INFORMATION TO USERS

This manuscript has been reproduced from the microfilm master. UMI films the text directly from the original or copy submitted. Thus, some thesis and dissertation copies are in typewriter face, while others may be from any type of computer printer.

The quality of this reproduction is dependent upon the quality of the copy submitted. Broken or indistinct print, colored or poor quality illustrations and photographs, print bleedthrough, substandard margins, and improper alignment can adversely affect reproduction.

In the unlikely event that the author did not send UMI a complete manuscript and there are missing pages, these will be noted. Also, if unauthorized copyright material had to be removed, a note will indicate the deletion.

Oversize materials (e.g., maps, drawings, charts) are reproduced by sectioning the original, beginning at the upper left-hand corner and continuing from left to right in equal sections with small overlaps.

Photographs included in the original manuscript have been reproduced xerographically in this copy. Higher quality 6" x 9" black and white photographic prints are available for any photographs or illustrations appearing in this copy for an additional charge. Contact UMI directly to order.

Bell & Howell Information and Learning
300 North Zeeb Road, Ann Arbor, MI 48106-1346 USA
800-521-0600

OPTICAL SPECTROSCOPIC OBSERVATIONS OF SPRITES, BLUE JETS, AND ELVES: INFERRED MICROPHYSICAL PROCESSES AND THEIR MACROPHYSICAL IMPLICATIONS

A

THESIS

Presented to the Faculty

of the University of Alaska Fairbanks

in Partial Fulfillment of the Requirements

for the Degree of

DOCTOR OF PHILOSOPHY

By

Matthew James Heavner, B.S., B.A.

Fairbanks, Alaska

May 2000

OPTICAL SPECTROSCOPIC OBSERVATIONS OF SPRITES, BLUE JETS, AND ELVES: INFERRED MICROPHYSICAL PROCESSES AND THEIR MACROPHYSICAL IMPLICATIONS

By

Matthew James Heavner

RECOMMENDED:

Advisory Committee Chair

Department Head

APPROVED:

Dean, College of Science, Engineering and Mathematics

Dean of the Graduate School

4-13-00

Date

Abstract

During the past decade, several new upper atmospheric phenomena associated with thunderstorms have been discovered. The four main types of optical emissions are now called sprites, blue jets, elves, and halos. Sprites are primarily red and appear between 40-95 km altitude and last between 1-100 ms. The dominant sprite emission is the molecular nitrogen first positive band, a relatively low energy emission also observed in the red lower borders of aurorae. The total optical energy output of a bright sprite is on the order of 50 kJ. Based on spectral observations, the total vibrational and electronic energy deposited in molecular nitrogen and oxygen in the upper atmosphere is 250 MJ-1 GJ. Blue jets last hundreds of milliseconds and span altitudes 15-40 km. Spectral observations of blue jets have not been obtained to date. Elves, the third type of observed optical emissions above thunderstorms, are red emissions at altitudes 75-95 km, lasting one millisecond or less. Elves and halos are similar phenomena, but are distinct based on altitude and duration. Halos typically last 3-6 ms and occur at lower altitudes than elves.

This dissertation describes the optical spectrum of sprites obtained by the University of Alaska Fairbanks during summer campaigns of 1995, 1996, and 1998, and its implication to the understanding of the electrodynamics of the middle atmosphere. The single most signficant result is the determination that a typical sprite deposits up to one gigajoule into the mesosphere. These forms of electrical energy coupling from tropospheric thunderstorms into the stratosphere, mesosphere, and thermosphere/ionosphere may have critical implications for the global chemistry and energy budgets in these regions.

Contents

List of Figures

List of Tables

Preface

> The study of nitrogen in the middle atmosphere can be subdivided into those processes occurring in the statosphere and those appropriate to the thermosphere. -Brasseur and Solomon [1986]

Little more than ten years ago, the first recorded sprite was presented at the 1989 Fall American Geophysical Union meeting. This dissertation describes contributions to understanding the phenomenology through the measurement and interpretation of sprites and other optical phenomena in the middle atmosphere. It has been exciting and gratifying to begin graduate work in a field in which a comprehensive literature search turns up several eyewitness reports and a few theoretical suggestions. The field has matured rapidly, and I have been fortunate that my graduate career has grown with the field. For the experimental portion of the work reported in this dissertation, I was able to leverage one of the major strengths of the Geophysical Institute, low light level optical observations. The analysis of the observations was possible because of an even greater strength of the Geophysical Institute–knowledge of video recording technology and analysis of optical spectroscopy. There is still a great deal of information about sprites to be gathered from optical measurements, and optical measurements will remain a primary part of all sprite observations. I am very fortunate to have had the opportunity to use and adapt readily available instruments to explore fundamental questions about the physics of sprites, with the support of all of the investigators of sprites and many people of the Geophysical Institute, whom I attempt to properly thank in the next section.

After the defense of this dissertation, during the final revisions state, Gene Wescott and Chris Berrington-Leigh met at the 1999 Fall American Geophysical Union and agreed on a distinction between elves and "sprite halos." A distinction of importance to this dissertation is that elves can generally not be observed at television rates. Because the distinction came just before the final stages of this dissertation, I have noted in the text several events as elves/"sprite halos."

Acknowledgements

It gives me great pleasure to acknowledge the help, cooperation, and patience I have received from many persons during my time as a graduate student. According to the UAF thesis guidlines, the abstract "will be the most read part of the thesis." I disagree–the acknowledgements will be the most read portion of this one (especially by the author). I attempt to include all of the folks who have made my research and graduate school experience a pleasure (mostly). I hope I include enough details to trigger memories and laughter every time I re-read these acknowledgments.

I could not have done this without Carolyn Elizabeth Talus. Thanks for the good times, the great travels, and the winter nesting, for everything and much more. I can't express my debt, my gratitude, or my love–but I will spend the rest of my life trying.

Davis Sentman has provided mentorship in the world of science, advice in the general pursuit of life, Green Slime, and an excellent graduate experience. Thank you for originally taking me under your wings as a graduate student in 1994, for providing me so many opportunities for research, collaboration, presenting my work, and learning how science gets done. I have been able to do more science and learn more about computers in the past eight years working with Dave than I could have begun to hope for when I started. Thank you so much!

Thanks to Don Hampton and Dana Moudry, *sine qua non*, for great friendship, great field work experiences, partnership in research and crime, a roof in Boulder and assistance paying those speeding tickets. Dana especially helped get this dissertation done while I was 5000 miles away from Fairbanks.

My committee members have all been crucial to my success in graduate school. I am indebted to Gene Wescott, for keeping me scientifically honest, giving me many great opportunities for field research, and providing a role model as a life of inquisitiveness, adventure, and scientific excellence. Hans Stenbaeck-Nielsen provided a foundation of optical expertise and experience, and offered great generosity of spirit. John V. Olson offered encouragement in science, taste in life, and crucial assistance in helping me successfully defend this dissertation during critical times.

My parents, Betsey and Jim, and by siblings, Kori and Ben, have shaped my life immeasurable, and I would not be who am I without them. Thanks, and I will keep my eye open for you all in every airport I am in–who knows when or where our paths may cross, but it is never often enough!

Curt Szuberla provided uafthesis.cls, got me startedin zymergy, provided many great discussions on the merits of CDparanoia, many moments of sanity and insanity, and much signal processing insight, and was an unflappable groom's gentleman.

Jeff Morrill provided perspective, expertise, synthetic molecular nitrogen curve, MOSART output, encouragement, good food, beer, big long distance phone bills, and discussion at AGU meetings. His attempts to convert me to a spectroscopist or maybe even a physical chemist helped get me interested in staring at grotrian diagrams. I feel dirty! Thank you very much. I look forward to many more productive collaborations. I feel lucky

to have met Dirk Lummerzheim, who provided much insight to spectroscopy, and a great example of an enjoyable life in pursuit of scientific knowledge–thanks! Tom Hallinan has been very generous is the use of instruments and the sharing of knowledge regarding the aurora and optical observations. Thanks to Carl Siefring and Eric Bucsela for scientific collaboration and guidance.

Many great friendships in addition to those mentioned above were necessary to make it through graduate school and life in general. Laura, Andrea, and Fred made my second comprehensive exam attempt more successful than my first, and also much more enjoyable. Laura and Martin are the most excellent folks I know for continually pursuing knowledge, adventure, and joy in life. Tom, Hans, Peter, and Jen made graduate school survivable with great music, hikes, and Easter egg hunts in addition to great friendship. Matt K. deserves thanks for friendship, being the dark Matt, and getting those opening night Phantom Menace tickets. Bevin, Hilary, and Darcie were a great part of Crane Court and helped survive Y2K in the wilds of New Zealand. Double n Tundra fueled the success of the heavnerhell studios, and provided good music and good distractions from this dissertation. Some of the many friends who have made life immeasurably better include: Matt Johnson, Alan Huang, Kerry Neis, Lizy, Ali, Kate, Dan, David, and Ellen (someday we'll find the perfect Margarita!). I am lucky to have found the friendship of Gina and Harlow, who have refueled my love of New Zealand and are great folks. They also introduced me to George, the best of the kiwis and an excellent protector against bogans for yanks abroad. I am grateful to John and Jason, you and I while we can, we'll listen to the music play. Thanks to Mace, for keeping live music alive in Fairbanks. Helena Symond and Paul Spong provided a beautiful haven on Hanson Island to begin chiselling this dissertation out of random electrons, and introduced me to some of the most intelligent creatures on the planet.

Many teachers have helped to spark my passion for learning. I owe them a great debt of gratitude, especially Bill O'Brien, Rob Roeder, Dr. Hilgeman, Tom Blackburn and Sara Duncan. Channon Price has taught me a great deal about physics and departmental politics, and kept me active in College Radio, as well as introducing me to J. Garcia.

Special thanks to Dave Covey, Scott Chesney, Don Rice, Chirk Chu and all of the other tolerant computer and network administrators of the UAF computer systems. In addition to keeping it all working, Dave Covey is a great cohort in pushing the use of computers and networking beyond any reasonable limits, and also provided friendship, running inspiration, and another tie to Lubbock. Thanks to Seth and J0seph for getting the UAFLUG going. Thanks to: Anne Trent, of the GI business office, for many smooth travels, and always helping me tag on that cheap flight to Lubbock (or New Zealand): Pennelope Noeker, for keeping the GI warm and working: Jim Desrochers, Dan Osborne, Bill Zito, and Kevin Abnitz provided expertise in instrumentation (especially the repair thereof!).

During the 1995 GASP campaign on Mt. Evans, Bob Stencel, Matti Jalakas, and Mark Jones of the University of Denver were most gracious hosts of the facilities at Womble Observatory. The University of Wyoming provided research facilities at the Wyoming Infrared Observatory. Walter Lyons and Tom Nelson at Yucca Ridge Field Station hosted instruments during the summer of 1996, and have provided helpful data, analysis, and discussion

regarding the phenomenon reported on in this dissertation. Researchers at Stanford University have been collaborators on analysis and provided many good discussions. Thanks to Umran, Tim, Steve (especially for the opportunity to do some field work in Fort Yuk), Victor, Elizabeth, and Christopher. I have been lucky to interact with researchers at New Mexico Tech/Langmuir Labs several times during my graduate career. I specifically thank Paul and Mark. Mike Taylor, of Utah State University, has been supportive of my graduate work, and has generously shared data, discussion, expertise, and beer. Many thanks for enlightening (and patient!) conversations with: Steve Reising, Dennis Boccippio (and for sharing one of the most expensive spaghetti dinners I've ever eaten, just off the plane in Osaka), Earle Williams, Stan Heckman, and Martin Fullëkrug.

Much of this dissertation would not have happened without the pilots, ground crew, and staff of AeroAir, most especially Jeff Tobolsky (for helping me to remember that for something to go up on the TV monitor, the plane has to tilt down..). Thanks!

Several data sets have been used for real time field observations and post-observation analysis. These include, the National Lightning Detection Network data, provided by Global Atmospherics and Steve Goodman and GOES data, specifically tailored for our needs by Dennis Chesters. Rick Howard, Ron Taylor, Sunanda Basu, and Mary Mellot at the NASA and NSF funding agencies have been very supportive of the research reported in this dissertation. USENIX, the American Geophysical Union, and the UAF graduate school all provided some travel funding.

This world would be a much worse place without the libraries and bookstores throughout the world, and I would be miserable as well. Thank you to everyone that keeps them going strong, especially to Connie at Into the Woods. This thesis has been brought to you by live music, Ben & Jerry's Ice Cream, and too much coffee.

And thanks to the Grateful Goddamned Dead!

Always pull tape

"All my attempts to adapt the theoretical foundation of physics to this new type of knowledge failed completely. It was as if the ground had been pulled out from under one, with no firm foundation to be seen anywhere, upon which one could have built. That this insecure and contradictory foundation was sufficient to enable a man of Bohr's unique instinct and tact to discover the major laws of the spectral lines . . . appeared to me like a miracle–and appears to me as a miracle even today. This is the highest form of musicality in the sphere of thought." – Albert Einstein (1951) Science 113, 82.

Chapter 1

Introduction

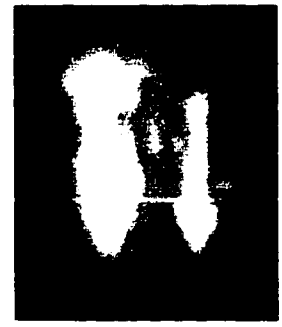

Over the past decade, middle atmospheric electrodynamics has experienced a surge of interest, primarily due to a single serendipitous recording (shown above, from Franz *et al.* [1990]) made by researchers cross calibrating imaging equipment to be used in conjunction with a sounding rocket experiment. This observation, made from O'Brien Observatory [1] in Minnesota on July 6, 1989 4:14:22, is the first recorded observation of optical emissions occurring in the middle atmosphere above active thunderstorms. Earlier eyewitness reports of possibly similar emissions date back to the late 1800's, but the above observation is the first known recording of the phenomenon now known as a sprite. Phenomena occurring above thunderstorms had been postulated [Wilson, 1925, 1956; Hoffman, 1960] and several unsuccessful attempts were made to detect them using high altitude aircraft [Vaughan and Vonnegut, 1989]. After the initial documentation of sprites by Franz *et al.* [1990], video observations from the space shuttle were examined and transient optical events identified as sprites were found in several of the recordings [Boeck *et al.*, 1992, 1995].

This dissertation presents three contributions to understanding this newly discovered facet of middle atmospheric electrodynamics. First, the rapid advancement of knowledge provided by observational efforts during the past decade is described in chronological order, and the significance of specific observations are highlighted. Second, the spectroscopic characterization of the optical emissions is discussed, focusing on measurements made by University of Alaska Fairbanks researchers. The third, and original, contribution of this

[1] O'Brien Observatory is operated by the University of Minnesota and located at 45.18°N, -92.77°E.

dissertation is the interpretation of the spectroscopic observations of sprites to determine the total energy deposited in neutral species of the middle atmosphere.

The largest source of energy into the middle-atmospheric region is via photo-dissociation of ambient chemical species by sunlight during daytime (this is the mechanism for production of ozone and the source of the heating which produces the temperature maximum at the stratopause) [Brasseur and Solomon, 1986]. Other sources of dynamic importance to the stratosphere and mesosphere include high latitude auroral processes and the upward mixing of tropospheric air. As an example of this mixing process, it has been hypothesized that lightning is the primary source of NO_x in the atmosphere. However, NO_x is trapped below the tropopause and transport across the tropopause to higher altitudes is a month to year long process. Gravity waves (generated by thunderstorm activity, orographic features, and other phenomena) and cosmic rays are additional energy inputs to the region of the atmosphere between the tropopause and the thermosphere [Dewan *et al.*, 1998; Fritts and vanZandt, 1993; Swenson and Mende, 1994]. The newly discovered transient optical events dramatically illustrate an electrical link between the lower atmosphere and regions up to the ionosphere. This link is of a much shorter time scale than other processes contributing to the dynamics of the region. The occurrence of brief, but bright, optical phenomena in the middle and upper atmosphere originating in thunderstorms may constitute a significant energy input into the region.

Observations of brief, low-light level phenomena, such as sprites, blue jets, elves, and halos above thunderstorms are difficult for several reasons. The middle atmosphere is relatively inaccessible to *in situ* measurements, lying above aircraft and balloon altitudes and below satellite altitudes. Only rocket observations, which pass through the region quickly and have only small likelihood of physically intersecting the transient events, are possible platforms for *in situ* experiments (one possible remote observation from a rocket has been reported by Li *et al.* [1991]). The more intense light from lightning is distracting to ground based naked eye observations. Sprites occur above less electrically active portions of storms, while the active regions of the storms are more interesting and therefore more likely to be the region of the storm observed. For these reasons, the recorded observations of these brief, low light level flashes in the middle atmosphere did not occur until the development of intensified video systems.

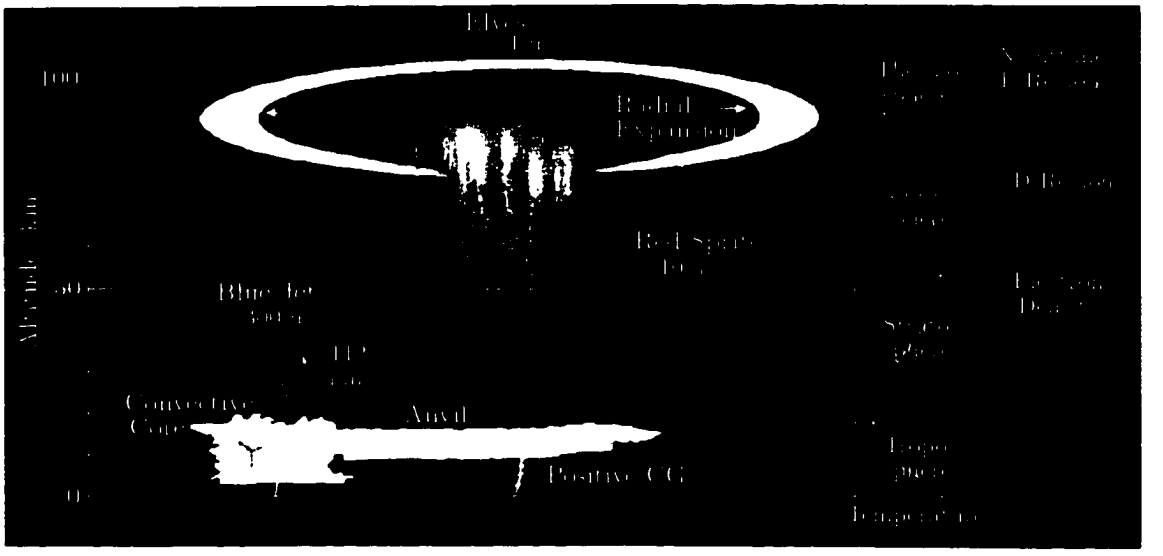

Figure 1.1. Summary of Sprites, Blue Jets, and Elves. Three types of transient optical events above thunderstorms recorded during the past decade are presented. Sprites occur in the altitude range 40-95 km and are associated with large positive cloud-to-ground lightning discharges. Blue jets are cones of light that propagate upward from the top of the electrically active convection core of thunderstorms to a terminal altitude of 35-40 km. Elves occur at the base of the ionosphere over both positive and negative CGs. They expand radially outward from a point in the lower ionosphere directly above the CG to horizontal diameters as large as ~500 km and exhibit vertical thicknesses of several km. This figure is based on a figure from Sentman *et al.* [1998a].

Since initial documentation in 1989, three main types of optical emissions in the middle atmosphere have been identified as summarized in Figure 1.1. An altitude axis, a typical vertical temperature profile, and a nighttime electron density profile are included to provide context for the three types of phenomena. Two main characteristics separate the phenomena into these groups: duration and altitude.

A sprite is a primarily red optical emission (with blue tendrils at lower altitudes) occurring between ~ 40-95 km above thunderstorms. The duration of sprites is on the order of few-to-tens of milliseconds. In addition to vertical extent, triangulation analysis (see Section 2.2) reveals that sprite emissions can span horizontal distances of up to 50 km [Sentman *et al.*, 1995b]. While the spatial volume of the optical emissions is quite large compared

to lightning,[2] spectral observations reveal sprites have a much lower energy density than lightning [Hampton *et al.*, 1996; Mende *et al.*, 1995].

Blue jets have average propagation speeds of 112 km/sec between cloud tops and terminal altitudes of ~40 km, with a duration of 200-300 ms [Wescott *et al.*, 1995b]. The obvious upward propagation, resolvable by human vision, led to the naming of these phenomena. Blue starters are similar to blue jets, propagating upward from storm tops. However, the starters extinguish at altitudes of ~25 km or less [Wescott *et al.*, 1996a].

A third phenomenon observed above thunderstorms is "ELVES" (or elves) (Emissions of Light and VLF perturbations due to EMP Sources [Fukunishi *et al.*, 1995]), which are brief (less than one millisecond) red emissions at the bottom of the ionosphere (at the upper altitudes of sprites). Optical "airglow enhancements" associated with lightning were first reported based on shuttle observations [Boeck *et al.*, 1992] and possibly also observed from a sounding rocket [Li *et al.*, 1991]. The phenomena were given the name elves after further documentation [Desroschers *et al.*, 1995; Lyons and Nelson, 1995] and photometer observations determined the lifetime of elves [Fukunishi *et al.*, 1996]. Recent triangulation shows that elves occur at altitudes ~99 km spanning up to ~530 km horizontally. In December 1999, a distinction between elves and "sprites halos" based on duration (and therefore detectability by current video rate instruments) was made by Gene Wescott and Chris Berringhton-Leigh at the American Geophysical Union meeting. Halos last 3-6 ms as observed by a 1000 frame per second imager (D.R. Moudry, personal communications). In addition to the longer duration, halos occur at ~77 km altitude, and are not as extended horizontally (Eugene Wescott, personal communications). The television rate imagery of both the shuttle, aircraft and ground-based observers mentioned above are now known as "sprite halos" while the photometric observations are elves.

All sprites, blue jets, and elves are observed above thunderstorms and have been found to be associated with thunderstorm lightning. Three main types of optical emissions and cloud-to-ground lightning have been determined by correlating observations with data from the National Lightning Detection Network (NLDN) (see Cummins *et al.* [1998] for a description of the NLDN). Sprites occur almost exclusively in spatial (within 100 km distance) and

[2]A typical lightning channel diameter is 10 cm [Uman, 1987].

temporal (delays of 300 ms maximum) proximity to large positive cloud-to-ground lightning[3] discharges [Boccippio *et al.*, 1995]. However, a few observations of sprites in conjunction with large negative cloud to ground flashes over one storm in August 1998 were reported by Stanley *et al.* [1998], and two additional examples were reported by Barrington-Leigh *et al.* [1999b]. Elves are observed in association with both large positive and negative lightning flashes [Barrington-Leigh and Inan, 1999]. The relationship between halos and thunderstorm activity has not yet been studied in detail. Blue jets and blue starters are observed in regions of storms associated primarily with negative lightning discharges, but are not temporally related to a specifc discharge and statistically are associated with a few second pause in lightning activity [Wescott *et al.*, 1995b]. Blue jets are associated with extreme convective activity and the occurrence of large hail.

Beginning in the northern hemisphere summer of 1993, there have been several large campaigns of both aircraft [Sentman and Wescott, 1993] and ground [Lyons, 1994] observations of sprites over the central United States. The majority of sprite observations to date have occurred over the central United States, but sprites have also been observed over South and Central America [Heavner *et al.*, 1995; Sentman *et al.*, 1995a; Wescott *et al.*, 1995a], Australia [Dowden *et al.*, 1997], and Japan [Fukunishi *et al.*, 1999].

The earliest observational efforts were directed at classifying basic spatial morphology of the various types of optical emissions, and work on refining descriptions of morphology is still ongoing. More recent observations, such as presented in Figure 1.2, have resolved sprites at higher spatial and temporal resolution, and have included non-optical measurements. Several studies of the lightning associated with sprite occurrence in the last decade have confirmed the association between sprites and positive cloud to ground lightning [Boccippio *et al.*, 1995; Nelson, 1997; Reising, 1998; São Sabbas, 1995]. The optical, infrared, and ultraviolet spectral signatures of sprites have been characterized [Hampton *et al.*, 1996; Heavner *et al.*, 2000; Mende *et al.*, 1995; Siefring *et al.*, 1997]. Using photometers and high speed imagers the temporal and spatial evolution of sprites and elves has been studied [Fukunishi *et al.*, 1996; Stanley *et al.*, 1999; Stenbaek-Nielsen *et al.*, 1999]. Radar signatures of sprites have been obtained [Roussel-Dupré and Blanc, 1997; Tsunoda *et al.*, 1998] (al-

[3]Lightning has been divided into 4 categories by Berger [1978] based on the direction of propagation and sign of charge of the leader that initiates the discharge.

Figure 1.2. July 26, 1998 Sprite Image. A low-light television image of a high resolution sprite from July 26, 1998 05:05:56.556 as observed from the EXL98 Gulfstream II aircraft (39.4142° North -104.4383° East, and 14.184 km altitude). Some streaking of the stars, due to a combination of intensifier persistence and aircraft motion, can be seen in the image. The brief duration of the sprite means that there is no streaking of the light from the sprites.

though other observers report no radar returns from sprites [Groves *et al.*, 1998]), including early observations of thunderstorm related phenomena [Rumi, 1957], which may or may not be related to sprites. Electromagnetic observations in the ULF/ELF/VLF frequency bands (Ultra-/Extremely-/Very- Low Frequency, ~.01 Hz to a few kHz) [Sentman *et al.*, 1994; Sentman and Wescott, 1994; Pasko and Inan, 1994; Inan *et al.*, 1995; Reising *et al.*, 1996; Cummer and Inan, 1997; Fukunishi *et al.*, 1997; Rodger, 1997; Rodger *et al.*, 1998; Reising, 1998; Füllekrug *et al.*, 1998; Reising *et al.*, 1999a] identify unique signatures related to both the current flow in sprites and ionospheric disturbances due to elves and sprites.

A principal result of this dissertation, based on analysis of the spectral observations, is the determination that a typical sprite is the electrical coupling of as much as 1 gigajoule from the tropospheric thunderstorm to the middle atmosphere. The optical energy radiated by a sprite was reported to be 10-50 kJ per event [Sentman *et al.*, 1995b], but radiated optical energy represents only a small fraction of the total energy deposited in the middle- and upper-atmosphere. Based on the optically radiated energy and a number of assumptions about the kinetic processes affecting the emissions in this wavelength range, estimates of the total energy deposition into O_2 and N_2 (vibrational and electronic states), range from

~250 MJ to ~1 GJ per event. One of the major goals of ongoing research is the confirmation of these estimates using independent methods of measurement.

One compelling reason for studying this new class of transient optical events is to assess their relevance in the context of global processes. Fundamental to this question is the amount of energy transported from the troposphere and deposited in the middle and upper atmosphere. The deposition of significant energy into the mesosphere by sprite processes may be important to the reactive chemistry of this region, but has not heretofore been included in chemical models of the upper atmosphere. Although much more speculative, sprites have even been suggested as a possible mechanism for production of the precursors to life on earth [Mojzsis *et al.*, 1999]. Studies of the production of amino acids via electrical spark have suggested that lightning could be a source for these molecules, but the extreme energy of a lightning flash is too large for the relatively weak bonds of amino acids. The lower energy of the sprites may provide a non-destructive path for amino acids production.

This dissertation represents the state of knowledge, as of November 1999, of the optical spectral characteristics of sprites. Chapter 2 is a chronologically organized description of observations including a discussion of the varieties of optical emissions that have been observed, other related (non-optical) observations, and a brief overview of the theoretical work developed to understand and explain the observations. The chronological discussion of observations highlights several original measurements of properties of sprites, blue jets, and elves. The spectral observations of sprites are briefly mentioned in Chapter 2 at the appropriate points in the chronology of observations.

Chapter 3 is the first comprehensive treatment of spectral observations identifying the emissions from sprites across the entire optical range of wavelengths. An illustrative comparison of spectral observations of similar atmospheric optical phenomena (aurora, lightning, and St. Elmo's fire) with sprite spectral observations is presented. The identification of primarily neutral molecular nitrogen emissions and the unambiguous observation of ionized molecular nitrogen emissions are discussed in Chapter 3. Only sprites have been spectroscopically observed and analyzed in detail, so the spectral discussions focus primarily on sprites.

Chapter 4 presents the detailed analysis of red spectral observations of sprites which include significant ionized molecular nitrogen Meinel emissions. The N_2^+ (Meinel) emissions

are from well below the published quenching altitude, so the intersystem collisional transfer (ICT) processes are described as a possible explanation for the observations of N_2^+ (Meinel) emissions at low altitudes. Blue spectral observations are complemented by blue filtered sprite observations, both of which find the dominant blue emissions are from the neutral molecular nitrogen second positive group, with ionized molecular nitrogen first negative group emissions a minor contribution. Based on the spectral observations, the total energy deposited in mesospheric neutrals is calculated to be between 250 megajoules and 1 gigajoule.

Chapter 5 summarizes the results of this dissertation and suggests several future obesrvations. Appendix A is the verbatim reproduction of several previously unpublished anecdotal reports of sprites. Appendix B describes the instruments used for the observations discussed in this dissertation.

Chapter 2

First Decade of Sprite Observations

This chapter describes the observations of sprites in the past decade, 1989-1999, in chronological order. Before the first documentation in 1989 of what is now called a sprite, only theoretical predictions and anecdotal reports of brief optical phenomena above thunderstorms existed. After the 1989 observation, space shuttle-based observations and continued ground based observations (at the O'Brien Observatory) were made with intensified cameras. In 1993, two campaigns, a NASA aircraft campaign over South America and the United States and a ground-based campaign from Colorado, provided unexpectedly high occurrence rates of sprites. After one decade of observations the total number of recorded sprites is on the order of ten thousand and growing rapidly. With the large number of observations, initial attempts at a classification of several types of sprites, jets, and elves have been made [Desroschers *et al.*, 1995; Moudry *et al.*, 1998; Heavner and Taylor, 1999].

The majority of sprite observations have been made during the northern hemisphere summers coincident with large thunderstorms over the midwestern high plains of North America [Lyons and Nelson, 1995; Lyons *et al.*, 1994, 1999; Sentman and Wescott, 1994; Sentman, 1998; Sentman *et al.*, 1998b; Dial and Taylor, 1999]. Aircraft campaigns over South America and Central America in February 1995 and August 1995 have also documented sprites [Heavner *et al.*, 1995; Sentman *et al.*, 1995a; Wescott *et al.*, 1995a]. Observations of sprites have been made in Australia during southern hemisphere summers

since 1997 [Dowden *et al.*, 1997]. In December 1998, sprites were observed above Japanese winter thunderstorms [Fukunishi *et al.*, 1999]. Few observations of sprites from a platform that provides a global view, such as from a satellite, have been made, although a total of seventeen sprites have been identified in the video observations from the U.S. space shuttle [Boeck *et al.*, 1998]. High energy particles originating from thunderstorm systems, detected in space by the Compton Gamma Ray Observatory satellite, may be associated with sprites [Fishman *et al.*, 1994], but the optical shuttle observations are the only reported space based observations of sprites.

The next section describes the first decade of sprite research and provides the framework for the next chapters of this dissertation regarding energetics of sprites in the optical passband.

2.1 Anecdotal Reports and Initial Documentation

Anecdotal reports from ground based observers and aircraft pilots have been collected for more than twenty years [Corliss, 1977; Vonnegut, 1980; Vaughan and Vonnegut, 1982; Gales, 1982; Vonnegut, 1984; Vaughan and Vonnegut, 1989; Rodger, 1999]. Preliminary investigations have not found any descriptions of flashes above thunderstorms that could be interpreted as sprites in mythological or pre-historical literature (D. Sentman, A. Ruggles, personal communications). Reports from the last 150 years include descriptions of "...continuous darts of light ... ascended to a considerable altitude, resembling rockets more than lightning" [MacKenzie and Toynbee, 1886], "...a luminous trail shot up to 15 degrees or so, about as fast as, or faster than, a rocket" [Everett, 1903], "...a long weak streamer of a reddish hue..." [Malan, 1937], "...flames appearing to rise from the top of the cloud..." [Ashmore, 1950], and a "...discharge [which] assumed a shape similar to roots of a tree in an inverted position..." [Wood, 1951].

Aircraft pilots have reported seeing similar phenomena. Ronald Williams, a U-2 pilot for NASA at the Ames Research Laboratory, describes observing a "bright lightning discharge, whitish-yellow in colour, that came directly out of the centre of the cloud at its apex and extended vertically upwards far above my altitude. The discharge was very nearly straight, like a beam of light, showing no tortuosity or branching. Its duration was greater than

an ordinary lightning flash, perhaps as much as five seconds." [Vonnegut, 1980]. The reported long duration does not match recorded observations of sprites or blue jets, but the report provided important documentation of a pilot's observation of optical events above thunderstorms which helped to generate scientific interest in the field. Conway Roberts, a NASA pilot at Wallops Flight Center, reported that while flying near a storm he observed that "approximately every 50th or 100th discharge would go from the top of a cloud upwards through the clear air toward the ionosphere" and estimated that "these vertical lightning bolts were extending from the tops of the clouds, which were between 50,000 and 60,000 feet [15.2 - 18.3 km], to an altitude equal to the height of the cloud. This would mean that the lightning flashes extended to an altitude of approximately 120,000 feet (± 20,000) [36.6 ± 6.1 km] before they could no longer be seen" [Vaughan and Vonnegut, 1982]. The reported altitude 'equal to the height of the cloud' is likely an angular comparison, rather than altitude comparison. Additionally, this was the limit of the pilot's visibility. Vaughan and Vonnegut [1989] provide 15 pilot observations of such things as "...a bolt of lightning [that] came straight out the top and went to a point about 2000 ft. [600 m] above us and shattered in all directions as an egg would do if it were thrown against a ceiling." Additional pilot reports are collected in Vonnegut [1984].

Serious scientific investigation of upper atmospheric optical phenomena associated with thunderstorms began on July 6, 1989 with the serendipitous observation of a "cloud-to-stratosphere" discharge [Franz *et al.*, 1990; Winckler, 1995]. The initial observation is reproduced in Figure 2.1 (B). The observation was obtained with an intensified low light level camera at O'Brien Observatory in Minnesota (45.18° N, -92.77° E), operated by the University of Minnesota. The camera was being calibrated for coordinated observations during an upcoming sounding rocket campaign. This first fortuitous observation of sprites from O'Brien Observatory led to the operation of a camera specifically for sprite observations during the ensuing decade [Winckler, 1998]. The initial report of the July 6, 1989 observation described the event as a "...discharge [that] began at the cloud tops at 14 kilometers and extended into the clear air 20 kilometers higher." These estimates of altitude were made with observations from only a single station and disagree with later results made using two station triangulation methods as well as single station observations using the NLDN for an estimate of the slant range to the sprite. However, the documentation of optical phenomena

Observatory	Lat.	Long.	Alt. (km)	Obs. Period
Bear Mountain	43.88	-103.75	2.15	8/99
Mt. Evans, Denver University	39.58	-105.63	4.05	'95,'98
Langmuir Laboratory, NMIMT	33.98	-107.18	3.2	'96-'99
O'Brien Observatory, U. MN	45.18	-92.77		'89,'93
Wyoming Infrared Observatory	41.10	-105.98	2.94	'96,'98,'99
Yucca Ridge Field Station	40.67	-104.93	1.65	'93-'99

Table 2.1. Observatory locations: latitude, longitude, and altitudes for the Bear Mountain Observatory near Custer, WY; the Womble Observatory, operated by Denver University atop Mt Evans, near Idaho Springs, Colorado; Langmuir Laboratory, near Socorro, New Mexico and operated by the New Mexico Institute of Mining and Technology; Wyoming Infrared Observatory on Jelm Mountain, near Laramie Wyoming; Forensic Meteorology Associates' Yucca Ridge Field Station, near Ft. Collins, Colorado are presented in this table. The years during which sprites have been reported from the stations are listed.

above thunderstorms generated interest among several groups of researchers.

One of the early efforts to record lightning related optical events was made by researchers from the University of Alaska Fairbanks using a NASA DC-8, flying over South America and the midwestern United States in 1993 [Sentman and Wescott, 1993]. Another early large campaign was based at the Yucca Ridge Field Station in Colorado [Lyons, 1994]. During the period 1992-1994 a low light level camera at O'Brien Observatory continued to observe sprites. One of the most active storms studied from O'Brien Observatory was a storm over Iowa August 9-10, 1993 [Winckler, 1995]. Table 2.1 summarizes the locations of ground sprite observations during the past decade.

The development of optical space based observations of lightning and related phenomena began in 1979, when an instrumented Belanca Viking aircraft was used as a test platform for a lightweight lightning detection and as a photographic system that was the basis for a system that later flew on the NASA space shuttle flights STS-2, STS-4, and STS-6 [Vonnegut *et al.*, 1983, 1985]. Successful observations of lightning from the Nighttime and Daytime Optical Survey of Lightning Experiment led to the use of handheld video cameras by crew members to record thunderstorm activity on several additional shuttle flights. After 1986 the Mesoscale Lightning Experiment [Boeck, 1987] observed lightning directly under the

shuttle and was a prototype for the development of the Optical Transient Detector, an instrument for observing lightning below an orbiting satellite. In 1988, the shuttle lightning observations were changed so that ground based controllers at Mission Control Center could operate the low light level TV cameras in the payload bay[1] to observe thunderstorms on or near the limb of the Earth. On October 21, 1989, the shuttle imaged the second recorded sprite [Boeck *et al.*, 1998]. One sprite[2] observed from the shuttle on August 5, 1991 at 1:29:08 is shown in Figure 2.1 (A). The example shown was observed over South America, with the cities of Uruguaiana, Goya, Reconquista, Concordia, Salto, Posadas, Resitencia and Corrientes identified in the foreground of the image. The nightglow layer (at ~85 km) provides a reference altitude, but the sprite occurs in the foreground of the scene, rather than on the limb. The estimated location of the sprite is -29.4° N and -52.3° E longitude, with an approximate slant range to the space shuttle of 1300 km. As of 1998, a total of seventeen sprite events have been observed from the shuttle and are included on the summary map of observations in Figure 2.17. Observations from the shuttle include 'airglow brightening' associated with lightning discharges [Boeck *et al.*, 1992], which are now identified as elves or sprite halos (see discussion in Section 2.3.3).

University of Alaska Fairbanks Geophysical Institute activities to study sprites with a 1992 proposal to NASA to perform measurements over South America in June, 1993 using the NASA DC-8 Airborne Laboratory. The global distribution of thunderstorms has been characterized based on several types of observations including daily variation of the fair weather electric field (Carnegie curve), Schumann Resonance amplitude daily variation [Sentman and Fraser, 1991], satellite observations of optical and radio lightning signatures [Christian *et al.*, 1999; Zuelsdorf *et al.*, 1997], and surface meteorological reports (see also Chapter 2 of Uman [1987] and Chapter 4 of Williams [1995]). The lightning maps generated by several independent observations all indicate that the greatest amount of global lightning activity occurs in three main tropical regions of the world: the Amazon basin of South America, sub-Saharan Africa, and the Malaysian Archipelago/Maritime continent extending from Southeast Asia across the Philippines, Indonesia, and Borneo into northwest Australia. The predominance of lightning activity in South America led to the decision to investigate

[1] Normally the cameras are used to observe crew activities in the payload bay. For lightning studies, the controllers turned the cameras to the limb of the earth when the crew was sleeping.

[2] From http://wwwghcc.msfc.nasa.gov/skeets.html.

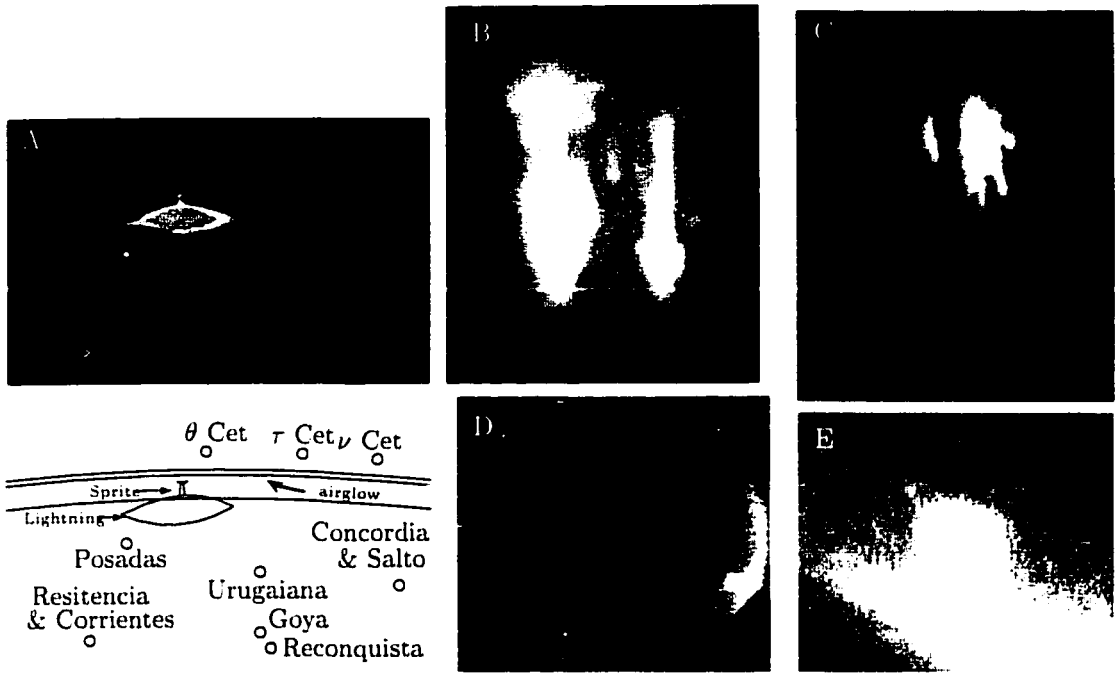

Figure 2.1. Early Sprite Observations. Images of the earliest observations of sprites. (A) was recorded from a space shuttle videocamera at August 5, 1991 1:29:48. The stars and cities are identified. The sprite is estimated to have occurred at 29.4° S, 52.3° W, at a range of ~1300 km from the shuttle. (B) is the first reported ground based sprite observation, from July 6, 1989 4:14:22. (C) is one of the first observations from Yucca Ridge Field Station, recorded July 7, 1993 at 6:07:39. (D) is one of the July 8, 1993 observation from a NASA DC-8 looking over a thunderstorm in Iowa using a fish-eye, all sky camera. (E) is a rotated, zoomed section of (D).

that region for sprites. However, nighttime flight scheduling difficulties during the South American campaign allowed only one night flight for observations, during which the DC-8 was able to circumnavigate a large thunderstorm over Bolivia with diameter ~100 km, as measured from the GOES infrared image. No optical emissions above the thunderstorm were observed. The single flight used only two flight hours of the eight provided by the NASA grant, but the DC-8 was scheduled to return to the United States, so no further observations were made in South America. Upon the return to the United States a small window of opportunity existed before the next scheduled DC-8 flights, so additional flight hours were added to the grant by NASA to provide one flight from California to the Midwest

on one of three possible nights. The first possible night, July 7, 1993 was canceled because of aircraft difficulties. On July 8, 1993, a large front of storms was creating severe flooding across Iowa. The DC-8 flew from NASA Ames Moffitt field in California to these storms and circled them while several low light level cameras made observations in the region above the thunderstorms. No obvious emissions were observed in real time during the flights, but upon careful review of the video tapes three unusual flashes were found that coincided with the thunderstorm activity.

After the initial identification of the three sprites, nineteen events total were found over two storms, one in central Iowa and a second in southeast Nebraska, through careful analysis of the video observations. Fifteen minute summary maps of the National Lightning Detection Network system were used to identify the possible region of the flash location, with the assumption that the flash was associated with the lightning activity. Using the distance between the airplane and the thunderstorms to estimate slant range and the starfield to determine elevation of the tops of the sprites, an estimate of the altitude range was calculated. The determination that sprites occurred in the mesosphere range of altitudes 60-100 km, rather than at lower altitudes as reported with other early observations, was the significant result from this campaign [Sentman and Wescott, 1993].

Figure 2.1 (D) and (E) shows one of the sprites observed (see Sentman and Wescott [1993] for several additional sprites observed from the DC-8). The observations were recorded by an intensified camera system with a fisheye lens, so the entire sky is monitored: (D) shows the all-sky image of a sprite observed at July 9, 1993 3:57:07. (E) is the cropped and rotated section of (D). The coarse spatial resolution of the all-sky imager provided minimal detail of the sprite ((B) and (C) are much higher resolution while the shuttle observations of (A) are even lower spatial resolution images of sprites). However, the aircraft observations from a single night over the central United States, with recorded sprites over two active thunderstorms, indicated that sprites are not rare phenomena. The Yucca Ridge Field Station and O'Brien Observatory observations from 1993 reported similar results regarding the frequency of sprite occurrence over active thunderstorms [Lyons, 1994].

The Yucca Ridge Field Station (YRFS) is located approximately 10 km outside of Ft. Collins, Colorado, on a small ridge east of the front range of the Rocky Mountains, with

an unobstructed eastward view of about 180° azimuth looking eastward. The convenient location for viewing thunderstorm activity on the great plains has attracted several groups of investigators, facilitating several major observational campaigns during summer months. YRFS began sprite observations during the northern hemisphere summer of 1993 and on July 7, 1993 imaged the sprite shown in Figure 2.1 (C) [Lyons and Williams, 1993; Lyons, 1994].

The origin of the term 'sprite' is of some interest since it runs counter to the more generally accepted usage of descriptive terms. Most descriptions of sprites in early reports attempted to include physical characteristics in the name which were conjectural or assumed information that was not known. Examples of such descriptive names, including "large upward electrical discharge" [Franz *et al.*, 1990], "cloud-to-stratosphere electrical discharges" [Lyons, 1993; Lyons and Williams, 1993, 1994], "luminous structures in the stratosphere" [Lyons, 1994], "cloud to space lightning" [Vaughan *et al.*, 1992], "stratospheric flash" or "lightning in the stratosphere" [Boeck *et al.*, 1995], and "cloud-ionosphere electrical discharges" [Winckler, 1995], have been used in early sprite reports. Unfortunately, these descriptive names were either only partially correct, or even incorrect. After the initial determination that the phenomena occurred at much higher altitudes than many of the early descriptions supposed [Sentman and Wescott, 1993], and because of the relative lack of knowledge of physical mechanisms and the actual direction of propagation, the name "sprite" was coined by D. Sentman as a nonjudgemental term to refer to these optical emissions. This term is now generally accepted, but the occasional use of misnomers continues to the present: a recent Ph.D. thesis at the University of Maryland was titled "The Physics of High Altitude Lightning" [Valdivia, 1997]; Gomes and Cooray [1998] use the term "glow phenomena" but then use "ionospheric lightning" in their abstract; [Boeck *et al.*, 1998] claims that "in addition to documenting the reality of *upward lightning discharges* that are now called sprites...": the term "mesospheric electrical discharges" [Winckler, 1998] is also found. A review of sprites, blue jets, elves, and TIPPS observations with the title "Red Sprites, Upward Lightning, and VLF Perturbations" was recently published [Rodger, 1999].

A definition of lightning is "a transient, high-current electric discharge whose path length is measured in kilometers" [Uman, 1987]. The amount of current flowing in a sprite is still under study, but estimates on the order of ten kiloamperes have been reported [Cummer and

Stanley, 1999]. For comparison, the causative lightning discharge may involve currents of approximately fifty kiloamperes. However, sprites are dissimilar to lightning, either cloud to ground, intracloud, or cloud-to-cloud discharges in a number of different aspects, including the volume of optical emissions and the spectral signatures of the emissions. In Chapter 3 (and specifically Figure 3.5) of this dissertation the very different spectroscopic signatures of sprite and lightning optical emissions are compared and discussed.

2.2 1994–Physical Dimensions, ELF/VLF, Blue Jets

Observations of sprites in 1993 established the existence of mesospheric optical emission that might extend up to altitudes as high as 100 km and suggested that sprites may not be uncommon [Sentman and Wescott, 1993; Lyons, 1994]. Results of the 1994 University of Alaska Fairbanks aircraft and Yucca Ridge Field Station ground observations include the frequency of occurrence of sprites to be up to about one sprite per minute, the accurate determination of the dimensions of sprites [Sentman *et al.*, 1995b], and the correlation of sprites with positive lightning flashes [Boccippio *et al.*, 1995]. The first coordinated optical and Extremely/Very Low Frequency (ELF/VLF) observations were also made in 1994, using a magnetic induction coil with response between 30 Hz-30 kHz deployed in Oklahoma during the University of Alaska 1994 aircraft campaign [Sentman and Wescott, 1994; Sentman *et al.*, 1994]. An outcome of these observations was the identification of a unique electromagnetic ELF/VLF signature associated with the occurrence of some sprites.

A primary goal of the University of Alaska 1994 aircraft campaign was the simultaneous observation of sprites and blue jets from two spatially separated locations. For this purpose, two corporate aircraft, a Westwind II and a Jet Commander, were used for observations. The two images obtained from the aircraft allow triangulation to accurately determine the latitude, longitude, and altitude of features in the event. The accuracy of the triangulation depends on the geometry of the two observers and the sprite, the quality of the star field in images, and the sharpness of the focus and field of view (angular pixel resolution). Image distortion due to the camera lens, especially severe for large field of view observations, are typically corrected using a calibration pattern, although the star field itself may also be used to make the correction. After distortions from the camera are removed, the stars in

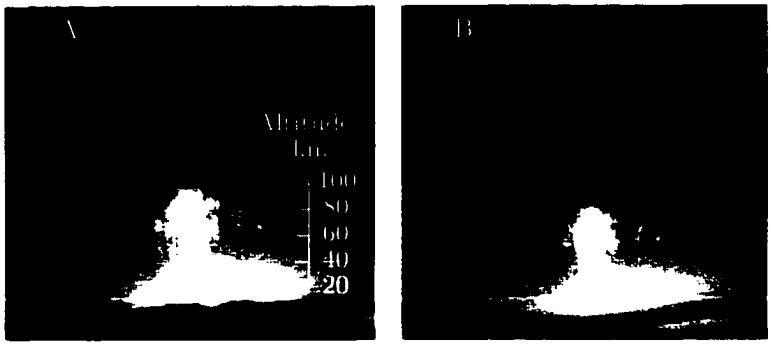

Figure 2.2. July 4, 1994 4:00:20 Triangulation. Aircraft stereo pair observations of a sprite at July 4, 1994 4:00:20 with triangulated height scales. These triangulation measurements were the first indication that sprites spanned the middle-atmosphere to the bottom of the ionosphere. This pair can be viewed in stereo 3D.

the image are identified using the STAR computer program[3], which uses the Smithsonian Astronomical Observatory star catalog to identify stars in images. Next, the STEREO computer program is used to locate common features of sprites in both images. The final output of these programs is the three dimensional absolute coordinates of the triangulated feature, yielding both the altitude and geographic position.

Figure 2.2 presents an example of a stereo pair used for triangulation from a July 4, 1994 4:00:20 sprite event. The images are cropped from the entire field of view, showing 18.6° H by 22.5° V section of the image. The triangulated elements of the event which are closest to each aircraft are at slant ranges of 255 km from the Westwind II (A) and 266 km from the Jet Commander (B). With the wide angle lenses used for observations in 1994, and for a slant range of 250 km and a good star fit, the pixel resolution gives triangulation errors of 720 m vertically. The maximum altitude of the event was 94.1 km while the lowest triangulated sprite emissions was at an altitude of 52.1 km. The scattered light from the associated lightning discharge makes lower altitude determination impossible. The altitudes triangulated during the UAF 1994 aircraft campaign [Sentman and Wescott, 1994] provided the first direct measurement of the true horizontal and vertical extent of sprites, improving on the previous estimates obtained in 1993 [Sentman and Wescott, 1993]. Detailed triangulation analysis of July 24, 1996 observations is presented in Figure 2.8. Accurate

[3]STAR and STEREO are written and maintained by Hans Stenbaek-Nielsen.

determination of the location of sprites is important for comparison and interpretation of sprite observations with non-optical (*e.g.* VLF) or satellite-based instruments.

In addition to land-based thunderstorms, at least one tropical storm has been studied to investigate the possible occurrence of sprites over water. On the night of July 3, 1994 the West Wind II aircraft of the Sprites'94 campaign flew near Tropical Storm Alberto, in the Gulf of Mexico. No sprites were observed, and very little lightning activity was recorded.

2.2.1 Blue Jets and Blue Starters

On July 1, 1994 University of Alaska scientists aboard the two Sprites'94 aircraft investigated an extremely active thunderstorm over Arkansas for sprite occurrence. Because of the storm/aircraft geometry (the cameras were viewing away from the sunset), the observations began about one hour earlier than other nights of aircraft flights. The aircraft made two observation passes by the storm. Few sprites were observed during the first pass of this storm, but fifty-six occurrences of luminous columns of light propagating up from the storm tops were unexpectedly observed and recorded during a twenty-two minute period. At the time of observation, these new phenomena were recognized as being qualitatively different from sprites in two ways: (1) the propagation speed was small enough that the upward motion was easily apparent at video rates (thirty frames per second) and (2) the emissions were blue, as observed using an intensified color camera. Due to the upward motion and the color of the phenomena, they were given the name blue jets [Wescott *et al.*, 1995b]. Thirty examples of blue starters, a related phenomena, were also recorded [Wescott *et al.*, 1996a].

Triangulation analysis of thirty-four blue jets observed simultaneously from both aircraft found an upper altitude of 37.2 ± 5.3 km and an upward velocity of 112 ± 24 km/s [Wescott *et al.*, 1998a]. The base of the jets was approximately 18 km, but may have been lower and simply obscured by the clouds because of the observational geometry: the aircraft altitude ($\sim$13 km) was below the triangulated base of the jets, and the National Weather Service reported radar observations of the anvil storm top at 19.2 km. One of the jets observed on July 1, 1994 is presented in the left two columns of Figure 2.3 (A). The left column is from the Jet Commander at 34.320° N, -95.074° E, 13.157 km altitude and the right column is from the West Wind at 34.088° N, -95.273° E, 12.876 km altitude. The top frame is from 03:13:46.176 and the bottom frame is from 03:13:46.410. The milliseconds after 03:13:46 are

labeled to the left of the jet images. The images are cropped video fields (17 ms resolution) from the black and white wide angle cameras on each aircraft for the jet observed July 1, 1994 3:13:46.

The blue jets do not occur in association with individual cloud-to-ground lightning strokes of either positive or negative polarity as reported by the National Lightning Detection Network. Instead, they occur over regions of storms with both high negative cloud-to-ground discharge rate and heavy hail [Wescott *et al.*, 1998a]. Newspapers from several towns near the triangulated locations of the jets reported large hailfall near the time of the blue jets, and the National Weather Service reported 5-7 cm diameter hail in cities in the region. Figure 2.3 (B) illustrates the spatial relationship between the blue jets and negative lightning discharge centers. The dark circles are the triangulated location of blue jets (thirty four total), while the light circles are blue jets only observed from a single aircraft (seventeen blue jets), so assumptions about their initial and terminal altitudes were required to estimate the range from the plane to the blue jet. The small circular dots show the location of all NLDN reported negative CGs during the time period of blue jets. Crosses mark the positive CGs recorded by NLDN. Three cities, Forman OK, New Boston TX and Texarkana TX are indicated by stars, along with the reported size of hail. The blue jets and lightning activity are clustered spatially, but the blue jets were not temporally associated with the negative CGs to within less than one second (as compared to sprites, which follow a positive CG within $\sim$.25 seconds).

During the second pass of the Arkansas storm, approximately one hour later, no blue jets were observed, but several sprites were recorded. Based on the observed temporal change between blue jet activity and sprite activity, Wescott *et al.* [1995b] hypothesized that the blue jets occur earlier in storm activity, over more active convective cells, while sprites occur over more mature storm systems. Six sprite groups were observed from the aircraft during the time period of blue jet observations. Triangulation revealed that the sprites occurred over a different part of the storm ($\sim$300 km east of the blue jets), and were associated with positive CGs. The temporal development of storm activity from blue jets to sprites is in agreement with the report of Mark Evans, reproduced in Appendix A.

Further analysis of the 1994 UAF aircraft video observations revealed a second type of event, a blue starter. Starters are similar to blue jets, propagating up from the top of

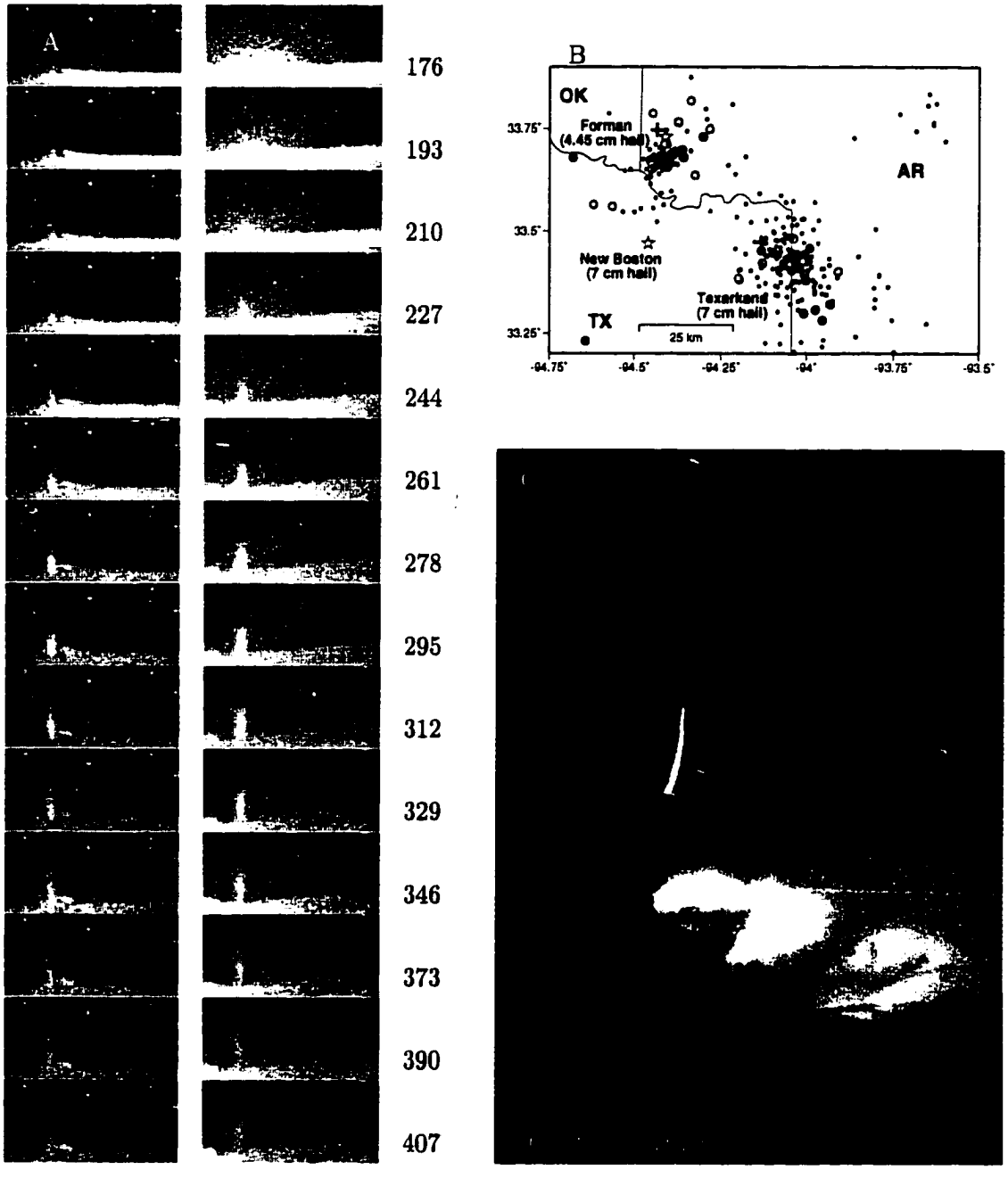

Figure 2.3. Section (A) is a series of television fields of a blue jet observation. The left column of (A) is from the Jet Commander and the right column is from the WestWind II. Milliseconds after 03:13:46 are labelled. A map of triangulated blue jets, negative lightning discharges, and reported hailfall from July 4, 1994 is shown in (B). The photograph of a blue jet from the ground is presented in (C) (courtesy of Patrice Huet).

the thunderstorms [Wescott *et al.*, 1996a]. However, blue starters terminate at an average altitude of ~25.5 km and have a velocity range of 27-153 km/s, with an average speed of 119.3 km/s. Intensified color camera observations record blue starters as the same color as blue jets. Thirty blue starters were observed in the same region of the July 1, 1994 Arkansas storm as the blue jets, during the same twenty two minute interval. On several other nights blue starters were observed over the active convective core of storms (with no blue jets recorded). Blue starters were also observed during the EXL98 mission (presented in Section 2.6 and Figure 2.13). The blue starters were observed in blue filtered images and also in the near infrared. The implications of these observations will be discussed below. A study of blue starters observed during the July 1, 1994 aircraft mission and the associated lightning found that the occurrence of blue starters was accompanied by a decrease in lightning activity [Wescott *et al.*, 1998a]. A similar study of the 1998 blue starter observations did not reveal the same temporary decrease in lightning activity in the storm.

Information regarding the nature of the optical emission source may be deduced by comparing observations made with different cameras and taking into account the camera responses. The color camera does not respond to light of wavelength less than ~400 nm while the monochrome camera response extends to ~380 nm (see Figure B.1). The monochrome cameras respond to the brightest emission in the N_2^+(1NG) group, 391.4 nm. The jets are visible solely in the blue channel of the color camera, but because the color camera is not as sensitive overall, and specifically because the blue channel is not responsive to the 391.4 nm emissions, the jet signal is much stronger in the monochrome camera. Wescott *et al.* [1998a] calculated the blue/red ratio for blue jets by assuming auroral emissions (from Vallance Jones [1974]) of N_2^+(1NG), N_2(1PG), and N_2(2PG) emissions and taking into account atmospheric transmission and altitude dependent quenching. Significant ionized emissions (N_2^+(1NG)) are required to describe the observed lack of signal in the red channel of the ACTP color camera (and correspondingly high blue/red ratio), indicating that ionized emissions are a substantial portion of the observed light from jets. However, conclusive observations of the ionized emissions from jets remained to be made. The EXL98 campaign (Section 2.6) was designed to make direct observations of N_2^+(1NG) emissions in sprites, blue jets and blue starters.

Almost all observations of jets have been from aircraft. In addition to the July 1, 1994 Arkansas observations and EXL98 blue starter observations, a single blue jet was observed on July 4, 1994 over Kansas, and another was recorded over South America in 1995. Blue jets occur at lower altitudes than sprites, so that the thunderstorm itself is more likely to obscure the view of the blue jets from the ground. The poor atmospheric transmission of blue light decreases the range at which blue emissions may be observed (compared to the 1000 km limit associated with sprites) further limiting the range of viewing geometries. However, several observations of blue jets made at ground level have been reported. One excellent example of a ground based observation of a blue jet was recorded from Reunion Island (near Madagascar) using 400 speed Fujicolor film and a two minute exposure from a regular 35 mm camera and is reproduced in Figure 2.3. The red, horizontal light in the image is a commercial aircraft. The camera was looking northward from La Reunion (20.85° S, 55.42° E) towards Madagascar. Fine streamer-like filaments can be seen near the brightest portions of the jet near the cloud tops.

Finally, a blue jet was visually observed January 6, 2000 22:38 UT by the author on a flight from Sydney, Australia to Los Angeles, California, USA. The plane was approximately midway between Nandi, Fiji and Apia, Western Somoa (estimated to be 15°S, 183°W). After the flight, the observation of the blue jet was confirmed by Chris Colvin, a pilot in the cockpit. Only a single blue jet was observed over a storm with a fairly low flash rate (approximately one flash per fifteen seconds) over the ocean. The low flash rate, compared to the Arkansas storm of July 1, 1994, and the observation of blue jets above the ocean indicate that blue jets may occur frequently on a global basis.

2.2.2 Palm Tree

The "palm tree" events were so named because of the distinctive features of the first event identified in the aircraft video observations of 1994. Following the occurrence of a large group of sprites, a vertical column of emissions appeared to propagate upward from the lowest resolvable altitudes near cloud tops ($\sim$ 20 km) to almost 60 km over a few video fields. Near the end of the event, two 'leaves' appeared to emerge from opposite sides of the top of the sprite column and propagate upward at approximately 45° angles.the top of the column.

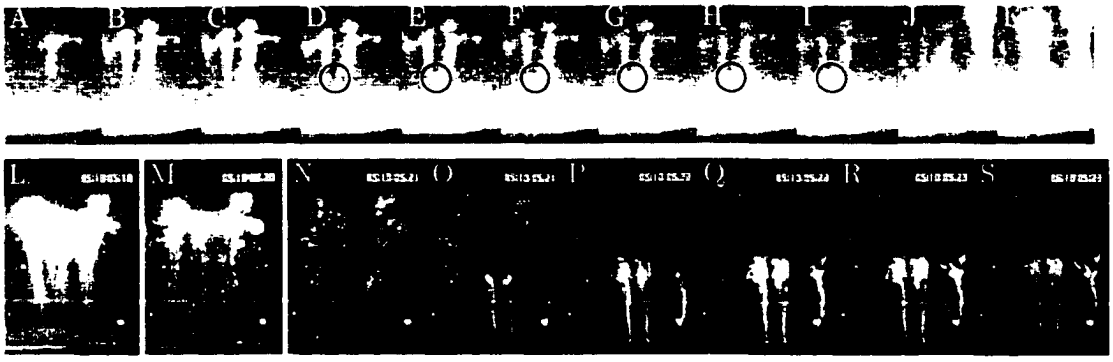

Figure 2.4. Palm tree sprite observed July 4, 1994 3:54:12.585. Temporal evolution is left to right, A-K, with 187 milliseconds of video data displayed. The palm tree is highlighted with a black circle. A second palm tree observed August 18, 1999 5:10:05 is included in images L-S. Each image is 17 millisecond apart, except two fields are dropped between L and M, and one field is dropped between M and N. Palm trees appear after a large group of sprites and are seen to propagate upwards.

The first palm tree event from July 4, 1994 3:54:12 was reported at the 1995 Fall American Geophysical Union meeting [Desroschers *et al.*, 1995][1] and is reproduced in Figure 2.4 A-K. The palm tree was associated with a large group of sprites. Because the sequence was observed by two spatially separated aircraft, accurate triangulation of the event was possible. The triangulated terminal altitude of the palm tree is 56 km, compared to the terminal altitude of the sprites of approximately 85 km. In the sequence of video frames A-K of the July 1, 1994 palm tree in Figure 2.4, the palm tree is apparently followed by a sprite in the same location. However, triangulation shows that the sprite and palm tree were separated by 30.1 km horizontally. The triangulation details of the July 1, 1994 3:54:12 palm tree are presented in Table 2.2. The palm tree was centered at 38.2° N -99.73° E. The sprite occurring after the palm tree was centered at 37.979° N, -99.436° E. The triangulation error of 730 m in the east-west direction, for this event is larger than the north-south directional error of 230 m. The palm tree was observed in the ACTP color camera to be the same red color as a sprite. In 1995, several palm tree observed by Mike Taylor of Utah State University were observed with a 665 nm filtered imager (M. J. Taylor, personal communication). The filtered observations show that the palm trees are the N_2(1PG) emissions (the same as sprites).

[1]See http://elf.gi.alaska.edu/heavner/rs/conf/fagu95/morph.html

Time	Object	Lat (N)	Long (W)	Alt (km)
July 4, 1994 3:54:12.719				
	Westwind II	36.283	97.153	12.79
	Jet Commander	35.860	97.846	10.51
	Palm Tree (A)	38.326	99.751	55.571
	Palm Tree (B)	38.195	99.696	36.183
	Palm Tree (C)	38.234	99.796	56.330
	Palm Tree (D)	38.235	99.690	56.090
3:54:12.593	NLDN +CG	38.503	99.903	
3:54:12.640	NLDN +CG	38.505	99.911	
3:54:12.825	NLDN +CG	38.535	99.408	
August 18, 1999 5:08:07.188				
	Palm Tree (A)	41.201	-98.921	50.596
	Palm Tree (B)	41.189	-98.947	32.382
	Palm Tree (C)	41.211	-98.913	52.065
	Palm Tree (D)	41.196	-98.926	50.289
	Palm Tree (E)	41.209	-98.934	46.034
	Palm Tree (F)	41.230	-98.917	48.397
05:08:06.469	NLDN +CG	41.163	-98.065	
05:08:06.829	NLDN +CG	41.260	-97.997	
05:08:06.948	NLDN +CG	41.306	-98.013	
05:08:07.113	NLDN +CG	41.477	-98.623	
August 18, 1999 5:10:05.705				
	Palm Tree (A)	41.220	-98.977	59.157
	Palm Tree (B)	41.186	-98.987	61.079
	Palm Tree (C)	41.187	-98.940	39.397
	Palm Tree (D)	41.191	-98.966	54.264
05:10:05.598	NLDN +CG	41.254	-99.675	

Table 2.2. Triangulated Palm Tree Locations. Summary of triangulated locations of palm trees, with aircraft locations for 1994 observations included. The location of associated NLDN reported lightning discharges are presented. The multiple triangulations of each palm tree represent different identified features in the event.

During the 1999 sprites campaign two palm tree events were recorded. One palm tree from August 18, 1999 5:10:05 is presented in the lower panel of Figure 2.4. The triangulated top altitudes of the events were at 50.6 km and 59.2 km.

2.3 1995-Equatorial Sprites, Optical Spectroscopy, Elves

Two University of Alaska Fairbanks aircraft campaigns were made during 1995 in order to study sprites outside of the United States. In February 1995, an instrumented aircraft was flown from Peru followed by a second campaign flown out of Costa Rica and Aruba in August. The first spectral observations of sprites were measured by University of Alaska Fairbanks researchers June 22, 1995, quickly confirmed by observations by Lockheed researchers on July 16, 1995. Photometric identification of elves was first made in 1995, and only recently (December 1999) has a discrimination between elves and "sprite halos" been proposed. In the summer of 1995 a sprite observation reporting mechanism was established on the World Wide Web as a link from a description of University of Alaska sprites observations at http://elf.gi.alaska.edu/. Out of the more than 60,000 visitors to the research reporting page, forty observations of sprites or jets have been reported. Some of the reports from the site include descriptions of watching sprites over storms in Arizona for several hours and sprites over storms in Africa. These and other reports are reproduced in Appendix A.

2.3.1 Equatorial Sprites

The original 1993 University of Alaska Fairbanks attempts to observe sprites over South America, one of the three major lightning activity centers of the world, were unsuccessful primarily because of difficulties with flight scheduling. Therefore, in February-March, 1995, an aircraft campaign based out of Lima, Peru was undertaken to provide the UAF researchers control of an aircraft to facilitate investigation of sprites in one of the major thunderstorm regions of the world, the Amazon basin. The Westwind II aircraft previously used during the Sprites'94 campaign was re-outfitted with the Auroral Color Television Project (ACTP) color camera, a wide angle panchromatic camera, the Fogle spectrograph (see Appendix B), and a commercial lightning flash detector. Several logistical difficulties hampered observations efforts (including an active border war between Peru and Equador).

One significant result from the observations of equatorial sprites was the lack of any structure aligned with the geomagnetic field. The equatorial field at 100 km is nearly horizontal, but no 'bending' of the tops of sprites was observed.

During the two week Peru campaign, approximately twenty sprites were observed [Sentman *et al.*, 1995a; Heavner *et al.*, 1995], fewer than had been expected. Several possible reasons for the dearth of observed events have been suggested. First, the logistical support for aircraft observations was less favorable than flights over the United States. Second, the lack of high quality lightning data such as from the National Lightning Detection Network for determining the location of the positive lightning discharges made locating the target thunderstorms more difficult. Third and more speculatively, meteorological differences between the small, strongly convective storms over South American rainforests and the large frontal systems across the midwestern United States may be significant for the production of sprites. Finally, another speculative explanation is the lower levels of pollution over South America may decrease the convection of aerosol particles and decrease the conductivity of the middle atmosphere [Shaw, 1998].

2.3.2 Optical Spectroscopy

In order to determine the source of the red emissions recorded by the color camera operated by the University of Alaska Fairbanks researchers during the 1994 and early 1995 observations, red spectroscopic measurements of sprites were required. Therefore, in the summer of 1995, a two month observational campaign, GASP'95, on Mt. Evans, CO, (see Table 2.1), was proposed to specifically identify the source of the optical emissions from sprites. The Mt. Evans observatory was selected in part because of its high altitude (4.3 km) and the decreased Rayleigh scattering and atmospheric absorption afforded by this high altitude. The Deehr spectrograph, described in Appendix B, was used for red observations (550-850 nm). The first optical spectral observations of sprites were obtained June 19, 1995 and revealed that the primary emissions of sprites are N_2(1PG) [Hampton *et al.*, 1996]. Figure 2.5 shows a typical sprite and spectrum obtained during the GASP'95 mission along with a bore mounted scene camera. The horizontal dashed line on the scene camera in Figure 2.5 (A) indicates the field of view of the slit in front of the spectrograph system. Figure 2.5 (B) presents the measured spectrum. The wavelength of the band-heads

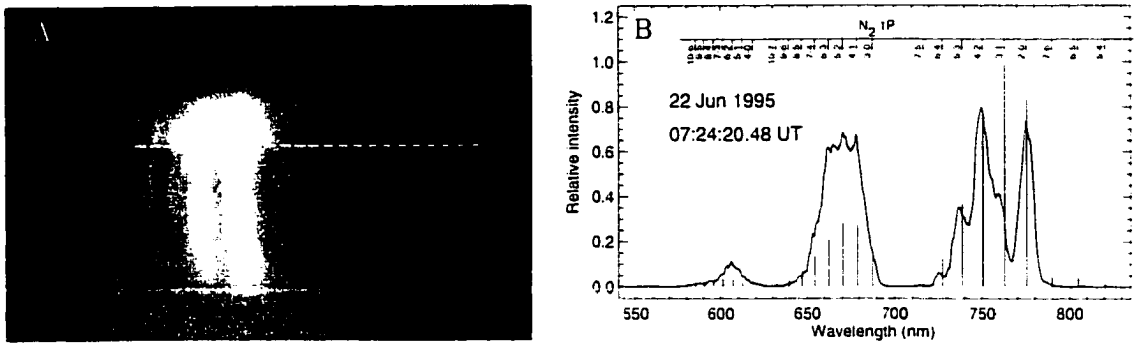

Figure 2.5. Optical Spectra of Sprite. Sprite observed June 19, 1995 7:24:20.48 showing sprite, slit, and spectrum observed. Reproduced from Figures 2 and 3 from Hampton *et al.* [1996]. The dashed line across the scene camera in (A) indicates the field of view of the spectrograph slit. The N_2(1PG) emissions are identified, with the line heights corresponding to observed auroral intensities. The spectrum has not been corrected for atmospheric transmission, as can be seen by the discrepancy in the N_2(1PG)(3-1) intensity at 762 nm, which is due to atmospheric absorption.

of the molecular nitrogen first positive group emissions (N_2(1PG)), with lines showing the relative amplitudes based on observed auroral spectra [Vallance Jones, 1974]. The most obvious difference between the observed sprite spectrum and the auroral amplitudes are the low observed sprite emissions at 762 nm, (from the N_2(1PG)(3-1) transition), which is resonantly absorbed by the (0-0) band of the molecular oxygen atmospheric group. The spectral observations are discussed in greater detail in Chapters 3 and 4. Approximately three weeks later, on the night of July 16, 1995 Mende *et al.* [1995] independently confirmed the identification of the red light from sprites to be N_2(1PG) emissions.

In addition to obtaining the first spectral observations of sprites, the GASP'95 mission also collected higher spatial resolution observations, which in turn allowed a more refined classification of sprites compared to previous studies based on their spatial morphology. The first main classification of sprites based on the GASP'95 observations was the distinction between classic and columniform type sprites [Wescott *et al.*, 1998b]. Columniform sprites (or 'c-sprites') are primarily thin vertical structures, while classic sprites exhibit much more spreading away from the vertical axis at both high and low altitudes. The June 21, 1995 storm over New Mexico produced almost exclusively c-sprites. Typically storms produce a majority of complex classic sprites with a lower percentage of c-sprites. A good example of

the columnar form of the c-sprites is from June 19, 1997 06:35:48 and is shown, along with results of triangulation, in Figure 2.6. By way of comparison, the events in Figures 2.1, 2.2, and 2.4 are all examples of classic sprites. No immediately obvious differences between c-sprite and classic sprite spectra are apparent–both are primarily $N_2(1PG)$ emissions (see Figure 8 of Wescott *et al.* [1998b]). High speed video observations (up to four thousand frames per second) indicate that all sprites begin as c-sprites at onset, and the event may develop more structured forms (Brook *et al.* [1997]; Stanley *et al.* [1999], see also Section 2.5).

Analysis of coordinated ELF and high speed photometer array observations found a slightly different classification of two types of sprites as "columnar" and "carrot" sprites [Reising *et al.*, 1999b]. "Columnar" sprites showed a delay of < 3 ms between the ELF radio atmospheric, and a smaller value of charge transfer within the causative cloud to ground positive flash, while "carrot" sprites have a delay of > 3 ms and a much larger charge transfer in the causative lightning flash [Reising *et al.*, 1999b]. This study was not based on optical morphology, and therefore the 'columnar' sprites do not strictly correspond to the narrow shape of the above mentioned optical c-sprites (as seen in Figure 2.8), and the 'carrot' sprites only roughly correspond to the classic sprites discussed above.

In addition to the first spectral observations of sprites and an initial morphology of sprites, the GASP'95 campaign was able to use observations obtained at Yucca Ridge Field Station in conjunction with the observations from Mt. Evans in order to triangulate observed sprites as part of the post-campaign analysis. Figure 2.6 shows the results of an analysis using dual camera triangulation, include the projection from the top and bottom of each element to the ground. The cross indicates the NLDN reported location of the causative positive lightning discharge, and great circles between the discharge location and each observatory are labeled. The entire sprite event is approximately 50 km wide and roughly centered on the NLDN reported discharge. Sprites are often triangulated to be more than 50 km offset from the location of the discharge as reported by NLDN. The triangulation analysis shows that the individual columns of the sprite do not focus on the +CG discharge, disproving the suggestion that multiple columns focus down to the causative tropospheric lightning discharge [Winckler, 1995].

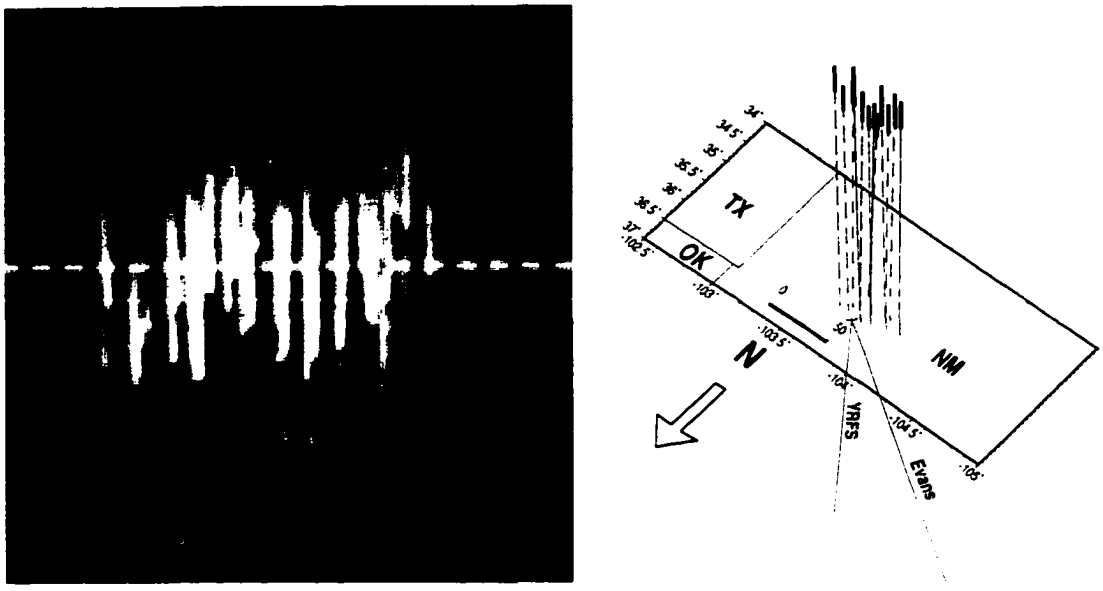

Figure 2.6. Columniform Sprite. Columniform sprite observed June 19, 1995 6:35:48.583 from Mt. Evans. This sprite was also observed from Yucca Ridge Field Station. These two images were used to triangulate the tops and bottoms of the columns. The results of the triangulation are plotted on the map, which is rotated to match the direction of observation.

2.3.3 Elves and "Sprite Halos"

In 1995, researchers at Yucca Ridge Field Station made observations of brief (less than one millisecond) red emissions hypothesized to lie at the base of the ionosphere at altitudes of ~95 km [Fukunishi *et al.*, 1995]. Optical "airglow enhancements" associated with lightning were first reported based on shuttle observations [Boeck *et al.*, 1992] and possibly from sounding rockets [Li *et al.*, 1991]. The phenomena were named elves (Emissions of Light and VLF perturbations due to EMP Sources) [Lyons and Nelson, 1995; Fukunishi *et al.*, 1996]. Observations of elves with the Fly's Eye Instrument [Inan *et al.*, 1997] find that elves occur in relation to the amplitude of the lightning EMP as measured in the VLF frequency range, and estimate single station lateral spatial extent of 200-600 km [Barrington-Leigh and Inan, 1999]. Recent comparison between photometer and high speed imager observations by Barrington-Leigh *et al.* [1999a] has led to the discrimination between elves and "sprite halos."

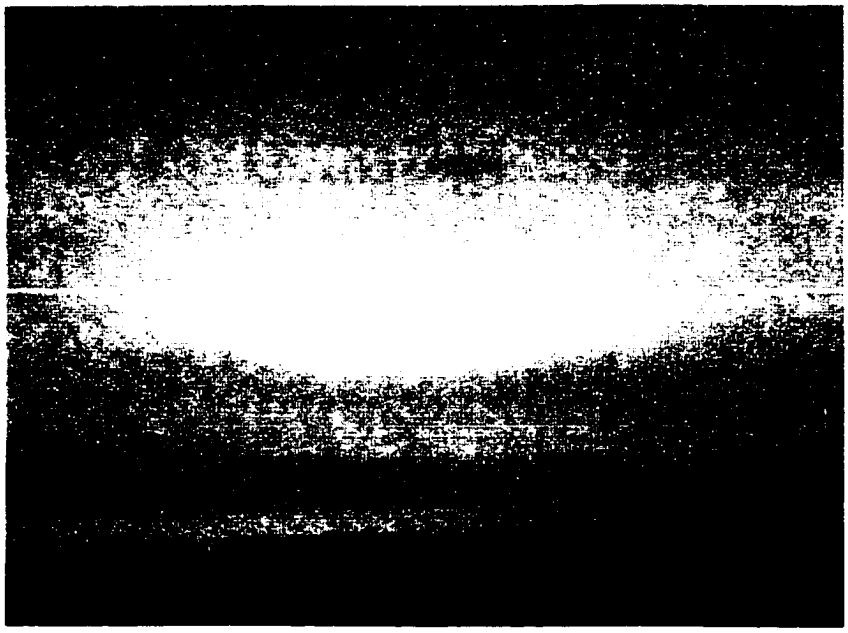

Figure 2.7. Sprite Halo Observation. A "sprite halo" observed from the Wyoming Infrared Observatory at July 28, 1998 5:06:26.303. The associated National Lightning Detection Network reported an 18.0 kA positive lightning flash with a multiplicity of two which occurred at 5:06:26.053 at a great circle distance 762 km from the observatory.

Discussion[5] at the 1999 Fall American Geophysical resulted in the classification of two separate elves-type events. The first type, 'true' elves, are generally not resolvable by video rate imagers. Higher temporal resolution instruments (such as photometers) record these very brief optical emissions. The second type of elves, now called 'sprite halos', may be similar to a sprite, but with no internal structure. Elves are very brief (less than one millisecond) emissions which generally cannot be observed with imaging systems operating at standard video rates of 30 fields per second. "Sprite halos" are morphologically similar to elves, but last between 3-6 ms (D.R. Moudry, personal communications), occur at lower altitudes, and are smaller than elves horizontally. Additionally, halos can be imaged by intensified imagers operating at standard video rates. Initial triangulation results show sprite halos are less than ten kilometers in vertical extent, occur at a mean altitude of 78±4 km with a horizontal diameter of ~65 km [Wescott *et al.*, 1999]. The shuttle observations were

[5]The discussions were primarily between the authors of two adjoining posters: Barrington-Leigh *et al.* [1999a] and Wescott *et al.* [1999].

most likely sprite halos (given that they were observed w/ an instrument operating at 30 frames a second).

An example of a sprite halo observed from the Wyoming Infrared Observatory on July 7, 1996 is presented in Figure 2.7. The National Lightning Detection Network reported an 18.0 kA positive lightning flash with a multiplicity of two which occurred at 5:06:26.053 at a great circle distance 762 km from the observatory. Both elves and sprite halos often precede sprites, but they are also observed without a following sprite. Additionally, while sprites are almost always associated with positive lightning activity, elves occur in association with both positive and negative discharges [Barrington-Leigh and Inan, 1999]. Halos seem to be associated with both positive and negative discharges as well. No spectra of elves have been obtained. Spectral observations of a sprite halo obtained in 1995 identify the optical emissions as primarily $N_2(1PG)$, and are presented in Section 3.6.

2.4 1996–High Spatial Resolution, NIR Spectra, and Blue Sprites

The active thunderstorm of July 24, 1996 provided excellent observations from both Wyoming Infrared Observatory and Yucca Ridge Field Station. Additionally, observers at Langmuir Laboratory made observations of many of the sprites over the same thunderstorm. Nelson [1997] studied this storm using both meteorological and NLDN data in conjunction with video observations of sprites to conclusively find that sprites occur over the anvil region and confirmed the association between sprites and +CG lightning discharges. One sprite from 1996 is presented in Figure 2.8, with multiple camera views of the event. The spectroscopic observations of the event are presented in panel C. Using observations of the same event by Utah State University researchers operating cameras at the Yucca Ridge Field Station, triangulation of various elements in the sprite is possible. The center of the field of view of the camera at Wyoming Infrared Observatory was at an azimuth of 140.737° and an elevation of 9.531°. The features of the sprite triangulated are circled in panel A and the triangulated locations are plotted on a map presented in Figure 2.8 D with a zoom in presented in panel E. The event occurs above the associated positive lightning discharge (indicated by a cross), but often the triangulated sprite occurs as much as 50 km horizon-

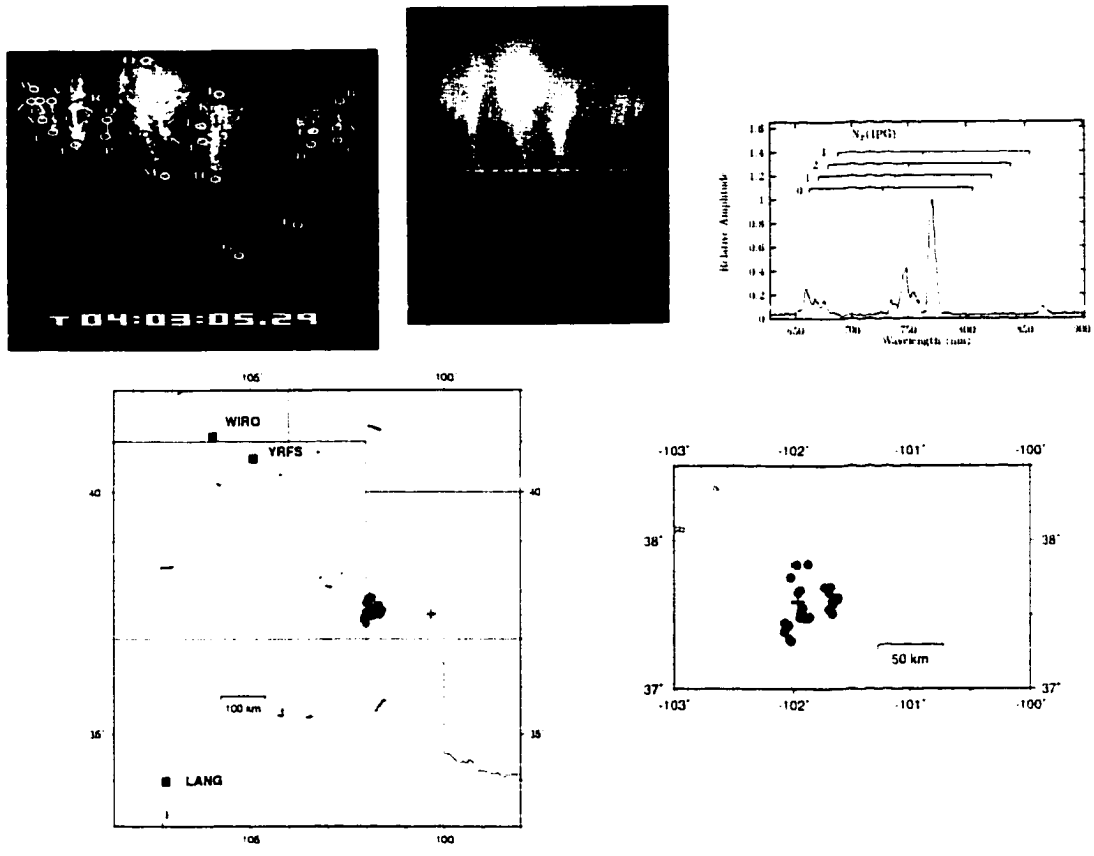

Figure 2.8. July 24, 1996 5:03:05 sprite. The July 24, 1996 4:03:05 event as seen from several cameras. Observations of the event from Yucca Ridge Field Station were used to triangulate the features indicated in the upper left image by circles and letters.

tally offset from the associated lightning discharge as reported by NLDN [Desroschers *et al.*, 1995].

Based on the improved spatial resolution of the 1996 sprite observations, horizontal banding was observed in many sprites [Sentman *et al.*, 1997]. No determination of the cause of the dark horizontal band within sprites has yet been made.

The direct observation of ionized emissions from sprites has been a goal of several narrow filtered imaging and photometric instruments. In 1995, Armstrong *et al.* [1998] used a filter centered at 431.7 nm with a FWHM (full width, half maximum) of 10.6 nm. In 1996, a second filter centered at 399.2 nm with a FWHM of 9.6 nm was used in conjunction with the 431.7 nm filter. Both of these filters include both $N_2^+(1NG)$ and $N_2(2PG)$ emissions

in their bandpass, making definitive observations regarding ionized emissions from sprites difficult. However, the ratio of the two filtered photometers is able to discriminate between lightning, sprites, and elves. The 399.2/431.7 ratio for lightning is 1, in agreement with the expected continuum radiation. For sprites, the 399.2/431.7 ratio is ~2 while elves alone (based on a lower number of observations) give a measured 399.2/431.7 ratio of ~3. The temporal evolution of the ratio of the two filters suggests an initial process with an electron temperature equivalent to ~10 eV (for less than 1 ms) followed by a longer lasting ~1 eV process. Similar observations were made by Suszcynsky *et al.* [1998] who used a 20 nm wide filter centered on 425 nm with a photometer to observe the 427.8 nm $N_2^+(1NG)(0,1)$ emission. However, the filter bandpass also included the lower energy $N_2(2PG)(1,5)$ emission at 426.8 nm as well as several other less intense $N_2(2PG)$ emissions which may have contributed to a portion of the observed signal. A blue filtered camera (response centered at 410 nm with a passband between 350-475 nm) was used in conjunction with the photometer. The important point to note here is that both of these studies indicate the presence of N_2^+ emissions during the initial portion of the sprite.

2.5 1997–High Speed Imagery, Australian Sprites, Blue Sprites

The University of Alaska Fairbanks group did not field any instruments in the summer of 1997. However, several groups made sprites observations at both Yucca Ridge Field Station and Langmuir Laboratories. The blue photometer observations at Yucca Ridge Field Station were continued by Armstrong, Suszynsky and colleagues, and a third filtered photometer (at 470.9 nm) was added to improve the classification of sprites, lightning, and elves through the ratio of the three photometers.

Kodak research loaned New Mexico Tech researchers an intensified camera system capable of recording images at rates of 1000, 2000, or 4000 frames per second. A sprite observed with this system on October 3, 1997 is presented in Figure 2.9. The analysis of the imagery indicates that all sprites initially appear as narrow c-sprites which may or may not then develop into more structured classic sprites [Stanley *et al.*, 1999]. A joint project by the University of Otaga, New Zealand, and Osaka University of Japan achieved the first

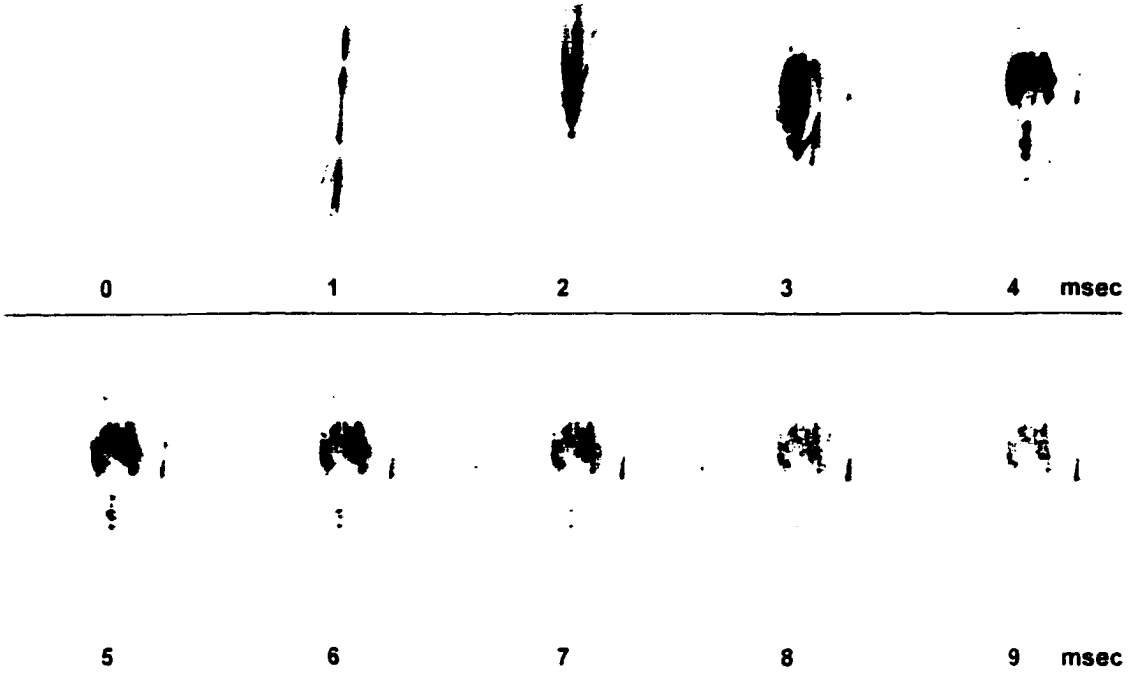

Figure 2.9. The October 3, 1997 8:43:57 sprite recorded by New Mexico Tech researchers using an intensified Kodak camera capable of making 1000, 2000, or 4000 frames per second recordings. Courtesy of Mark Stanley, NMT.

observations of sprites over Australia [Hardman *et al.*, 1998].

2.6 1998–Blue Spectra, NUV Sprites, High Spatial Resolution, Japanese Sprites

EXL98 [Sentman *et al.*, 1998b] was a multi-station aircraft and ground-based observing campaign designed to investigate energy budget effects in the middle and upper atmosphere due to electrical processes excited by lightning. A Gulfstream II aircraft was flown during the moon-down period of July 1998 with instruments from the Geophysical Institute, University of Alaska Fairbanks (GI-UAF), Air Force Phillips Laboratory (AFPL), and the Naval Research Laboratory (NRL). GI-UAF flew several cameras on the aircraft: a wide field of view (about 60°), a panchromatic (400-850 nm) camera for finding sprites, a 14° field of view

panchromatic (400-850 nm) scene camera, a 14° field of view (bore-sighted to the unfiltered narrow FOV camera) filtered (423.8 nm and 427.8 nm) camera, and the ACTP color camera with a variable field of view. A middle infrared (MIR) imager (provided by AFRL) was intended to search for emissions from vibrationally excited CO_2 and NO. An NRL camera was flown, and could be operated in several modes: an unfiltered near-ultraviolet imager, a filtered imager (340.7 nm), and a near-ultraviolet (near-UV, 320-460 nm) spectrograph. NRL also flew a near infrared (NIR) camera was also part of the EXL98 instrumentation.

Specific EXL98 Observations

Several sprites recorded with multiple instruments during the 1998 EXL98 campaign are presented in the following sections. The first example, from July 19, 1998, 9:06:59, is chosen because three bright stars are observed in the 427.8 nm filtered observations. The three stars are used to calibrate counts recorded by the imager with photons received from the stars.

The July 22, 1998 4:57:43 event provides the best example of strong ionized $N_2^+(1NG)$ emissions observed with the 427.8 nm filtered imager. The next example, from July 28, 6:41:01, was observed with the near-UV/blue spectrograph. The lack of ionized emissions indicated from both the 427.8 nm filtered imager and the spectral observations of the sprite are in agreement and indicate that some sprites have very little ionized emissions, while the July 22, 4:57:43 event shows that others have significant ionized emissions.

July 19, 1998 9:06:59

The July 19, 1998 9:06:59 event shown in Figure 2.10 is an example of an event observed in several cameras, including the 427.8 nm filter. The stars ϵ Ursae Majoris, ζ Ursae Majoris, and η Ursae Majoris (the three 'handle' stars of the big dipper) are bright stars observed in the 427.8 nm filtered image which provide good stellar sources. Although these three stars are saturated in the unfiltered camera, many other stars are visible in the unfiltered observations, so that the photon flux of that event can also be calculated for the unfiltered camera. In this section the star calibrations are presented with the 427.8 nm filter to establish an upper limit on optical emissions from the $N_2^+(1NG)$ ionized emission band.

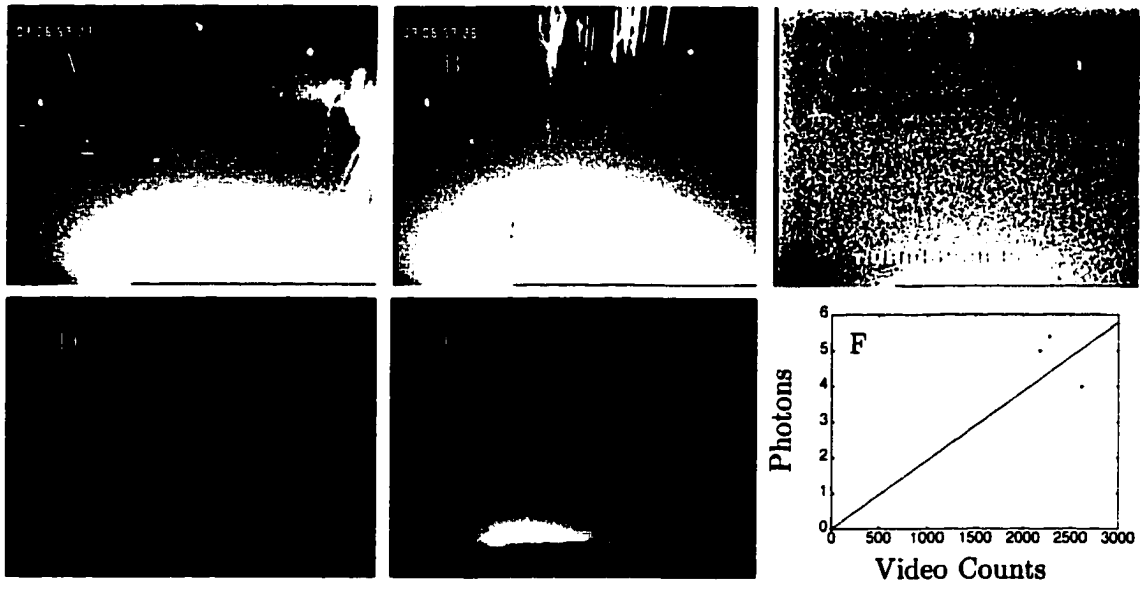

Figure 2.10. The July 19, 1998 9:06:59 sprite as seen from several cameras on the EXL98 aircraft. (A) and (B) are the narrow FOV unfiltered scene camera observations separated by 90 milliseconds. (C) is the 427.8 nm filtered observation (with histogram equalization applied), showing no ionized $N_2^+(1NG)(0\text{-}1)$ band emissions. (D) and (E) are the color camera observations corresponding to (A) and (B). (F) is a plot of photons vs. video counts for the three stars that can be seen in the 427.8 nm imager. Note the associated halo in panel (A).

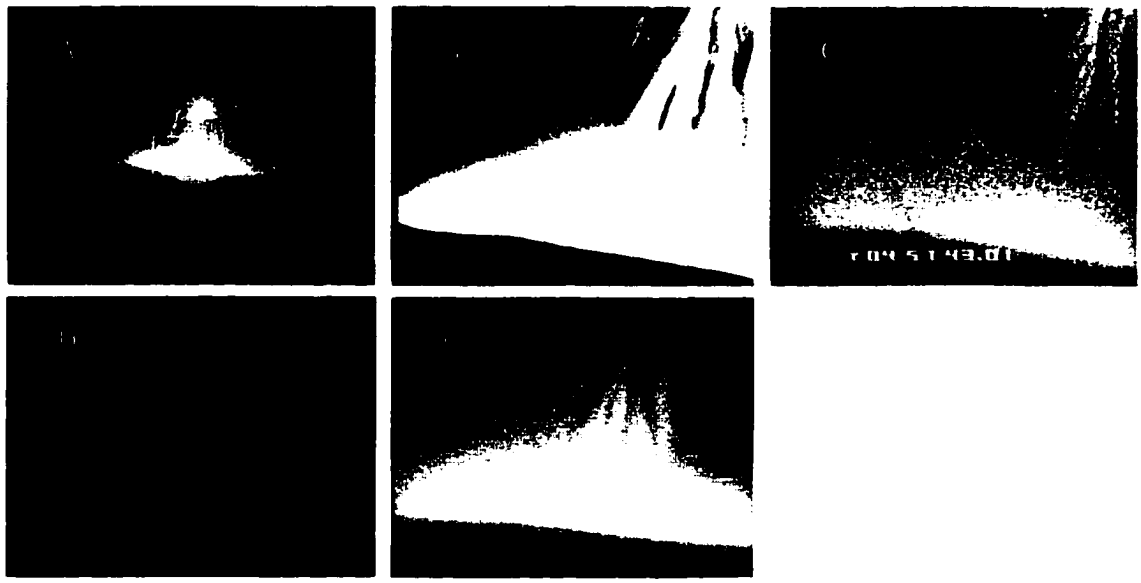

Figure 2.11. The July 22, 1998 4:57:43 sprite as seen from several cameras on the EXL98 aircraft. No other observatory imaged this sprite, so triangulation is not possible. The great circle distance between the NLDN reported positive cloud to ground flash associated with the sprite was 197 km. Note the associated halo in panel A.

July 22, 1998 4:57:43

The July 22, 1998 4:57:43 event presented in Figure 2.11 is the closest observation of sprites from the EXL98 campaign, with a great circle distance between the aircraft and the NLDN reported 39.4 kA positive flash of 197 km. Figure 2.11 (A) shows the panchromatic wide field of view camera image of the sprite, with the small square indicating the field of view of the narrow field camera, (B) is the panchromatic narrow field imager, (C) shows the 427.8 nm filtered camera (with the same field of view as (B)), (C) is the composite image from the ACTP color camera, and (E) is the blue channel of the ACTP color camera. Emissions from the lower region of the sprite are observed in the 427.8 nm filtered imager. Because the sprite is near the upper right corner of the imager, careful analysis was required to confirm that the photons observed are not leakage from the N_2(2PG) 426.8 nm emissions due to the off axis change in filter response. The 427.8 nm filter is a 1.44 nm FWHM filter actually centered at 428.3 nm, specifically selected slightly red of the N_2(2PG) 426.8 nm emissions which would contaminate the filter if it had been centered on 427.8 nm. The

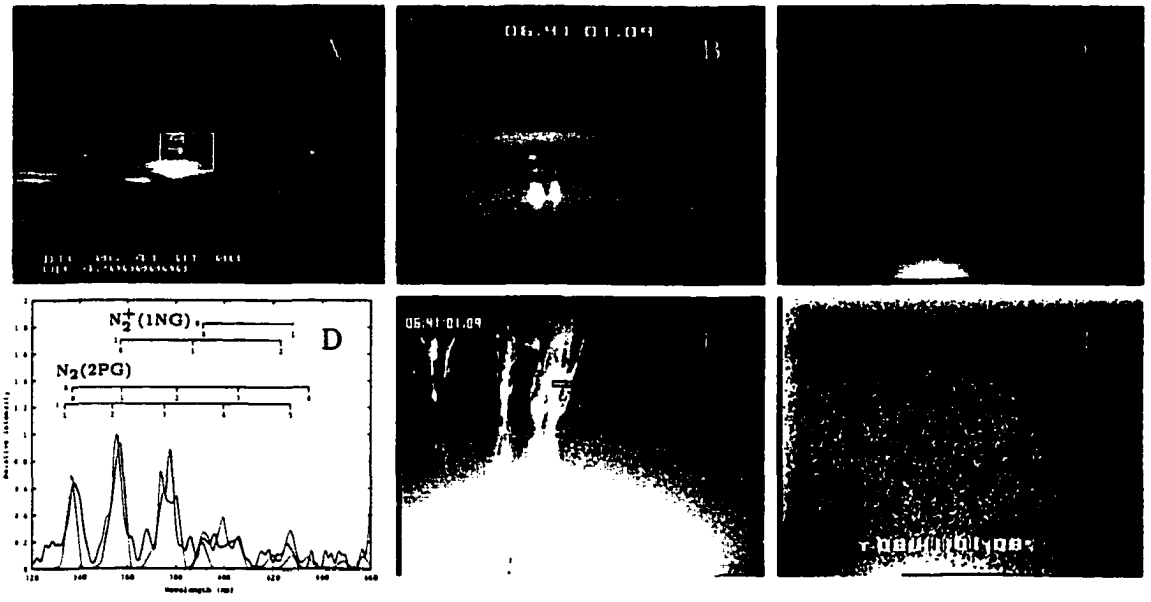

Figure 2.12. The July 28, 1998 6:41:01 sprite as seen from several cameras on the EXL98 aircraft and the broadband camera from the Wyoming Infrared Observatory (WIRO) on Jelm Mountain, Wyoming. (A) is the wide field of view (FOV) unfiltered camera and the square represents the field of view of the other cameras. (B) is the event observed from WIRO. (C) is the color camera observations of the sprite. (D) is the observed spectrum from the near-UV/blue spectrograph. (E) is the unfiltered narrow FOV camera and the black box indicates the near-UV/blue spectrograph field of view. (F) is the 427.8 nm filtered observations, which has been processed with histogram equalization. There is no signature of ionized molecular emissions from this sprite. The observations from (E) and (F) are in agreement about the lack of detectable ionized emissions, and are discussed in more detail in Section 3.5.

426.8 nm leakage issue is covered in more detail in Appendix B. The unfiltered camera image was taken four fields after the event because of image saturation during the event.

July 28, 1998 6:41:01

The sprite from July 28, 1998 6:41:01.278 is shown in Figure 2.12. (A) is the wide field of view camera from the aircraft, (B) is a narrow field of view unfiltered imager at WIRO, and (C) is the color camera observations of the sprite from the aircraft. (D) is the observations from the near-UV spectrograph. After gamma correction and background subtraction of the video image of the near-UV spectrograph output, three video fields were averaged together (for a total time integration of 50 ms), and then the 10 video scan lines over which spectral

information was present were also averaged, to improve the signal-to-noise ratio.. (E) is a panchromatic imager with a 9.3° x 7.0° field of view. The black box is drawn to illustrate the field of view of the near-UV spectrograph. Figure 2.12 (F) is the image from a bore-sighted 427.8 nm filtered imager, with the same 9.3° x 7.0° field of view as the panchromatic imager. The 427.8 nm image has been processed using histogram equalization to stretch the dynamic range of the image. No signature of the sprite is evident in the 427.8 nm image.

The National Lightning Detection Network [Cummins *et al.*, 1998] reported a positive cloud-to-ground lightning flash associated with this event at 36.525° N, -99.016° E occurring at 6:41:01.261 with a multiplicity of 1 and reported current of 37.7 kA. The NLDN-reported discharge was at a great circle distance of 329 km from the EXL98 aircraft. Observations from Jelm Mountain, Wyoming also captured the sprite at an azimuth of 127.9° and a distance of 789 km. Unfortunately, locally cloudy conditions in Wyoming and the large distance between Jelm and the sprite made poor triangulation conditions.

Other EXL98 Campaign Results

A blue starter observed July 17, 1998 during the EXL98 campaign is presented in Figure 2.13 [Deehr *et al.*, 1998]. The left panel is view of the 340.7 nm (a neutral N_2(2PG) emission) filtered observation. The right panel is the unfiltered narrow imager, and the center panel is the 427.8 nm filtered image. The starter is bright in the 427.8 nm filtered camera. This confirms the suggestion of ionized emissions in starters (and likely blue jets as well). Blue jets possibly have the signature of higher total energy processes than either sprites or elves because of the ionized emissions, and blue jets last 10-100 times longer than other phenomena. Wescott *et al.* [1998a] estimate that the average blue jet or starter transfers about 10^9 J of energy to the stratosphere.

In addition to blue emission, jets have been observed in the near-IR during EXL98. These emissions are most likely some combinations of N_2(1PG) and N_2^+ (Meinel). Considering the quenching heights in Table 3.1 N_2(1PG) and N_2^+(Meinel) emission should be strongly quenched. However, energy transfer processes may enhance the population of the lower vibrational level of the N_2(1PG) and N_2^+(Meinel) upper electronic states. Another possibility would be emission from atomic species (O and N) as is observed in lightning. The existence of atomic emissions would indicate a much more energetic process than is

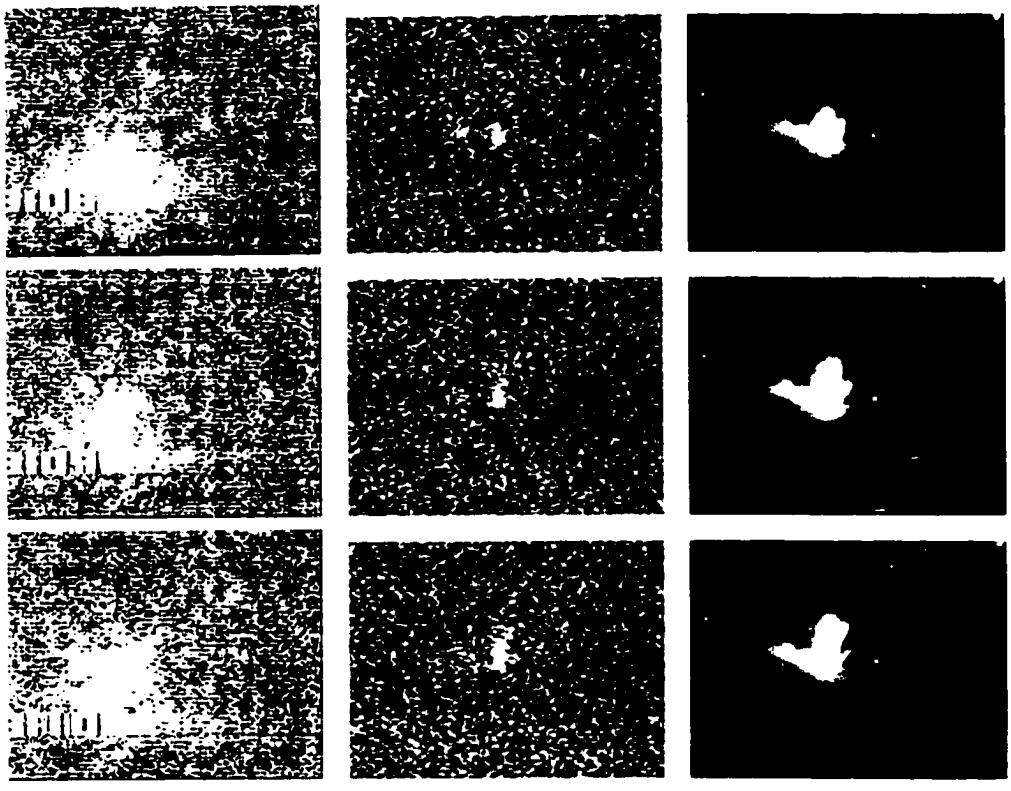

Figure 2.13. Observations of a starter with a 340.7 nm filtered imager (left), 427.8 nm filtered imager (center), and panchromatic imager (right). The 340.7 nm and 427.8 nm images have been histogram equalized. The emissions at 427.8 nm indicate significant ionization in blue starters.

thought to occur in sprites and elves. Spectroscopic observations of blue jets and starters will be required to resolve this issue.

From the Wyoming Infrared Observatory, a photometer was used to observe sprites and two representative results are shown in Figure 2.14. The interpretation of the 7:53:49 event is that a bright, brief transient event (most likely an elves or sprite halo) is followed approximately 20 ms later by a longer lived sprite. The 8:08:34 event does not have the indication of the elves in the photometer record, but shows several events brightening, which may either be a "rebrightening" of a the observed forms, or indication that first one sprite 'turned-on' followed by later sprites. The most intense optical emissions are observed to last for only a millisecond in this event.

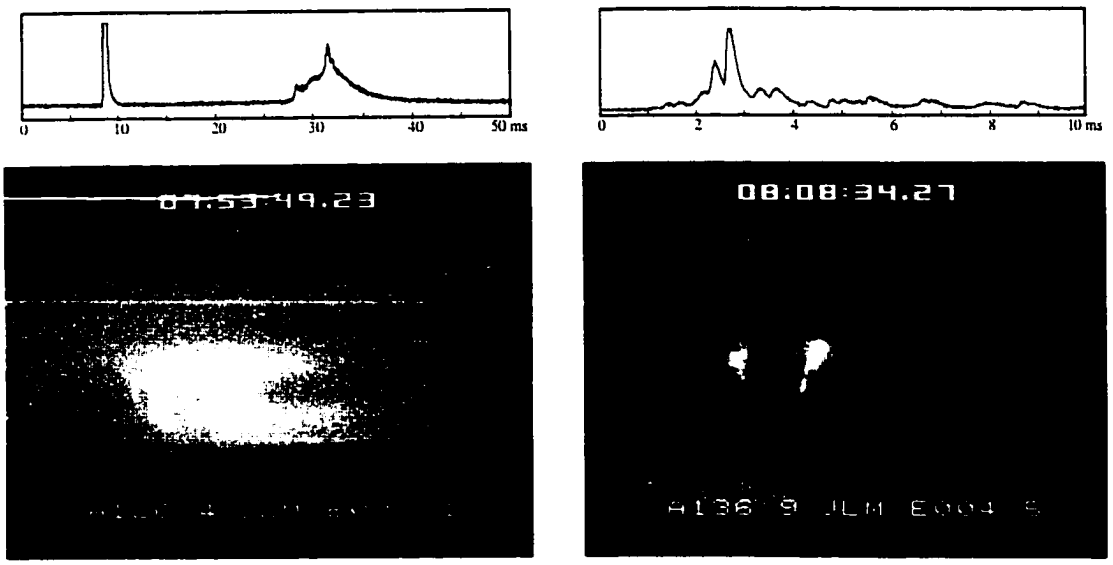

Figure 2.14. Photometer Sprite Observations. Photometer traces recorded at 100 kHz and associated TV images. The two events were recorded at Jelm Mountain, Wyoming, on 28 July 1998 (left) and 31 July 1998 (right). The left photometer sequence covers 50 ms of data while the sequence on the right only covers 10 ms. The corresponding TV images, with 17 ms time integration, show the sprites associated with the traces.

Non-EXL98 observations

In 1998, observations of sprites at Yucca Ridge Field Station continued, including interesting observations of the effects of the Mexican fires on thunderstorms [Lyons *et al.*, 1998]. Thunderstorms in the midwestern United States, spatially associated with smoke from large fires in Mexico, had unusually large percentage of positive cloud-to-ground discharges. No sprites were observed, but Lyons *et al.* [1998] suggested that thunderstorms associated with smoke from large fires may produce more sprites than non-smoke thunderstorms. The possible enhancement of sprites would be significant in regions with common large burns, such as Indonesia and the rain forests of the Amazon region of South America.

At Langmuir Laboratory, the use of a telescope [Gerken *et al.*, 1998; Inan *et al.*, 1998] achieved very high spatial resolution images of sprites, as shown in Figure 2.15. The telescopic imager resolved sprite structure to 6 m resolution. The mean horizontal wind speeds at 30° latitude at an altitude of 65 km is greater than 80 m/s [Kantor and Cole, 1964], so during 1/60 of a second, the neutral motion will be greater than 1.33 m on average. Hence

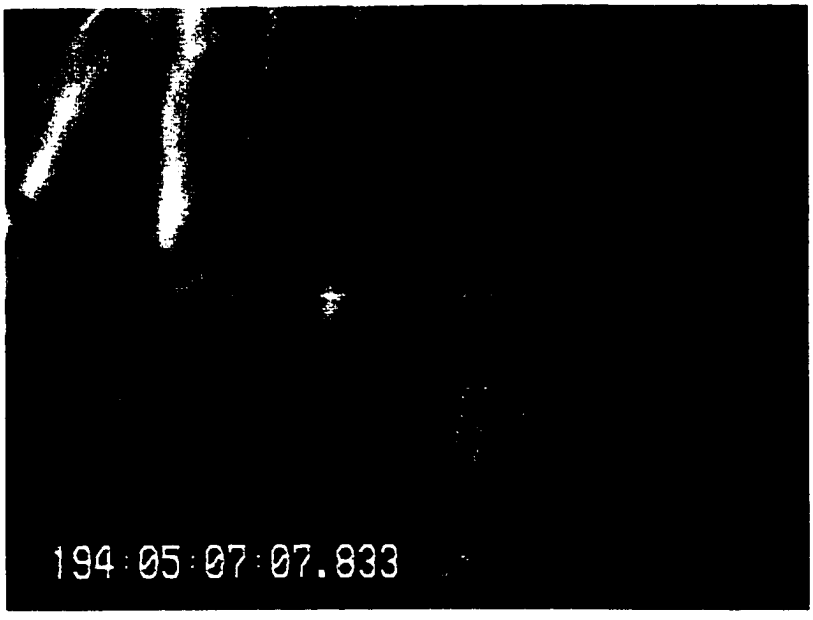

Figure 2.15. Telescopic Sprite Observation. Sprite observed from Langmuir Lab with a telescope system. This sprite was recorded by Stanford University researchers on July 13, 1998 at 05:07:07.833. The great circle distance between the observers and the NLDN identified positive flash was 531 km at an azimuth of 201.9°.

the neutral motion speed may be a smearing factor for high spatial resolution sprite observations with relatively low (video) temporal rates. The high spatial resolution observations resolved spatial structures, such as the vertical branching and horizontal gaps in emissions that were previously only hinted at in some lower resolution sprite observations [Sentman *et al.*, 1996b, 1996a].

An observation campaign by researchers from Tohoku University during December 1998 and January 1999 made the first observations of sprites and elves above winter Japanese thunderstorms [Fukunishi *et al.*, 1999]. Sixteen channel array photometers and CCD cameras operating at Dodaira Astronomical Observatory (36.0° N, 139.2° E) and Sendai (39.3° N, 140.9° E) observed sprites and elves above the Sea of Japan near the Hokuriku region. The meteorology and phenomenology of Japanese winter thunderstorms is quite different from the large midwestern United States thunderstorms above which most sprites have been observed. In general, the freezing level and bottom of the storm are much lower and the percentage of positive lightning discharges is much higher [Takeuti *et al.*, 1978].

The observations of sprites above the Japanese winter thunderstorms on January 25, 1999 were of several c-sprites, which were triangulated from the two locations to have tops and bottoms of 87 km and 73 km respectively. The total vertical extent of thirteen sprites observed above Japanese winter storms was found to be between 8-15 km, similar to the c-sprite altitudes observed over the midwestern United States (Wescott *et al.* [1998b] reported mean bottoms of 76 km and mean tops of 86 km for the event shown in Figure 2.6). The observed elves appeared to have similar spatial and temporal development compared to elves observed above the large midwestern mesoscale convective systems, with horizontal extent between 250-420 km [Fukunishi *et al.*, 1999].

2.7 1999-NASA Sprites Balloon, High Speed Imagery

The 1999 northern hemisphere summer sprites observations were focused on supporting the NASA 1999 sprites balloon campaign [Bering *et al.*, 1999]. The balloon payloads were instrumented by University of Houston researchers with dual three axis electric field detectors, three axis fluxgate and induction magnetometers, X-ray scintillation counter, Geiger-Mueller tube, upward looking high-speed photometer, vertical current density ammeter, conductivity measurements, and an ambient thermometer. The University of Alaska Fairbanks research group operated cameras and other instrumentation at the Wyoming Infrared Observatory and at Bear Mountain, near Custer, South Dakota. The instrumentation included a newly built high speed imager operated at Wyoming Infrared Observatory. The observations of the August 18, 1999 6:25:18 sprite are presented in Figure 2.16. The observations from the high speed (1000 frames per second) imager illustrate that even one thousand frames per second is insufficient to resolve the temporal development of sprites.

Observations from Yucca Ridge Field station in support of the balloon flights included observations from a high speed imager, color video camera, ELF/VLF sensors, and filtered photometers [Lyons *et al.*, 1999]. During the 1999 campaign season, a TVR-900CCD color camera system was added to the array of instruments at YRFS.

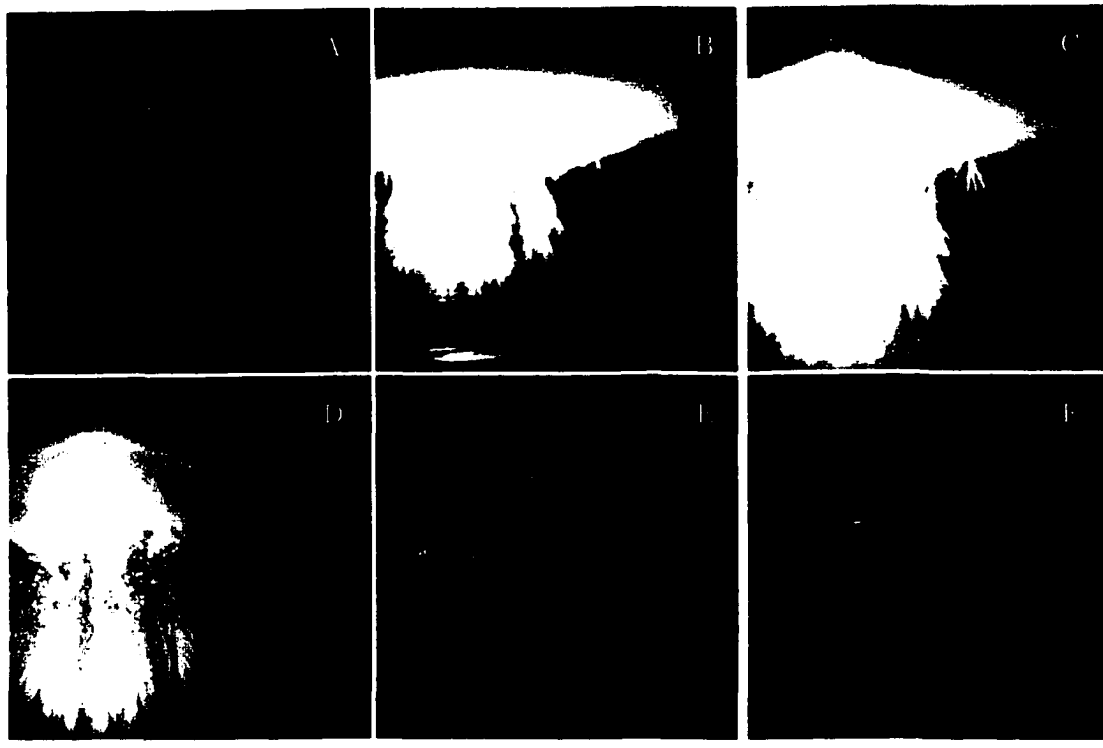

Figure 2.16. High Speed Imagery of August 18, 1999 6:25:18. Observations of the August 18, 1999 6:25:18 sprite using a high speed imager with 1 ms temporal resolution. The camera was operated at Wyoming Infrared Observatory in conjunction with the NASA 1999 sprites balloon campaign. These observations demonstrate that the characteristic time scale for sprite development is less than the 1 ms resolution of the camera. The figures, running temporally A-F, represent 6 ms of observations. Note that a coincident halo is clearly seen beginning in frame B.

2.8 Summary of Observations

The global distribution and rate of occurrence of sprites is very poorly characterized by current observations. Observations over the central United States have shown that sprites occur over virtually every storm possessing positive cloud-to-ground lightning activity. By way of contrast, there was a surprising dearth of sprite activity over South and Central America [Sentman *et al.*, 1995a; Heavner *et al.*, 1995]. 'Airglow enhancements', as first reported from space shuttle observations (probably what are now identified as sprite halos), seem to occur over many sprite-producing thunderstorms associated directly with both pos-

	C-Sprite	Classic Sprite	Palm Tree	Jet	Starter	Elves
Max Alt. (km)	87	95	60	40	25	85
Lightning	Pos	Pos	Pos	Neg	Neg	Both
No. Observed	1000+	10000+	5+	57+	30+	1000+
Duration(ms)	3-10	3-10	<17	~250	~100	<1
ELF/VLF	Yes	Yes	?	?	?	Yes

Table 2.3. Summary of Observations. The types of upper atmospheric flashes and various parameters are presented. Halos have not been included in this table because they were identified so recently (December 1999) that such analysis has not yet been completed.

itive and negative cloud-to-ground lightning discharges [Barrington-Leigh and Inan, 1999]. Blue jets are associated with thunderstorms which are very electrically active and produce large hail or at least have very strong upward convection. The blue starters are apparently blue jets which fail to meet some critical requirement for propagation upward to 40 km [Wescott *et al.*, 1996a]. The palm tree events are of brief duration (like the sprites), but do not reach the terminal altitude associated with sprites. C-sprites are apparently similar to sprites, but show less structure, and possibly a different time delay between the causative lightning flash and the emission onset [Wescott *et al.*, 1998b; Reising *et al.*, 1999b]. Differences in storm conditions, atmospheric conditions, or ionospheric conditions could be determining factors in the appearance of optical transients observed between thunderstorm tops and the ionosphere, leaving much room for both theoretical work and joint studies that cross traditional discipline boundaries.

The observations reported in this chapter are broadly summarized in Table 2.3. Figure 2.17 summarizes the spatial locations of all reported sprite observations to date. Ground based observatories, shown as stars in the lower panel, have a maximum optical sprite detection distance of approximately one thousand kilometers. Observations of sprites from the space shuttle are plotted as squares on the upper map. The Japanese observations and Australian observations are plotted as diamonds on the upper panel. The flight paths of the EXL98 aircraft observations are plotted on the upper global map, while the earlier aircraft observations are plotted on the lower panel map. Table 2.4 summarizes all observational campaigns to date.

In order to approach the questions of global rates and distributions of sprites, elves, halos, and blue jets, more observations are required. The identification of a global synoptic detection method of these events would enhance such measurements. Attempting to estimate the global occurrence of sprites is an elusive problem. The latest estimate of the global cloud to ground lightning flash rate of between $10s^{-1}$ and $14s^{-1}$ [Mackerras *et al.*, 1998]. Positive flashes are less than 10% of the total lightning flashes, and not every positive flash produces an optically detectable sprite. Therefore the global occurrence of sprites can be estimated at less than 1 per second. However, this is based on the assumption that the global sprite distribution is similar to global lightning distribution. While current observations are biased geographically, lightning and sprites do not appear to necessarily have the same spatial distribution. Blue jets are rarely recorded by ground based observers, and even aircraft campaigns record many more sprites than blue jets/starters. However, the dearth of jet observations may be partially explained by Rayleigh scattering and observational difficulties described earlier. The long duration of blue jets and the observation of strong $N_2^+(1NG)$ emissions indicate that blue jets may be an important energetic process in the stratosphere. Elves are associated with both positive and negative cloud-to-ground lightning, so the global elves occurrence rate is probably higher than the global sprite rate.

2.9 Theories of Sprite and Jet Production

Before any documented observations of sprites, several theories postulating thunderstorm effects on the middle and upper atmosphere were advanced. Wilson [1925, 1956], noting that electric field of thunderstorm charge re-arrangement decreases with altitude as r^{-3}, while the breakdown field strength of the atmosphere decreases more rapidly as e^{-r/h_0} (where h_0, the scale height of the neutral atmosphere, is approximately seven kilometers), suggested that thunderstorms may produce heating in the atmosphere. Hoffman [1960] hypothesized that upward discharges from thunderstorms lead to the production of some types of whistler signals. Inan [1990]; Inan *et al.* [1991] proposed modification of VLF propagations due to thunderstorm heating and ionization of the middle and upper atmosphere.

Three separate models have been proposed to describe sprites, which can be differentiated according to the principal features of their respective physical mechanisms: quasi-

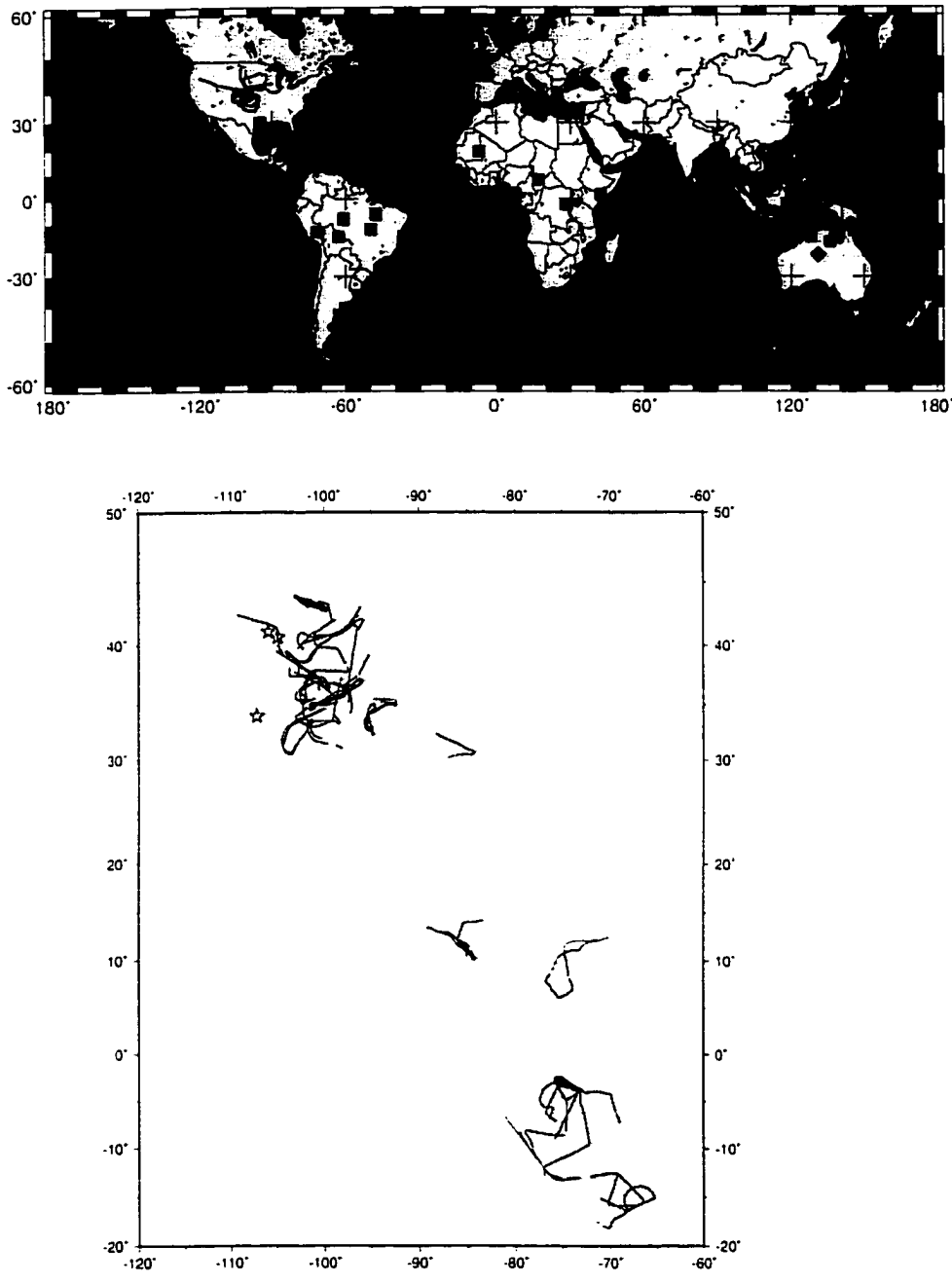

Figure 2.17. Map of Sprite Observations. Maps illustrating the locations of sprite observations. The top panel summarizes the global distribution of observations. The bottom panel shows the aircraft tracks of University of Alaska aircraft campaigns 1994-1998.

Name	Date	Location	Platform	Results
Sprites'93	1993/07	South America, U.S.	Aircraft	Height Est.
SPRITES'93	1993/07	Yucca Ridge	Ground	Sprites
Sprites'94	1994/07	Central U.S.	Aircraft	Triangulation, Jets
SPRITES'94	1994/07	Yucca Ridge	Ground	Sprites
Peru '95	1995/02	South America	Aircraft	Few Sprites
GASP '95	1995/06-07	Mt. Evans	Ground	Specta
SPRITES'95	1995/07	Yucca Ridge	Ground	Sprites
Blue Sand '95	1995/08	Central America	Aircraft	Sprites, Jet
SPRITES'96	1996/07	Yucca Ridge	Ground	Sprites
NMT'96	1996/07	Langmuir	Ground	Sprites
Sprites '96	1996/06-07	WIRO & YRFS	Ground	Triangulation
SPRITES'97	1997/07	Yucca Ridge	Ground	Sprites
SPRITES'98	1998/07	Yucca Ridge	Ground	Sprites
NMT'98	1998/07	Langmuir	Ground	Telescope, Daytime
EXL '98	1998/07	Central U.S.	Aircraft	Blue Spectra, Jet
Balloon '99	1999	Central U.S.	Balloon	6-Axis E-Field

Table 2.4. Major Sprite Campaigns Summary. Sprite observational campaigns from 1993 to the present.

electrostatic heating, or runaway electron mechanisms (see Rowland [1998] for a detailed review). These models all take a tropospheric lightning discharge as the initial energy source, and result in electron impact excitation of middle- and upper-atmospheric molecular nitrogen.

The quasi-electrostatic heating model [Pasko *et al.*, 1998] postulates electric fields that are a result of the reconfiguration of thunderstorm charge due to lightning. A large positive cloud to ground flash removes positive charge from the upper charge center (*e.g.* 300 C removed from 10 km altitude) which produces a large change in the electric field (greater than 100 V/m at 70 km altitude). The field persists for approximately the local relaxation time (milliseconds at 85 km altitude, but seconds at 45 km altitude). The strength of the field is determined by charge moment ($\int qdl$) of the lightning flash. In order to test the

model, experimental determination of charge moment from ELF/VLF (10 Hz - 30 kHz) measurements has been developed [Cummer *et al.*, 1998]. Similar to the quasi-electrostatic model is the EMP induced breakdown model, which includes the addition of an upward propagating EMP associated with a large lightning stroke that can produce breakdown at altitudes above 60 km [Fernsler and Rowland, 1996; Rowland *et al.*, 1995, 1996; Milikh *et al.*, 1995].

The runaway electron model postulates a high energy (relativistic) seed electron (possibly a cosmic ray secondary) accelerated by the electric field above a thunderstorm [Roussel-Dupré *et al.*, 1998; Taranenko and Roussel-Dupré, 1996; Lehtinen *et al.*, 1996]. If the seed electron has enough kinetic energy, a collision between the seed electron and a neutral molecule produces a high energy secondary via impact ionization, resulting in two relativistic electrons. This cascade process is predicted to produce a beam of runaway electrons. Optical emissions produced from this mechanism would have a much higher characteristic energy than the quasi-electrostatic heating model predicts.

Three models based on streamer-type phenomena have been proposed to explain blue jets [Pasko *et al.*, 1997; Sukhorukov and Stubbe, 1998; Yukhimuk *et al.*, 1998a]. Based on modeling efforts, a single jet has been postulated to cause local density perturbations of nitric oxide (10%) and ozone (0.5%) at 30 km altitude [Mishin, 1997].

The optical emissions of sprite halos have been identified as originating from N_2(1PG). Originally, the spectral signature was classified as that of elves, but with the recent distinction between halos and elves, the spectral observations have been properly re-identified as the spectral signature of a sprite halo. The shorter duration of elves and halos suggests that elves are less important energetically than sprites or jets. However, elves may represent the high energy component of lightning discharges transferring energy to the middle atmosphere, only the strongest of which produce optical emissions. Elves have been described by models as heating from the EMP from tropospheric lightning [Inan *et al.*, 1997; Pasko *et al.*, 1998]. Lower energy lightning discharges may not stimulate optical emissions, but the majority of tropospheric lightning discharges can still cause neutral heating in the middle and upper atmosphere. Before the documentation of elves, the neutral heating of the upper atmosphere by lightning was proposed as a mechanism for creating a long-term (hour time scale) infrared glow above thunderstorms [Inan *et al.*, 1991; Picard *et al.*, 1997].

This mechanism describes the vibrational excitation of ground state N_2 by electron impact followed by energy transfer to neutral CO_2 via the process $N_2(X^1\Sigma_g^+)(v>0)\rightarrow CO_2$. Elves are observed to occur above both positive and negative CG's and therefore are likely occur more frequently than sprites.

Chapter 3

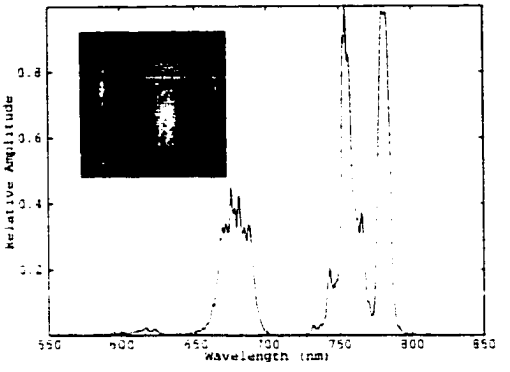

Spectral Observations

The detection of previously unknown optical phenomena of electrical origin in the middle- and upper-atmosphere described in the previous chapter suggests a possible new component to the understanding of middle atmosphere dynamics. In order to determine the signficance of sprites, blue jets, and elves in the terrestrial system, the nature of the energetic processes involved in their creation must first be identified.

Based on 1994 color camera observations, the total optical (395-700 nm) output of sprites has been reported to be 50 kJ[1] [Sentman and Wescott, 1998]. This energy calculation used known stellar sources as absolute calibration references to derive photon fluxes from the sprite. The identification of the source of the optical emissions, as either scattered light from an external source or as volume emissions from the apparent source region itself, is necessary for establishing the processes producing optical emissions. In the first case, the optical energy of the sprites may be of little importance to the middle- and upper-atmosphere. However, in the latter case, sprites provide direct observations of energetic processes occurring in the mesosphere, even though the radiated optical energy represents only a small fraction of the total energy deposited in the middle- and upper-atmosphere. For example, the total photon flux from a rainbow can be much greater than a sprite. However, spectral analysis of the light from a rainbow reveals a solar spectrum, so no local energetic process creates the photons. The light is only from the diffraction of solar light by atmospheric water droplets. One early (incorrect) explanation of elves/halos was that

[1]The brightness of 1-5 kJ in Sentman *et al.* [1995b] is underreported by a factor of 4π.

light from tropospheric lightning was resonantly excitating metallic elements, particularly sodium, which was then re-radiating the light. The strong NII nitrogen lightning emission at 568.0 nm was proposed as a possible candidate for resonant excitation of the 568.2 nm sodium line [Boeck *et al.*, 1992]. Spectral observations of halos identifying molecular nitrogen emissions, rather than atomic emissions, rule out the explanation of resonant excitation via optical emissions from lightning.

The spectrum at the beginning of this chapter is typical of the first sprite spectral observations [Hampton *et al.*, 1996] and is discussed in Section 3.1. These ground based 460-1000 nm spectral observations of sprites identified the molecular nitrogen first positive group (N_2(1PG)) emissions responsible for optical emissions from sprites. The N_2(1PG) corresponds to the lowest energy optical emissions of molecular nitrogen, requiring ~7.5 eV electrons for excitation. Below 90 km altitude, molecular nitrogen is ~80% of the atmosphere and molecular oxygen is almost all of the remaining 20%, so many common atmospheric emissions originate from excited oxygen or nitrogen species [Rees, 1989].

In this chapter, the identification of the optical emission source of sprites is described, followed by a general discussion of the relevant optical emissions of molecular nitrogen and oxygen. Atmospheric transmission is included in the discussion because it is critical for the interpretation of low elevation observations through the dense atmosphere. A comparison between sprite, lightning, St. Elmo's fire, and auroral spectra illustrates the differences in energetic excitation processes leading to optical emissions in the phenomena and the microphysical processes related to the relaxation of the energy.

Optical emissions of the molecular nitrogen first positive group require the lowest energy excitation mechanisms of all optical molecular nitrogen emissions. Other optical molecular nitrogen emissions require higher excitation energy mechanisms, and therefore have been the subject of more recent spectral investigations of sprites. In 1998, the EXL98 aircraft campaign measured the first blue spectral observations (320-460 nm) of emissions from sprites. The dominant emissions across this wavelength band are nitrogen second positive group emissions, requiring almost 11.5 eV electrons for the electron impact excitation of molecular nitrogen. The filtered and spectral observations of ionized molecular nitrogen emissions from sprites requires electron energies >18 eV for electron impact excitation. The spectra of sprite halos are predominantly the nitrogen first positive group emissions,

similar to the red emissions from sprites. Spectral observations of elves and blue jets have not yet been made. Filtered observations of blue jets and starters provide some information about the emissions and are discussed in the Chapter 4.

After describing measurements made to understand the energetic processes associated with sprites, and how the energy of sprites, blue jets, and elves relaxes into the ambient upper atmosphere, this chapter concludes with suggestions of future observations to improve the understanding of the energetic processes producing optical emissions.

3.1 Spectral Observations (550-1000 nm)

Sprite spectral observations from the Womble Observatory and Yucca Ridge Field Station in 1995 spanned the wavelength range 550-840 nm [Mende *et al.*, 1995; Hampton *et al.*, 1996]. Analysis of the observed sprite spectra characterized the source of red sprite emissions to be solely from the first positive group of molecular nitrogen (N_2(1PG)), the lowest energy N_2 optical emissions. The 1995 GASP'95 (Section 2.3) and 1996 sprite observations (Section 2.4) were made with spectrograph systems consisting of optical elements to gather and focus the sprite light, a dispersion grating, and intensified television camera systems to record the signals. Initial processing of the imaged spectrum includes background subtraction using an earlier video field and gamma correction.

The earliest spectral observations of sprites independently identified molecular nitrogen first positive group (N_2(1PG)) as the predominant emission from sprites [Mende *et al.*, 1995; Hampton *et al.*, 1996]. Figure 3.1 is a representative example of a sprite observed June 22, 1995 at 7:10:48 from Mt. Evans, showing both a cropped portion of the scene camera and the measured spectrum. The unfiltered image of approximately 10.7° x 11° image of a sprite is presented on the left portion of the figure. The dashed line indicates the field of view of the slit of the spectrograph. The spectrograph field-of-view intersects the sprite in the 'hair,' so is estimated at an altitude 80 km. Only the portion of the large central sprite is included in the spectrum on the right side of Figure 3.1. The N_2(1PG) and N_2^+ (Meinel) emissions are identified above the spectrum. The horizontal lines indicate emissions originating from the same upper vibration states. The vertical ticks identify the wavelength location of the bandhead for each transition to a lower state vibrational state.

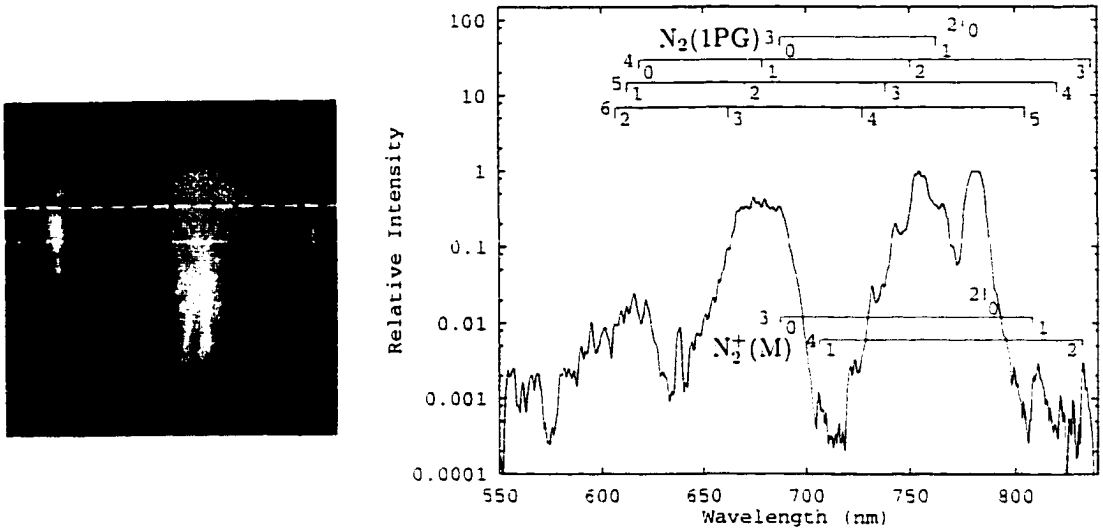

Figure 3.1. Spectral observations of June 22, 1995 7:10:48. The cropped video field showing a 10.7° x 11° field of view is the right panel. The dashed line indicates the field of view of the slit spectrograph system. The spectrum observed from the bright central sprite is shown at left. The location of $N_2(1PG)$ and N_2^+ (Meinel) emissions are identified. The spectrum from this event is shown on a linear scale at the beginning of this chapter.

The spectrum is plotted on a semilogarithmic scale to illustrate the quality of the observations. The peak is more than three orders of magnitude above the background noise. The $N_2(1PG)(2\text{-}0)$[2] band (775 nm) in figure 3.1 is saturated, indicating that the Deehr spectrograph (described in Appendix B) used for these observations could be successfully used for observations with improved time resolution. This observation and all other spectral observations presented in this dissertation are 17 ms resolution as recorded with standard video systems. Photometer observations show temporal evolution in sprite emissions at time scales of less than one millisecond (McHarg *et al.* [1999] see also Figure 2.14).

Spectral observations of sprites were also performed during a second campaign in 1996, operating from Yucca Ridge Field Station and the Wyoming Infrared Observatory. These observations confirmed the identification of the $N_2(1PG)$ emissions that had been made the

[2]Molecular nitrogen transitions which generate optical emissions are between different electronic states. Within both the upper and lower electronic states exist vibrational states. There are several common notations, but as written (2-0) describes that the $N_2(1PG)$ is from an upper state vibrational level 2 to a lower state vibrational level 0. Another equivalent notation is (v'=2, v"=0).

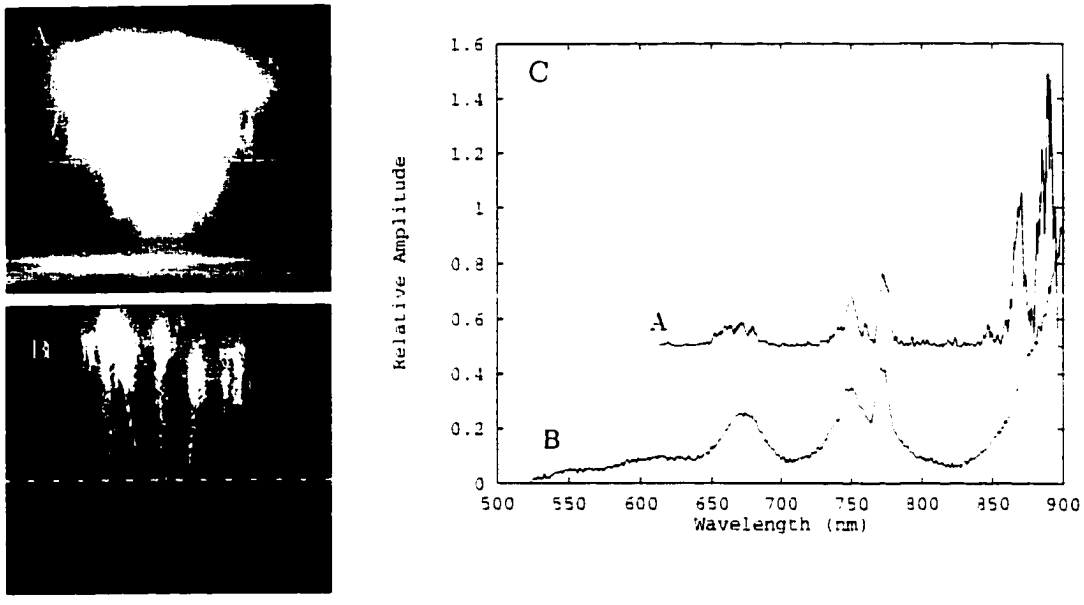

Figure 3.2. July 24, 1996 4:09:19.559 Spectra. Summary of July 24, 1996 4:09:19.559 spectral observations. Two spectrograph systems operating at the Wyoming Infrared Observatory observed the sprite simultaneously. The lower scene camera and spectrum are from ~7 km lower in the sprite. The 1996 events extended the red measurements of sprites to include the $\Delta v = 1$ transitions of N_2(1PG).

previous year. Figure 3.2 shows a representative sprite spectrum from the 1996 campaign. The view recorded by the scene camera bore-mounted with the Deehr spectrograph is Figure 3.2 (A), and the image from the scene camera bore-aligned with the Fogle spectrograph is presented in Figure 3.2 (B). Figure 3.2 (C) shows the observed spectra which have been averaged over several scan lines of the video data.

As discussed in the next sections, the observations that sprite emissions are primarily N_2(1PG) suggest the optical sprite emissions are due to energy processes that are low compared to both lightning and aurora. After the initial observations of a fairly low energy spectral signature from sprites, experimental effort has recently been directed towards measurements of more energetic processes in sprites, jets, and elves (such as by observations of ionized molecular or atomic emissions).

3.2 Optical Atmospheric Emissions

Molecular nitrogen (N_2) is the primary constituent (~78%) of the atmosphere in the stratospheric and mesospheric regions (20-90 km) where blue jets, sprites, and elves occur, with molecular oxygen (O_2) a secondary constituent of the atmosphere across these altitudes, at ~21%. The remaining 1% is predominantly argon, with several other trace gases. Optical spectroscopy of molecular nitrogen involves transitions between vibrational sublevels of different electronic states. Rotational substructure in the vibrational bands also exists, but requires ~.2 nm resolution to observe so is not resolvable with the instruments used to date for spectral observations of sprites.

Potential energy curves of electronic states of a diatomic molecule such as N_2 or O_2 are represented graphically in a Grotrian diagram, which for diatomic molecules is a plot of the potential energy of the electronic states as a function of the internuclear distance. A partial Grotrian diagram of molecular nitrogen, including several electronic states of interest for discussing observed sprite, blue jet, and sprite halo emissions, is in Figure 3.3. (A more comprehensive set of N_2, O_2, N, O, and NO Grotrian diagrams can be found in Appendix 3 of Rees [1989].) The Grotrian diagram in Figure 3.3 was produced using the RKR vibrational levels compiled in Tables 79 and 81 of Lofthus and Krupenie [1977] [see also Gilmore *et al.*, 1992]. The Grotrian diagram illustrates possible electronic transitions which may produce optical emissions if excited. From the relationship $E = hc/\lambda$, optical photons (with wavelengths between 320-1050 nm) are produced by transitions between states with energy differences between 1.18-3.87 eV. The transition probability between two states is determined from the respective wave functions of the upper and lower energy states. The symmetry of the states can be used to determine if transitions are favorable (requiring only electronic dipole transitions) or unfavorable (requiring higher order electronic transitions, or magnetic transitions).

The electronic states of diatomic molecules are enumerated according to the energy level and symmetry of the state [Herzberg, 1989; Harris and Bertolucci, 1989]. For both neutral and ionized molecular nitrogen and oxygen, the electronic excitation levels were originally labelled by capital Roman letters, X, A, B, C, ... with X representing the ground state energy level, A the next energy level above X, *etc.*. After the initial identification, additional

electronic energy states were identified, requiring labelling such as B' and W. The capitalized Greek letter, or term symbol, of the state represents the overall spin angular moment of the molecule about the internuclear axis, and the other symbols represent symmetries or degeneracies of the molecule.

The symmetry of a diatomic molecular state is determined by considering the states of the separated atoms. (For states of molecules with the same two atoms in identical states, see Table 28 of Herzberg [1989]. Terms for identical atoms with electrons in different states are presented in Table 30.) For all diatomic molecular species, the Σ state has a degeneracy (regarding the sign of the total electric moment, M) which splits into two different states (written $\Sigma^{\pm}$). For the case of homonuclear diatomic molecules (with identical atoms: N_2, for example), a degeneracy occurs because of the possible interchange of the two atoms that are in the same state. The u and g symbols indicate the "gerade" or "ungerade" (German for even or odd, respectively) parity of the wavefunction of the state, similar to the atomic notation. For example, given two like atoms with spin ${}^1S_g + {}^1P_u$, the possible molecular states are two ${}^1\Sigma^+$ and two ${}^1\Pi$ states. The parity of the molecular state is based on work by Wigner and Witmer [1928], who show the interaction of the two atoms at small internuclear distances causes the splitting of the states into even and odd symmetry states. So in the above example, the molecule will have states ${}^1\Sigma_g^+$, ${}^1\Sigma_u^+$, ${}^1\Pi_g$, and ${}^1\Pi_u$.

Early studies of optical emissions from excited gases were made using a Geissler tube (glass tube) with a cathode and anode to produce electric fields to accelerate electrons and excite the gas in the tube. N_2, when studied in a Geissler tube, exhibits three distinct bands of colored emission in the tube. Red emissions closest to the cathode were named first positive. Blue emissions near the cathode, but not as close as the first positive, were named second positive. Similar to the cathode, there is a group of blue emissions near the anode, which were called first negative. These and other N_2 optical emissions are discussed in the following sections.

The N_2(1PG) optical emissions from sprites and elves/halos are produced by electron impact of molecular nitrogen similar to the processes that produce auroral emissions [Vallance Jones, 1974] caused by impact excitation of molecular nitrogen in the upper atmosphere by energetic electrons streaming earthward along magnetic field lines. Electron impact excitation is the process by which energetic electrons (e^{-*}) transfer kinetic energy

Name	Upper State	Lower State	Lifetime	Quench Altitude	Quench Particle	Threshold Energy
N_2(1PG)	$N_2(B^3\Pi_g)$	$N_2(A^3\Sigma_u^+)$	6 μs	53 km	N_2	7.50 eV
N_2(2PG)	$N_2(C^3\Pi_u)$	$N_2(B^3\Pi_g)$	50 ns	30 km	O_2	11.18 eV
N_2^+(1NG)	$N_2^+(B^2\Sigma_u^+)$	$N_2^+(X^2\Sigma_g^+)$	70 ns	48 km	N_2, O_2	18.56 eV
N_2^+ (Meinel)	$N_2^+(A^2\Pi_u)$	$N_2^+(X^2\Sigma_g^+)$	14 μs	85-90 km	N_2	16.54 eV
N_2(VK)	$N_2(A^3\Sigma_u^+)$	$N_2(X^1\Sigma_g^+)$	2 s	145 km	O	6.31 eV
O_2^+(1NG)	$O_2^+(b^4\Sigma_g^-)$	$O_2^+(X^2\Pi_g)$	1.2 μs	60 km	N_2	18.2 eV

Table 3.1. Atmospheric Species. Several neutral and ionized N_2 and O_2 optical emissions that are observed in the aurora. The earliest spectral observations of sprites identified N_2(1PG) emissions. which are the lowest threshold energy of the N_2 states that emit optically.

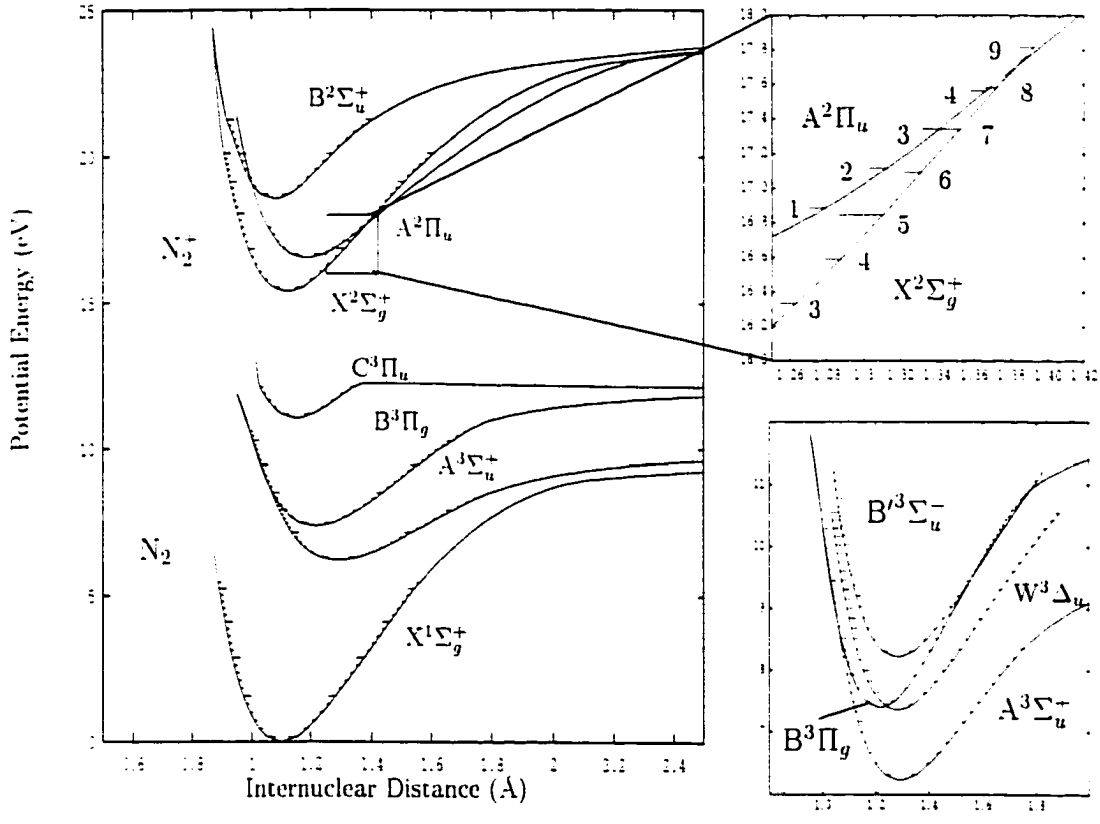

Figure 3.3. Molecular Nitrogen Grotrian Diagram. N_2 Grotrian diagram showing potential energy curves for some electronic states with vibrational levels indicated by horizontal ticks. The expanded section of the Grotrian diagram shows the close overlap in vibrational energy levels of the $N_2^+(X^2\Sigma_g^+)$ and $N_2^+(A^2\Pi_u)$ states, discussed in Section 3.2.3. The expanded section in the lower right shows the $N_2(B'^3\Sigma_u^-)$, $N_2(B^3\Pi_g)$, and $N_2(W^3\Delta_u)$ vibrational potentials discussed in Section 3.2.1.

to another species through collisions. For molecular nitrogen, this process is indicated by

$$e^{-*} + N_2(X^1\Sigma_g^+) \rightarrow e^- + N_2(\gamma), \quad \gamma \equiv A^3\Sigma_u^+, B^3\Pi_g, W^3\Delta_u, C^3\Pi_u, \textit{etc.}$$

A similar process is impact ionization

$$e^{-*} + N_2(X^1\Sigma_g^+) \rightarrow 2e^- + N_2^+(\zeta), \quad \zeta \equiv X^2\Sigma_g^+, A^2\Pi_u, B^2\Sigma_u^+, \textit{etc.}$$

in which the molecular nitrogen is ionized. While the energizing mechanism of electrons which create sprite emissions is different than for the aurora, the common observation of N_2(1PG) emissions in both has permitted the theory of auroral emissions to be applied to sprite observations. Other common auroral emissions that are also associated with electron impact have been the basis for proposed continued spectral observations of sprites.

Several auroral emissions are summarized in Table 3.1 and discussed in the following sections. The upper and lower states of the emissions are electronic states of N_2 and O_2. The threshold energies in Table 3.1 are the energies between the lowest vibrational level of the upper state and the lowest vibrational level of the N_2 ground state[3]. Several transitions of N_2, O_2, and O are not included in Table 3.1 either because they do not lead to optical emissions or are forbidden transitions, leading to long lifetimes, so that the upper state is collisionally deactivated before a photon is emitted. The threshold energies of N_2 are based on Tables 79 and 81 of Lofthus and Krupenie [1977] and the threshold energy value for the excited O_2 state is from Table A4.1 of Rees [1989]. The quenching altitude is the altitude below which more than 50% of the population of upper electronic states are collisionally deactivated before undergoing radiative decay. Significant emissions from a band below the quenching altitude may mean that a large population of the excited upper state exists, or that a process is continually populating the upper state (such as intrasystem collisional transfer [Morrill and Benesch, 1994; Katayama, 1984]).

Observations of a given emission can be characterized in terms of a monoenergetic electron beam with energy sufficient to excite the upper state (*e.g.* the observation of N_2(1PG)(4-2) at 750 nm requires population of the upper state ($B^3\Pi_g$(v=4)) at 8.32 eV above the ground state ($X^1\Sigma_g^+$(v=0)) and therefore requires an 8.32 eV monoenergetic electron beam). The energies of the various N_2 electronic states are used in conjunction with

[3]The peak electron impact excitation cross-section occurs at slightly higher energy [Vallance Jones, 1974].

the observed emissions to determine the energetics of processes associated with sprites, blue jets/blue starters, halos, and elves. State energies are often characterized in terms of monoenergetic electrons as can be measured in the laboratory while physical processes in nature generally have a more complex energy distribution. Two independent steady state models of sprite spectra find a 1 eV Boltzmann electron distribution fits the published spectra [Green *et al.*, 1996; Milikh *et al.*, 1997]. Green *et al.* [1996] suggested that a Druvysteyn distribution (a modified Boltzmann distribution with a high energy tail) is probably more realistic. However, a monoenergetic electron beam energy is convenient for comparisons of the energetic implications of observations of various N_2 electronic states.

The lifetime, τ, of a vibrational state i is $\tau_i = \Sigma_j 1/A_{ij}$ where A_{ij} is Einstein A coefficient [Rybicki and Lightman, 1979], or the transition probability between states i and j per unit time for spontaneous emission of a photon. The summation over j represents all upper states from which the system can relax into lower state i. Several excited states of N_2 have lifetimes of $\sim 10\mu$s or less, so generally emit a photon via spontaneous emission before they are de-energized through collisional processes. The lifetime of an electronic state is generally given as the lifetime of the longest lived vibrational state.

In their collective totality, blue jets, sprites, halos and elves span the altitude range 20-100 km, corresponding to more than 10 atmospheric pressure scale heights. The optical emissions of these phenomena therefore occur over regions of vastly different rates for excitation, optical transmission, and collisional deactivation all of which depend on pressure. For example, $N_2^+(A^2\Pi_u)$, the upper state of the Meinel emissions, has a quenching altitude of 85 km. This means the atmosphere at 85 km is dense enough that the $N_2^+(A^2\Pi_u)$ state is as likely to be collisionally de-activated as it is to radiatively de-activate. The shorter lifetime state $N_2(B^3\Pi_g)$ is significantly quenched at approximately four more atmospheric pressure scale heights below this (at 53 km).

The branching ratio between two transitions from an upper vibrational states to two different lower vibration states must be reflected in the intensity ratio of emissions from the two bands (at the source). For example, an electron in the $B^3\Pi_g$(v=4) vibration level will produce a 750 nm photon when dropping to the $A^3\Sigma_u^+$(v=2) vibration level. The $B^3\Pi_g$(v=4) to $A^3\Sigma_u^+$(v=1) transition results in an emitted 678 nm photon. The branching ratio of these two bands is the ratio of probability of spontaneous emission into each of the

lower states. The Einstein A-coefficients are:

$$\left\langle \Psi(\mathrm{N_2B^3\Pi_g} v=4) \right| r \left| \Psi(\mathrm{N_2A^3\Sigma_u^+} v=2) \right\rangle = 0.836 \times 10^{-5}$$

$$\left\langle \Psi(\mathrm{N_2B^3\Pi_g} v=4) \right| r \left| \Psi(\mathrm{N_2A^3\Sigma_u^+} v=1) \right\rangle = 0.302 \times 10^{-5}$$

The ratio of the Einstein A coefficients is 2.77 so the ratio of the radiated photon flux at 750 nm to 678 nm must also be 2.77. This provides a verification of instrumental and atmospheric transmission corrections.

As indicated earlier, the names "first positive group" (N_2(1PG)) and "second positive group" (N_2(2PG)) given to molecular nitrogen emissions derive from laboratory experiments. However, the emissions are central to the discussion of sprite observations, so the following several sections describe the principal microphysical characteristics of these transition groups.

3.2.1 Molecular Nitrogen First Positive Emissions

The molecular nitrogen first positive group (N_2(1PG)) of electronic transitions produces optical emissions between 575-1187 nm, with brightest emissions between 775-1050 nm [Piper, 1988b]. These N_2(1PG) transitions between the $N_2(B^3\Pi_g)$ and $N_2(A^3\Sigma_u^+)$ electronic states are responsible for the brightest optical emissions observed in sprites [Hampton *et al.*, 1996; Mende *et al.*, 1995]. The lowest vibrational level of $N_2(B^3\Pi_g)$ (the upper state of N_2(1PG)) is 7.5 eV above the ground state $N_2(X^1\Sigma_g^+)$(v=0). Therefore the observation of N_2(1PG) emissions requires electrons with energy of at least 7.5 eV. The most energetic $N_2(B^3\Pi_g)$ vibrational level resolved in sprite spectral observations is from vibrational level 8, requiring 9.09 eV. These energy levels, of a few eV, therefore indicate the characteristic energy of the processes involved in sprite emissions.

Electron impact excitation of molecular nitrogen is believed to be the source of energy for the population of excited vibrational levels of the $B^3\Pi_g$ (upper state of the N_2(1PG) transition) [cf Stanton and St. John, 1969]. However, electron impact is not the only process which can populate the $N_2(B^3\Pi_g)$ vibrational state. The $N_2(B^3\Pi_g)$ vibrational levels overlap the vibrational levels of other N_2 electronic levels, such as $N_2(W^3\Delta_u)$, $N_2(B'^3\Sigma_u^-)$, and upper vibrational levels of $N_2(A^3\Sigma_u^+)$. This close overlap (illustrated in the expanded Grotrian in the lower panel of Figure 3.3) of vibrational states from multiple electronic manifolds can

extend the lifetime of the $N_2(B^3\Pi_g)$ population via intersystem collisional transfer (ICT). ICT is collisional transfer of energy between (for example) the $B^3\Pi_g$ and $W^3\Delta_u$ electronic states. The $W^3\Delta_u \rightarrow X^1\Sigma_g^+$ transition is unfavorable, so the energy remains in an excited $W^3\Delta_u$ state for a longer time period than it would remain in the excited $B^3\Pi_g$ state [Morrill and Benesch, 1996, and references therein]. Both quenching and the intrasystem collisional transfer process becomes more significant as pressure increases, and intrasystem collisional transfer has been suggested to explain the red lower border in aurora [Morrill and Benesch, 1996]. Severe pressure effects at the relatively low altitudes of aircraft (13.83 km in this case) increase the significance of intrasystem collisional transfer, and may be responsible for the high vibrational N_2(1PG) emissions observed from St. Elmo's Fire (see Figure 3.5). Intrasystem collisional transfer rate coefficients reported in Table 2 of Morrill and Benesch [1996] between $B^3\Pi_g(v=8) \leftrightarrow W^3\Delta_u(v=9)$ and $B^3\Pi_g(v=9) \leftrightarrow A^3\Sigma_u^+(v=19)$ are both large relative to the intrasystem collisional transfer rates for other vibrational levels (43.4 and 35.3 10^{-12} cm^3/molecule-s respectively). Therefore a peak in the N_2(1PG) emissions near v=8 is expected from intrasystem collisional transfer, and is measured in the St. Elmo's fire observations discussed in a later section.

The $N_2(B^3\Pi_g)$ state is also populated via cascade from spontaneous emissions from the $N_2(C^3\Pi_u)$ state (this is the N_2(2PG) transition discussed in the next section). Because electron impact $N_2(B^3\Pi_g)$ population is enhanced via both cascade (from $C^3\Pi_u$) and intrasystem collisional transfer (from $W^3\Delta_u$, $A^3\Sigma_u^+$, and $B'^3\Sigma_u^-$), the determination of processes involved with sprite emissions via only N_2(1PG) is complicated. This issue is discussed in the Section 3.7 under future observations, as well as in Chapter 4.

3.2.2 Molecular Nitrogen Second Positive Emissions

The molecular nitrogen second positive group, N_2(2PG) blue emissions, associated with the $N_2(C^3\Pi_u \rightarrow B^3\Pi_g)$ electronic transition, are observed between 268-546 nm [Piper, 1988a; Shemansky *et al.*, 1995]. $C^3\Pi_u$ is the upper state, and is not affected by either cascade or intrasystem collisional transfer populating processes. Ground based observations of N_2(2PG) emissions from sprites are difficult because blue light is strongly Rayleigh scattered by the atmosphere, but some ground based blue observations of three sprites from July 24, 1996 have been reported [Suszcynsky *et al.*, 1998]. These observations are discussed in detail in

Section 4.1.

Although the intrasystem collisional transfer and cascading processes are fairly well understood, these processes do not contribute to populating the $C^3\Pi_u$ state. Therefore the analysis of N_2(2PG) spectral observations to determine N_2 triplet state excitation are simpler than comparable N_2(1PG) and $B^3\Pi_g$ excitation determinations. The energy required to produce N_2(2PG) emissions is greater than 11.1 eV (compared to 7 eV required for N_2(1PG) production), so observations of blue emissions in sprites implies somewhat higher electron excitation energies to produce the emissions.

3.2.3 Ionized Molecular Nitrogen Meinel Emissions

The red N_2^+ (Meinel) emission is due to the electronic transition $N_2^+(A^2\Pi_u \rightarrow X^2\Sigma_g^+)$ and lies between 550-1770 nm. The process of electron impact excitation of $N_2^+(A^2\Pi_u)$ is discussed by Stanton and St. John [1969] and Piper *et al.* [1986]. The quenching altitude for N_2^+ (Meinel) is 85 km [Vallance Jones, 1974; Piper *et al.*, 1985], indicating that at this altitude 50% of the energy in the $N_2^+(A^2\Pi_u)$ state is collisionally lost. The intrasystem collisional transfer processes discussed in Section 3.2.1 occurs between the $N_2^+(A^2\Pi_u)$ and $N_2^+(X^2\Sigma_g^+)$ states in addition to cascading between the two states [Katayama *et al.*, 1980; Morrill and Benesch, 1996]. The upper expanded portion of the Grotrian diagram in Figure 3.3 shows the $N_2^+(X^2\Sigma_g^+)$ and $N_2^+(A^2\Pi_u)$ potential wells and vibrational levels. The $A^2\Pi_u(v = 3)$ and $X^2\Sigma_g^+(v = 7)$ are separated by only 0.00446 eV [Katayama *et al.*, 1980; Katayama, 1984]. The combination of quenching, which may strongly affect observed N_2^+ (Meinel) emissions, and the effects of intrasystem collisional transfer processes extending lifetimes of the upper state, complicate the analysis of N_2^+ (Meinel). Although characterizing the ionizing processes occurring in sprites by measuring N_2^+ (Meinel) observations is complicated by these factors, the observation of weak N_2^+ (Meinel) emissions indicates that some ionization must be occurring.

3.2.4 Ionized Molecular Nitrogen First Negative Emissions

The blue emissions (330.8-586.4 nm) of the ionized molecular nitrogen first negative group (N_2^+(1NG)) are due to the $N_2^+(B^2\Sigma_u^+ \rightarrow X^2\Sigma_g^+)$ electronic transition [Stanton and St. John, 1969; Van Zyl *et al.*, 1983]. The brightest N_2^+(1NG) emission in the visible is the (0-0) band

[Borst and Zipf, 1970], with the band head at 391.4 nm. The second brightest band is the (0-1) vibrational transition at 427.8 nm. The branching ratio of the 391.4 nm to 427.8 nm emissions is 3.28. Detection from low altitudes of the $N_2^+(1NG)$ blue emissions originating in the upper atmosphere is difficult because of Rayleigh scattering between the source region and the observer. In a relationship similar to that of the $N_2(1PG)$ and $N_2(2PG)$ neutral N_2 emissions, the N_2^+ (Meinel) upper state $A^2\Pi_u$ has complicated collisional processes which must be accounted for in analysis, while the $N_2^+(1NG)$ intensity is directly proportional to the amount of ionization [Vallance Jones, 1974].

3.2.5 Atmospheric Transmission

Most sprite observations have been made using ground based instruments (see Chapter 2). Aircraft have been used as observational platforms primarily in order to get above the thickest part of the atmosphere. Some observations from the space shuttle have looked at or very near to the limb of the earth. The ground based, aircraft, and space shuttle observations are all made through the atmosphere at low elevation angles (looking almost horizontally through the atmosphere, rather than vertically up through the atmosphere near zenith, as are most auroral or astronomical observations). Because of the long path length through the dense atmosphere, atmospheric transmission effects must be taken into account in interpreting the spectral observations. One reference model used for atmospheric transmission correction is provided by Guttman [1968]. This model is based on filtered intensity observations at only six wavelengths from only three locations (Valley Forge Pennsylvania, White Sands New Mexico, and Kwajalein island). Much better atmospheric transmission models are available, either MOSART (as reported in this section) or the realistic inclusion of several contributions to the attenuation of light through the atmosphere, as has been done by Milikh *et al.* [1998b].

MOSART, the Moderate Spectral Atmospheric Radiance and Transmittance model, is a local thermodynamic equilibrium model which uses a band approach to radiation transport to calculate low altitude optical backgrounds and transmission in the ultraviolet through microwave spectral region, approximately 0.2-50 microns, at a spectral resolution of 2.0 cm^{-1} combining features of MODTRAN [Berk *et al.*, 1989] and APART [Cornette, 1990]. The radiative transfer model used to calculate atmospheric transmission and path radi-

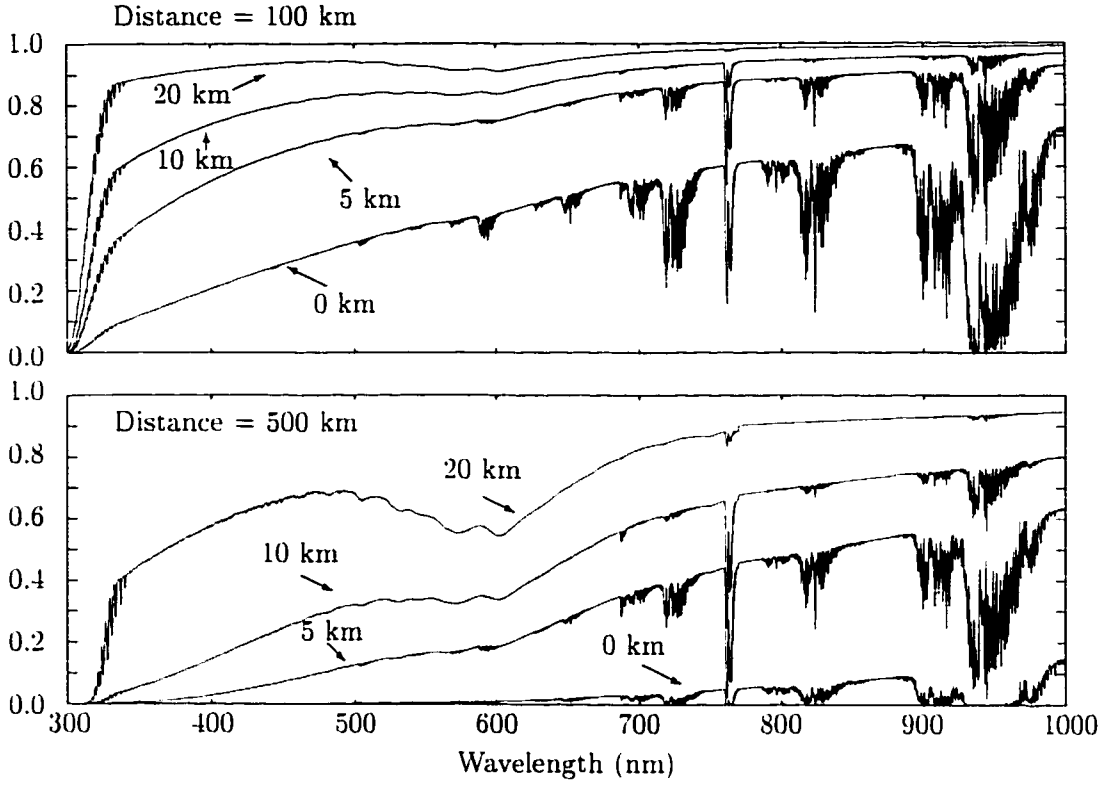

Figure 3.4. Atmospheric Transmission, calculated using MOSART. The upper panel shows an optimistic source observer geometry, with a path length of 100 km for 4 altitudes. The lower panel shows a more realistic source observer geometry, with a path length of 500 km for the same 4 altitudes.

ance is driven by detailed descriptions of atmospheric profiles (i.e., model atmospheres), aerosols, hydrometeors, terrain backgrounds, space backgrounds, and atmospheric turbulence. MOSART contains an extensive set of data bases that describe each of these atmospheric elements. In addition, MOSART incorporates global data bases which provide mean values of these atmospheric elements at any terrestrial location. The MOSART code also contains several global data bases that contain average sets of values for characterizing the environment at any location on the globe.Transmission effects include absorption of light by various atmospheric molecules (O_3, H_2O, OH, CO_2, and O_2).

Figure 3.4 illustrates the nature of Rayleigh scattering and atmospheric absorption for several geometries relelvant to ground and aircraft based observations of sprites. The upper

panel shows a MOSART model [Cornette *et al.*, 1994] output [4] for emissions originating from an altitude of 65 km to observers at four different altitudes (0 km/sea level, 5 km to approximate a tall mountain, 10 km for aircraft, and 20 km for high-altitude aircraft), with a path length between emitter and observer of 100 km. One specific example of atmospheric transmission effects in sprite observations is the O_2 atmospheric band (0,0) absorption at 761.9 nm which overlaps with the N_2(1PG)(3,1) band. The Rayleigh scattering at the blue end of the optical band can be severe, especially for low altitude observers. Only a few sprites have been observed at slant ranges of less than 200 km, and none have been observed at less than 100 km. A more typical source observer geometry is given with an approximate 500 km path length. The atmospheric transmission for this geometry (same four observer altitudes) is shown in the lower panel of Figure 3.4. For a sprite 500 km distant, the atmospheric transmission at 427.8 nm is less than 5% for 5 km altitude observers and ~20% for 10 km aircraft observers. The atmospheric transmission plots illustrate the difficulties of low elevation angle observations through the atmosphere. Two atmospheric transmission profiles from MOSART are included on the instrumental response and atmospheric emission plots in Figure B.1.

3.3 Comparison of Sprite, Auroral, Lightning, and St. Elmo's Fire Spectra

Lightning, aurora, sprites, blue jets, elves, halos, and St. Elmo's fire are all atmospheric electrical phenomena accompanied by optical emissions. A review and comparison of their spectrographic signatures is instructive for the interpretation of sprites spectra. Blue jets have not been observed spectrographically to date, therefore can not be included in this discussion. The spectral observations of halos are discussed separately in Section 3.6 (the sprite halo spectral signatures are similar to sprite observations). The molecular species in Table 3.1 are the sources of several optical emissions in the aurora, and several have also been identified in sprite emissions. Spectral observations of St. Elmo's fire, lightning, aurora, and sprite are all presented in Figure 3.5. The emissions are identified and discussed in detail in the remainder of this section.

[4] The MOSART results presented here are courtesy of Stan Berg and Jeff Morrill, both of NRL.

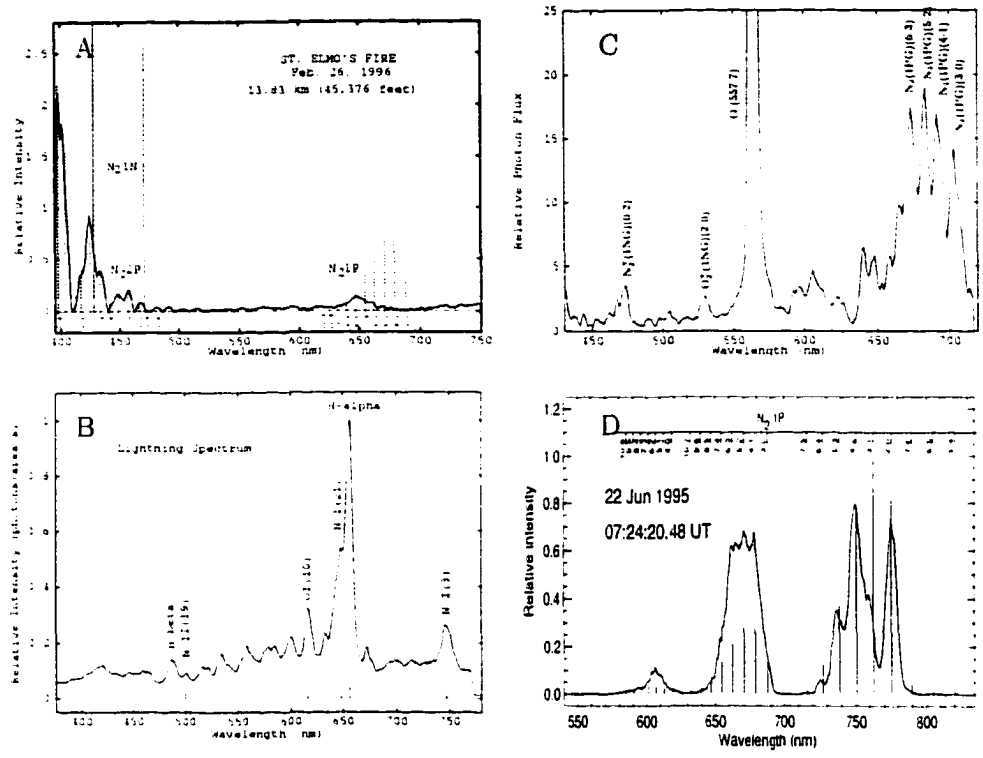

Figure 3.5. Sprite, Lightning, Aurora, St. Elmo's Fire Spectra. Observations of (A) St. Elmo's First spectrum with primarily neutral molecular nitrogen signatures. (B) Lightning spectrum, showing ionized atomic emissions, indicating a higher energy density than St. Elmo's Fire. (C) Auroral spectrum, with signatures of a combination of atomic emissions and both ionized and neutral molecular emissions. (D) an observed sprite spectrum, with only N_2(1PG) emissions observed. (Note that the wavelength scales on the four spectra are different.)

Sprite Spectrum

Sprite N_2(1PG) emissions have been identified in Section 3.1 and discussed in more detail in other sections of this chapter. The sprite spectrum from June 22, 1995 is shown in Figure 3.5 (D) for comparison to the spectral signatures of the other phenomena. Blue spectral observations (340-460 nm) of sprites are primarily N_2(2PG) emissions at video rates. The blue spectral observations of sprites are discussed in Section 3.5.

Auroral Spectrum

The auroral spectrum presented in Figure 3.5 (C) was observed April 6, 1995 at 10:26:45 from Poker Flat, Alaska. The auroral observations were measured with the Deehr spectrograph and is reproduced from Hallinan *et al.* [1997]. Two prominent features are the emissions from molecular N_2(1PG) and strong atomic oxygen emissions at 557.7 nm. The N_2^+(1NG)(0-2) emissions at 470.9 nm indicate stronger ionization than is observed from sprites. The N_2^+ (Meinel) emissions are observed in most auroral spectra, but this example is from the lowest regions of optical emissions from the aurora, so N_2^+ (Meinel) emissions are strongly quenched. The N_2^+ (Meinel) emissions observed in most auroral spectra are missing from most sprite spectral observations, but it is not a priori clear if the upper state of the N_2^+ (Meinel) transition are excited and quenched, or is not excited at all. The interpretation of spectral signatures of the aurora in Vallance Jones [1974] provided the motivation for the analysis of sprite spectra.

Comparing emissions in the lowest auroral regions and the upper portions of sprites shows that the excitation mechnisms in aurorae is higher energy than the sprite excitation mechnism. The presence of atomic emissions in the auroral spectrum indicates higher energy processes occurring in the aurora than in sprites because more energetic electrons are required to dissociate the molecular gases of the atmosphere. The 630.0 nm emission is due to the $O(^1D) \rightarrow O(^3P)$ transition. This is a forbidden transition with a long lifetime of 110 seconds. The atomic oxygen transition (the oxygen 'red line') was first observed in the aurora, where low densities allow long lived upper states to exist for sufficient time to radiatively emit photons via spontaneous emission. However, the 630.0 nm emissions are not observed in the auroral spectrum presented in Figure 3.5, because it is from the lower hem of an auroral arc. The 557.7 nm emission, the atomic oxygen 'green line' from the $O(^1S) \rightarrow O(^1D)$ transition, has a much shorter radiative lifetime of 0.74 s and is the most prominent emission in the observed auroral spectrum.

Lightning Spectrum

Lightning is a relatively high energy tropospheric phenomenon where N_2, O_2, and H_2O are dissociated into atomic constituents, which are then ionized, emit photons, and finally re-

combine. A spectrum of lightning emissions that was observed with the Fogle spectrograph (described in Appendix B) during the 1995 South America Sprite Campaign is shown for comparison in Figure 3.5 (B). The spectral signature is predominantly from atomic electronic transitions. The atomic species are produced by the dissociation of molecular species present in the atmosphere. The strong H_α emissions present in lightning are a signature of high temperatures (30,000 K) occurring in the discharge process. Much higher energy processes are required to explain the observed optical spectrum of lightning compared to aurora, sprites, or St. Elmo's fire. However, the physical dimension of lightning is much smaller than the other phenomena: lightning has a diameter of ~10 cm, while the horizontal extent of large sprite events can be ~50 km. Vertically, lightning can be tortuous and does not normally extend above the tropopause (below 20 km) while sprites span 70 km vertically. An excellent review of lightning spectroscopy is found in Chapter 5 of Uman [1994] and several detailed examples of spectral observations of lightning are presented by Salanave [1980]. Lightning spectral emissions are not discussed in detail in this dissertation because no atomic emissions have been observed in sprites.[5]

Comparing lightning and auroral spectra requires consideration of the atmospheric region in which each phenomenon occurs. Lightning occurs in the dense troposphere dominated by molecules, while the aurora in the thermosphere is at many orders of magnitude lower density. The lower auroral altitudes are in a region of mixed atomic and molecular species, while the higher auroral altitudes are regions dominated by atomic species. The lower altitude auroral spectra have the signature of a lower energy density process than lightning spectra because the lightning emissions show primarily atomic emissions, while the auroral observations include both molecular and atomic emissions. The processes in lightning leading to atomic optical emissions require more energy because the tropospheric molecular species must first be dissociated, while auroral atomic emissions come from both dissociation of molecular species and excitation of thermospheric atomic species.

[5]Observations of starters by a NIR imager during the EXL98 aircraft campaign, with no signature in the red channel of the color camera, may be indication of atomic emissions in blue jets and starters. This is discussed in more detail in Section 2.6.

St. Elmo's Fire Spectrum

During the 1995 aircraft sprite campaign in South America (Section 2.3) the aircraft flew into clouds for several minutes and the pilot and researchers observed St. Elmo's as a visible glow forward of the wing tips and the nose of the aircraft [Wescott *et al.*, 1996b]. The video cameras and Fogle spectrograph were recording observations during the St. Elmo's fire. The Fogle spectrograph was on the plane for sprite observations and captured the spectrum of St. Elmo's fire between 400-750 nm, which is presented in Figure 3.5 (A). The color camera on board the aircraft recorded the glow as predominantly blue, in agreement with the spectral observations indicating N_2(2PG) emissions. N_2(1PG) emissions from transitions originating in the high vibrational levels can be explained by strong intrasystem collisional transfer of energy between triplet states of N_2 (discussed in Section 3.2.1). The lack of atomic oxygen, nitrogen, and hydrogen emissions indicates that St. Elmo's fire has a lower energy density than lightning.

The comparison of sprite, auroral, lightning, and St. Elmo's fire spectra illustrates the usefulness of spectral observations for parameterizing the energetics of processes leading to the optical emissions. The lightning spectral signature is characteristic of energetic processes, while the auroral emissions are not as energetic, and the sprite emissions are spectroscopically of even lower energy. The importance of the collisional effects (which increase with increasing density) and the effects of atmospheric transmission are both evident in observed spectra of the four phenomena.

3.4 Variability of Observed Spectra

In their totality, blue jets, elves, and sprites span approximately ten pressure scale heights (20-90 km) and the quenching altitudes of all of the molecular nitrogen emissions discussed in Section 3.2. Variations in the spectral signature of sprites as a function of altitude may therefore be expected. The color camera observations of sprites obtained in 1994 detected blue emissions at low altitudes (below $\leq$50 km) and red emissions at middle and upper altitudes ($\sim$50-90 km). The optical spectrum depends on several parameters that may vary significantly over the altitude range where sprites occur, or between thunderstorms. For example, (A) Sprites, blue jets, and elves are directly associated with underlying tropo-

spheric lightning discharges, so variations between lightning discharges may lead to associated changes in the spatial structure and spectral signature of sprites. (B) The total optical brightness of a sprite may be related to the total energy associated with the event, and therefore the energy of the spectral observation (determined by higher vibrational level population within the $N_2(1PG)$ band, or by higher energy emissions such as N_2^+ (Meinel) or $N_2^+(1NG)$). (C) Proposed long-term (hour time scale) heating of the middle atmosphere above thunderstorms [Picard *et al.*, 1997] would change the $N_2(X^1\Sigma_g^+)$ vibrational population, leading to changes in the $N_2(B^3\Pi_g)$ vibrational distribution following electron impact. This would result in a change in the observed the first positive band distribution, leading to a spectral variation on hour time scales observed with storm development. (D) Spectral variability observed between sprites observed over different thunderstorms may be due to ambient conductivity differences of the middle atmosphere or possibly even differences in ionospheric conditions.

Section 4.2.5 of Vallance Jones [1974] discusses variations of auroral spectra, and classifies the differences as follows: simple height effects, simple energy spectrum effects, and complex energy spectrum effects. Quenching effects correspond to the auroral 'simple height effects,' and spectral variations correlated with changes in lightning are similar to auroral 'simple energy spectrum effects.' A study based on the set of 1995 spectral observations examined variations of the observed $N_2(4-2)/N_2(2-0)$ intensity ratio [Heavner *et al.*, 1996]. This ratio is the ratio of the two most prominent features in a sprite spectrum. The correlation of the spectral variability with any of the above factors (A-D) was inconclusive. The variability observed and suggestions for future studies attempting to correlate spectral variations with above mentioned parameters are presented in this section.

Figure 3.6 illustrates an enhancement in the $N_2(B^3\Pi_g)(v'=4)$ state with an increase in altitude. This is seen as increased intensity, relative to the rest of the $N_2(1PG)$ emissions, at the $N_2(1PG)(4-2)$ (750 nm) and $N_2(1PG)(4-1)$ (678 nm) emissions. The sprites were observed from Jelm Mountain, WY, on July 22, 1996. The upper image and spectrum in Figure 3.6 (A) were recorded at 5:55:09.142. The slit FOV was at the top of the sprite and the estimated altitude of the spectral observations is 85 km. Because this is near the quenching altitude of N_2^+ (Meinel) emissions, the lack of significant N_2^+ (Meinel) emissions is curious. The increase in upper vibrational levels indicates possible higher energy excitation

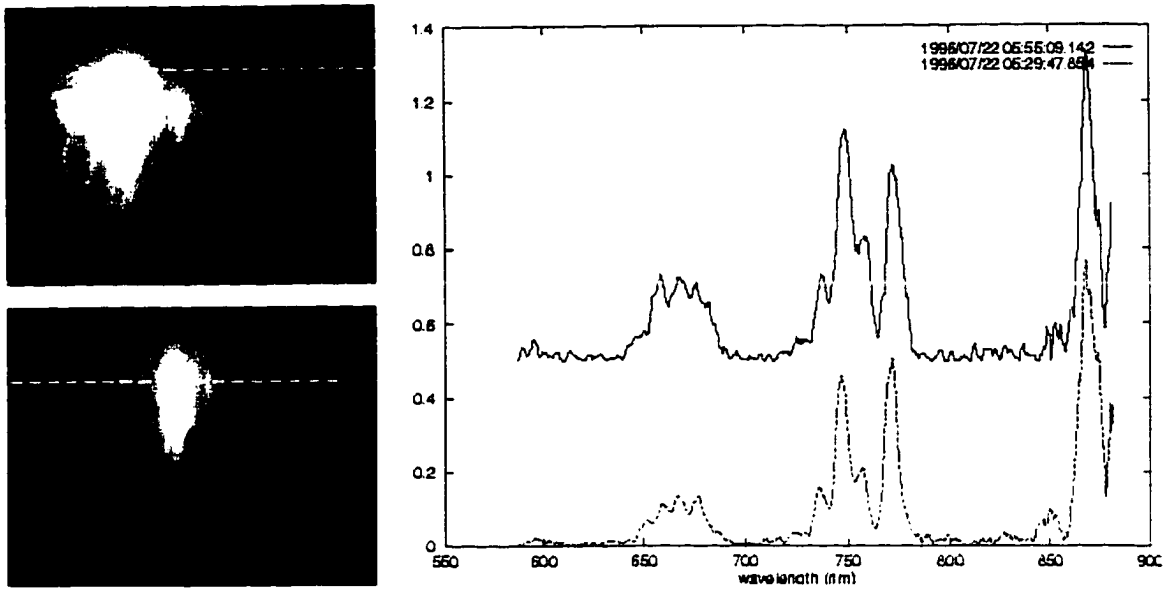

Figure 3.6. Spectral Variations with Altitude. The scene camera and processed spectral observations from two events, July 22, 1996 5:55:09.142 and July 22, 1996 5:29:47.854, are shown. Events from the same night were chosen in order to minimize changes in the intervening atmospheric composition, so that atmospheric corrections can be safely ignored when intercomparing two different events. The spectrograph slit was looking at approximately 85 km altitude in the sprite for the 5:29:47 event, while for the 5:55:09 the slit is at a lower altitude of approximately 75 km.

processes, but the lack of N_2^+ (Meinel) emissions indicates that it cannot be too much higher. This issue is discussed in more detail in the Chapter 4. Presented in Figure 3.6 (B), the 5:29:47.854 event, the spectrograph is looking at an altitude of approximately 78 km. The emissions from the higher vibrational levels of the N_2(1PG) are not elevated as in the 5:55:09.142 spectrum. The quality of these observations is similar to the event presented in Figure 3.1, with a similarly good signal-to-noise ratio. The coincident increase in the N_2(1PG)(4-1) emissions in conjunction with the N_2(1PG)(4-2) emissions adds confidence in this observation, because the branching ratio of these two states must agree with the intensity ratio of the emissions.

Figure 3.7 illustrates a change in the $N_2(B^3\Pi_g)$ vibrational distribution as a function of total sprite brightness. The sprites were both observed from Mt. Evans on June 22, 1995. The black vertical lines on the images from the scene camera indicate the regions of the

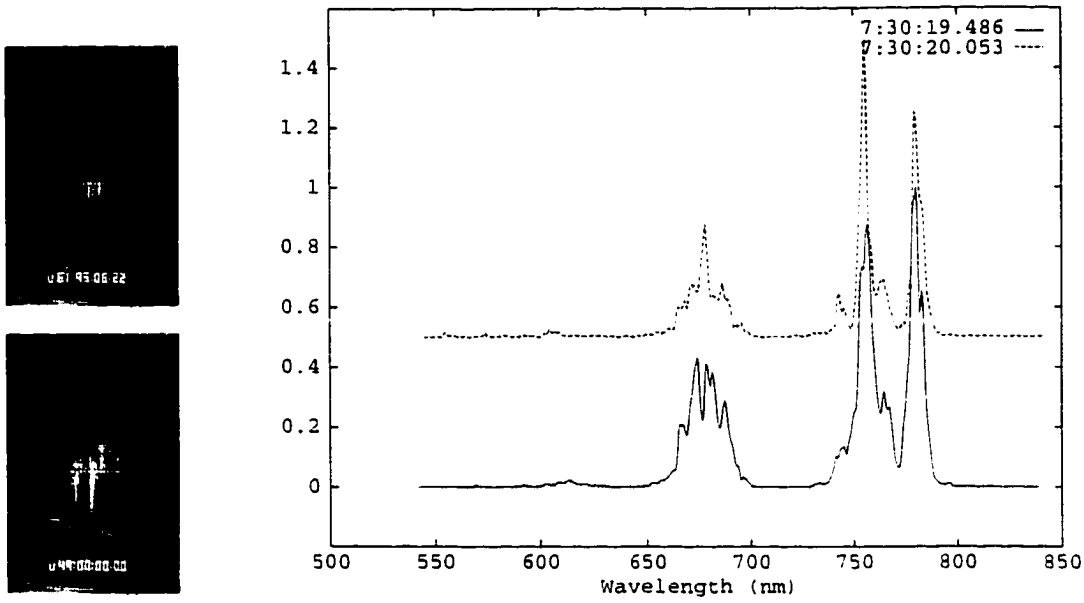

Figure 3.7. Spectral Variations with Brightness. Spectral observations from June 22, 1995 7:30:19.486 and a second sprite 467 ms later. These two events were chosen to minimize the effect of any parameters other than the total optical output of the sprite.

slit used to produce the spectra presented. Only one NLDN positive CG flash is reported at the time of both sprites. This illustrates the coarse nature of the NLDN data, and one difficulty in correlating spectral variations with NLDN reported properties of the lightning discharge. The overall brightness of the 7:30:19.486 event is greater than the 7:30:20.053 event and there is a corresponding pronounced enhancement in the higher vibrational bands ($N_2(1PG)(4-1)$, $N_2(1PG)(3-2)$, and $N_2(1PG)(4-2)$). This example shows increased upper vibrational population, and therefore slightly more energetic processes, correlated with more intense optical emissions.

The two comparisons of spectra presented are examples of the variability exhibited in optical spectrum associated with sprites. Understanding the variability observed in sprite emissions is critical for modeling the processes at work in sprites. Milikh *et al.* [1998b] propose a model that allows the evaluation of the electric field associated with the causative lightning discharge. Pasko [1996] discusses the effect of different lightning discharge characteristics (*e.g.* time scale of charge removal) and the effect on optical emissions. The proposed models are discussed in relationship to the observed variations in Chapter 4. The effects of

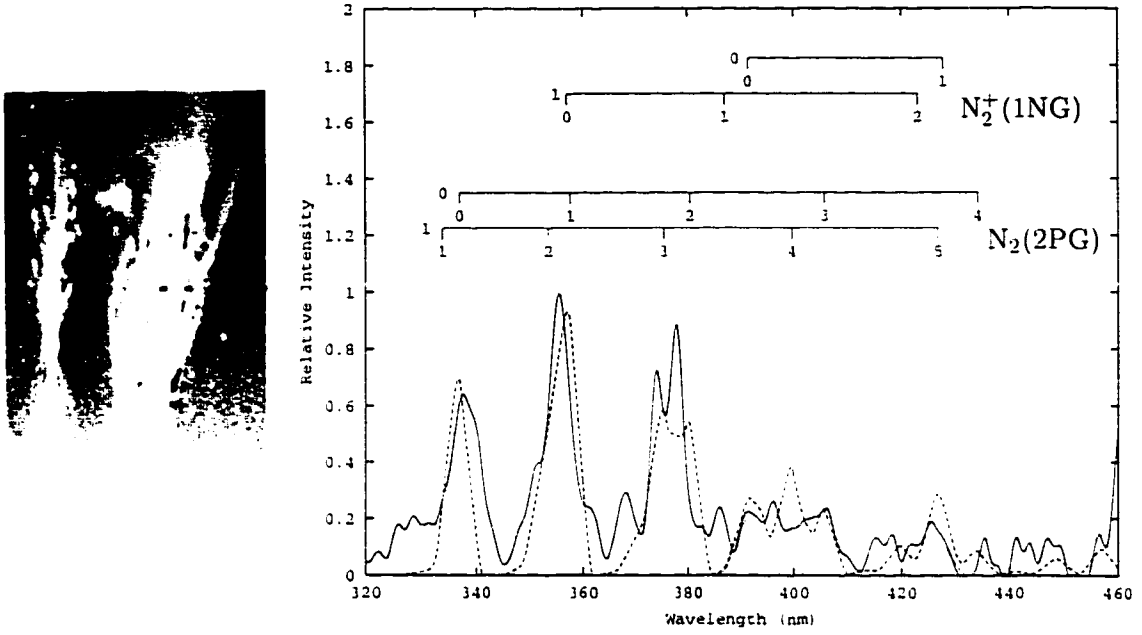

Figure 3.8. Blue Spectrum of July 28, 1998 Sprite. The spectrum recorded from the EXL98 aircraft using NRL's near-UV/Blue spectrograph on July 28, 1998 at 6:41:01.278. The observed spectrum is the solid line. The dashed line is the synthetic fit to the observations using methods described in Section 4.1. The dashed line shows the total fit including both neutral $N_2(2PG)$ and ionized $N_2^+(1NG)$. The ionized contribution to the fit is shown as a dotted line (primarily near the 391.4 nm and 427.8 nm bands). The signal-to-noise ratio of these observations is approximately 5. The broadband image of the sprite is shown at left with a black dashed line indicating the field of view of the slit spectrograph. The 427.8 nm imager data is shown in Figure 2.12. The imager detected no 427.8 nm emissions, agreeing with the lack of any such signature in the spectral observations.

intrasystem collisional transfer should increase with pressure (and therefore become more important at the lower altitudes of sprites). The analysis of observed sprite spectra, which span several pressure scale heights, provides a natural setting for testing theoretical and laboratory understanding of molecular nitrogen.

3.5 Spectral Observations (340-460 nm)

Because of the severe quenching expected for the red N_2^+ (Meinel) emissions at sprite, blue jet, and elves altitudes, optical observations of ionized molecular N_2 must be studied in the

blue. The N_2(2PG) and N_2^+(1NG) bands are blue (< 450 nm, with brightest emissions < 400 nm). Due to strong Rayleigh scattering of blue light at low elevation angle observations through the atmosphere, atmospheric transmission in the blue is poor (*cf* Figure 3.4), and observations need to be made from high altitudes, such as from an aircraft, to minimize these effects. One reason for investigating the blue N_2(2PG) band is that the upper state of N_2(1PG), $B^3\Pi_g$, is filled via cascading [$B^3\Pi_g$ is the lower electronic state of N_2(2PG)], so that analysis of N_2(1PG) is not straightforward. There is not the problem of cascading into the upper states of N_2^+(1NG) and N_2(2PG). Quenching issues are not as severe for the N_2^+(1NG) and N_2(2PG) upper electronic states. Additionally, N_2(1PG) is energetically the lowest emission of the four, so observations of other bands indicate higher excitation energies of the electrons which are impacting on the N_2.

The cropped image and the observed blue spectrum of the July 28, 1998 6:41:01.278 sprite are presented in Figure 3.8. The blue spectral observation was made from the EXL98 aircraft, which was used in order to minimize the severe atmospheric transmission problems by getting above the densest portions of the atmosphere. Despite the improved atmosphereic transmition associated with aircraft observations, the signal-to-noise ratio of the blue spectral observation is not as good as the signal-to-noise ratio in the red spectral observations (*cf* Figure 3.1). The blue spectral observations of sprites is a challenging experiment even from aircraft altitudes. After gamma correction and background subtraction of the video image of the near-UV spectrograph output, three video fields were averaged together for a total time integration of 40 ms (the spectral observations were on the upper portion of the scan read-out imager, so the time integration only includes a portion of the third field and is not the entire 50 ms of the three fields), and ten video scan lines were also averaged in order to improve the signal strength. The lack of ionization in the spectral observations of the sprite agree with the lack of a signature of the sprite in the 427.8 nm filtered imager, which is filtered to only record N_2^+(1NG) emissions (*cf* Figure 2.12). Even without ionized emissions, the spectral identification of N_2(2PG) increases the required excitation electron energies to above 11.18 eV.

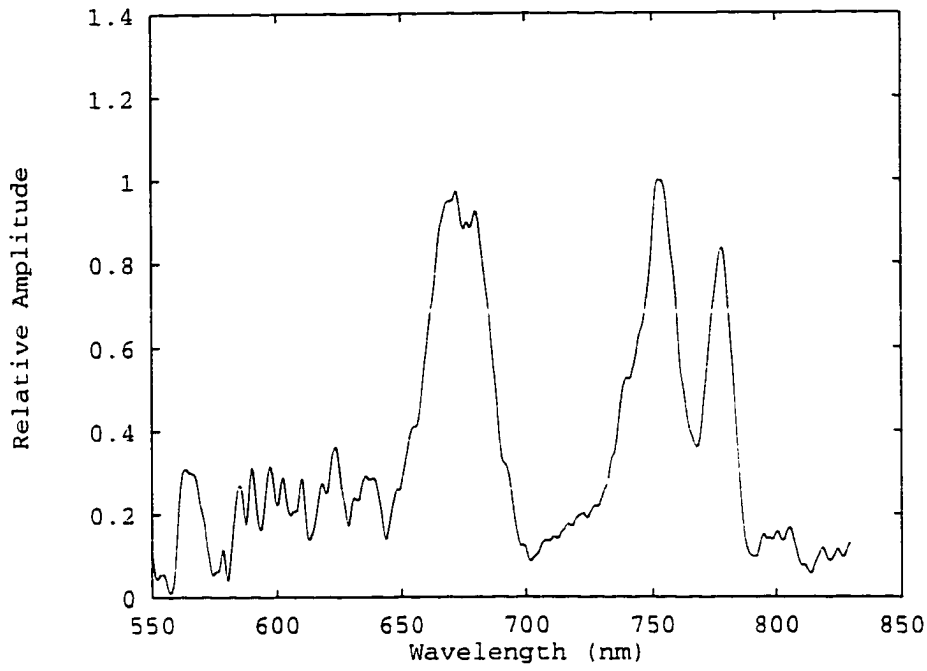

Figure 3.9. Sprite Halo Spectrum. The spectrum of a halo recorded June 22, 1995 at 7:10:48. The primary emission is N_2(1PG), and the spectrum looks very similar to the observe sprite spectra. One difference is the much higher noise level in the data (less than one order of magnitude) especially at wavelengths less than 600 nm. This is for two reasons: the duration of the halo is 3-6 milliseconds and the observations were made looking directly over Denver, Colorado.

3.6 Spectral Observations of Halos

Figure 3.9 presents an observed halo spectrum. The low signal levels (*cf* Figure 3.1) of the halo is due to the very brief duration of the emissions compared to standard video rates. High speed video observations indicate that halo emissions last 3-6 ms (D.R. Moudry, personal communications). The signal between 550-600 nm in the spectrum is scattered anthropic light because the observations were made from Mt. Evans looking directly over Denver, Colorado, so there is a great deal of scattered light from the city. The observed N_2(1PG) halo emissions are similar to sprite emissions, but have not been analyzed in as much detail.

3.7 Conclusions and Suggestions for Future Observations

This chapter began with the identification of N_2(1PG) as the primary source of the red light of sprites. A discussion of molecular nitrogen optical emissions was presented as a prerequisite for the remainder of the dissertation. Several atmospheric phenomena, including sprites, lightning, aurora, St. Elmo's fire, and halos, were discussed with a focus on the energetics and emissions. The emissions observed in aurora were discussed in some detail, to provide a context for the discussion of the observations in this chapter and to provide necessary background for the spectroscopic analysis presented in the next chapter. Results from a preliminary study of the variability of spectral observations were presented. The recent blue spectral observations of sprites provide emissions of additional molecular nitrogen bands-specifically N_2(2PG). The chapter concluded with the description of blue spectral observations of sprites and spectral observations of halos.

Based on discussion in the chapter, additional spectral observations of sprites should be made in the future improve spatial and temporal resolution over what is currently available. Using better temporal resolution, the identification of initial high energy processes (10 eV) followed by a lower energy 'after-glow' (1 eV) [Armstrong *et al.*, 1998] could be verified. Such a temporal evolution of the characteristic energy of the processes producing optical emissions implies that ionized N_2 is produced only during the intial phase of sprite emissions and improved time resolution of the spectral observations would permit detection of the associated N_2^+ (Meinel) emissions. An imaging spectrograph would provide two-dimenionsal spatially resolved spectral observations of a sprite and study of sprite process dependence on altitude. The limited number of photons from a sprite provides instrumental design challenges for both high time resolution and spatially resolved spectral observations of sprites.

Chapter 4

Spectrographic Analysis

The previous chapter discussed spectrographic observations of sprites and elves/"sprite halos" and identified the associated molecular nitrogen optical emissions. This chapter presents a detailed comparative analysis of two sprites, one simultaneously observed with two separate red spectrographs (640-900 nm) and a second sprite observed with a blue spectrograph (320-640 nm). The analysis includes comparison of observations with the predicted spectral emissions of several proposed models of sprites. The spectral fit that best agrees with the red spectral observations (specifically between 780-820 nm) requires ionized N_2^+ (Meinel) emissions at ~53 km (several pressure scale heights below the 85 km quenching altitude). The presence of N_2^+ (Meinel) emissions is significant for the interpretation of both non-optical observations and the modelling of processes leading to optical emissions. Their occurrence significantly below the quenching altitude also indicates that sprites may provide a natural laboratory for studying microphysical processes associated with energized molecular nitrogen. For example, the pressure dependent processes of intrasystem collisional transfer (ICT) of energy between various electronic states of N_2, can be studied through altitude resolved spectral observations of sprites.

The spectral observations of sprites at near-UV/blue wavelenghts (320-460 nm) are discussed, along with the corresponding filtered imager and photometer observations. The blue emissions predicted by several theoretical models are discussed. Stellar flux calibrations are used to determine the absolute photon flux of the observed emissions and converted to the corresponding optical energy flux of ~50 kJ. This energy measurement and the red spectral

observations are combined to determine the population of $B^3\Pi_g$ state of electronically excited molecular nitrogen associated with sprite emissions. The relative excitation rates of the upper electronic N_2 producing the observed spectral emissions to the excitation rates of all excited electronic states of N_2 gives a total population of electronically excited N_2 associated with sprites. Similarly, the N_2 vibrational energy is calculated. The relative densities of O_2 and N_2 are used to obtain an initial estimate of the total electronic and vibrational energy of a typical sprite of 250 MJ-1 GJ. A brief discussion of possible chemical effects of sprites is followed by suggestions for further spectral analysis and observation.

4.1 Red Spectral Analysis

As discussed in the previous chapter, the emissions from the molecular nitrogen first positive group (N_2(1PG)) have been identified as the main source of optical emissions from sprites. Fitting a synthetic spectrum to the observed spectrum is achieved by constraining the relative populations of the vibrational levels of the upper electronic states of the emissions ($N_2(B^3\Pi_g)$ in the case of N_2(1PG) emissions) to achieve a least-squares spectral fit to the observations (*cf.* Bucsela and Sharp [1997]). The low elevation angles of most sprite observations requires atmospheric transmission effects be taken into account. The analysis presented in this disseration uses atmospheric transmission corrections generated by the MOSART model. as discussed in Section 3.2.5.

4.1.1 Observations

In 1996. both the Fogle and Deehr spectrographs were used to obtain coincident observations from WIRO. The two scene camera images and the Deehr spectrograph observations from the July 24. 1996 3:58:24 event are presented in Figure 4.1. Figure 4.1 (A) was recorded from the scene camera co-aligned with the Deehr spectrograph. The dashed line on the scene camera indicates the field of view (FOV) of the Deehr spectrograph. The scene camera co-aligned with the Fogle spectrograph was looking at a slightly different azimuth and only imaged the edge of the sprite, as indicated by the white box superposed on the Deehr spectrograph scene camera image. Figure 4.1 (B) is from the Fogle scene camera. The FOV of the Fogle spectrograph slit is indicated by a solid line on panel (A), and a

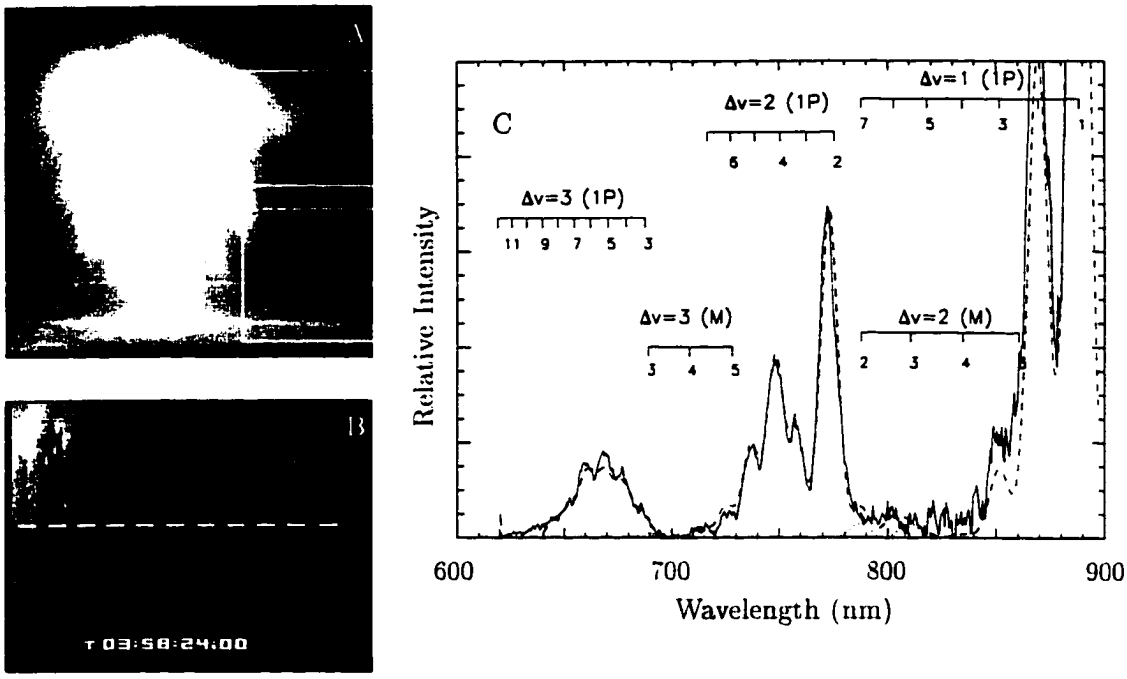

Figure 4.1. July 24, 1996 3:58:24 Sprite Spectra. Summary of the July 24, 1996 3:58:24.982 observations. The Deehr and Fogle spectrographs, both located at the Wyoming Infrared Observatory, recorded the July 24, 1996 3:58:24 sprite. The Deehr and Fogle system scene images are presented in (A) and (B) respectively. The spectrum shown at right is from the Deehr spectrograph. The solid line is the observed spectrum, the dashed line is a fit composed of both N_2(1PG) and N_2^+ (Meinel) emissions, and the dotted line is the N_2^+ (Meinel) contributions to the fit.

dashed line on panel (B).

The observations from the Deehr spectrograph, corrected for instrumental response and atmospheric transmission determined via MOSART, are presented in Figure 4.1 (C). The instrument response begins decreasing at ~800 nm and therefore the signal to noise ratio decreases with increasing wavelength. The relative vibrational populations from the synthetic fit to the Deehr spectral observations are shown in Figure 4.2. The spectrum is well described with a spectral fit requiring only N_2(1PG) emissions. N_2^+ (Meinel) emissions were included in the least squares fit analysis, but the $N_2^+(A^2\Pi_u)$ population required for a robust spectral fit was below the noise limit of these observations.

The Fogle spectrograph observations are presented in Figure 4.3 with two different

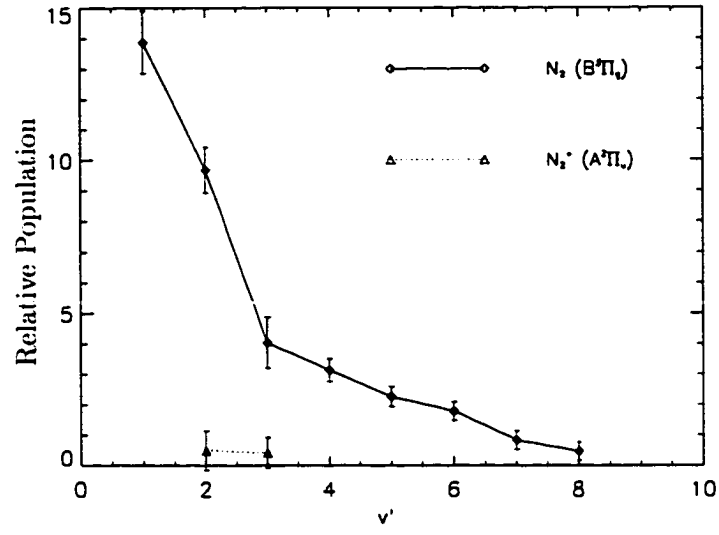

Figure 4.2. July 24, 1996 3:58:24 Deehr Vibrational Distribution. The vibrational distribution determined from a spectral fit of the July 24, 1996 3:58:24.982 Deehr spectrograph observations. $N_2(B^3\Pi_g)$ is the upper electronic state of the N_2(1PG) emissions and $N_2^+(A^2\Pi_u)$ is the upper electronic state of the N_2^+ (Meinel) emissions.

spectral fits to the observations of the July 24, 1996 3:58:24 sprite. The three panels all use a solid line to show the observed spectrum and a dashed line for the spectral fit. Figure 4.3 (A) shows the best spectral fit combining both the N_2(1PG) emissions and N_2^+ (Meinel) emissions. The dotted line represents the N_2^+ (Meinel) contribution to the fit.

The presence of an N_2^+ (Meinel) component is unexpected because quenching is the dominant energy release mechanism for the upper state ($N_2^+(A^2\Pi_u)$) of N_2^+ (Meinel) below 85 km altitude [Piper *et al.*, 1985] and the observations are from emissions at an altitude of 53 km. Only the N_2(1PG) contribution to the synthetic fit is shown in Figure 4.3 (B). Obviously, the region between 770-810 nm is poorly fit. The fit in this region can be improved by increasing the population of the high vibrational levels of the N_2(1PG)(Δv=1) progression. Figure 4.3 (C) shows a spectral fit of only N_2(1PG) emissions, with the least squares fit constrained to wavelengths greater than 750 nm (resulting in a 'high-v' fit). The 770-810 nm region is more accurately reproduced in the 'high-v' fit than by the N_2(1PG) only fit to the entire spectrum. In (C) however, between 640-670 nm and 700-730 nm the synthetic 'high-v' fit is poor. The increased population of the higher vibrational levels to achieve the fit without any ionized emissions leads to increased emissions between 640-670 nm and 700-

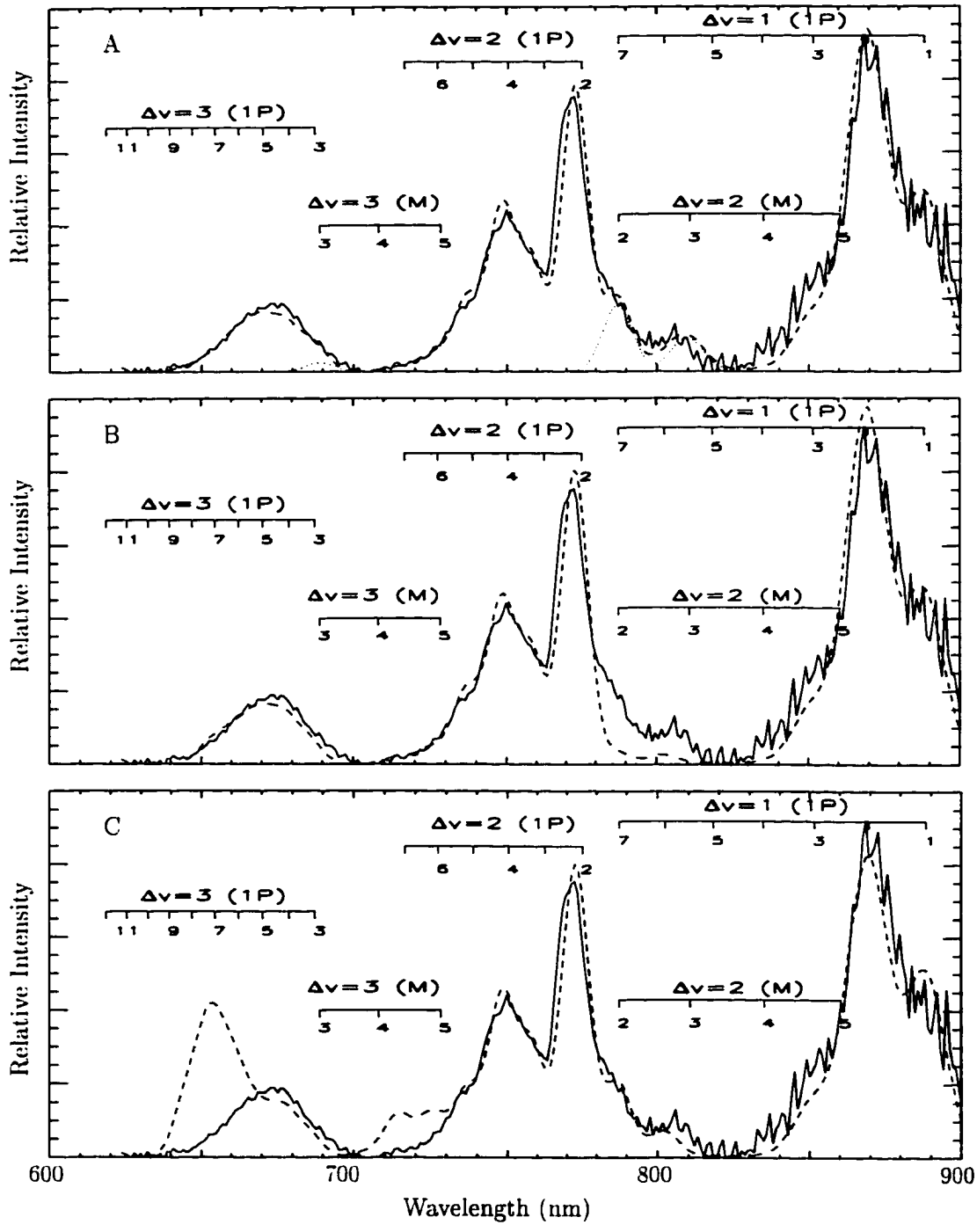

Figure 4.3. July 24, 1996 3:58:24 Sprite Spectral Fits. Spectral fits of the July 24, 1996 3:58:24 Fogle spectrograph observations from sprite emissions coming from an altitude of ~53 km. The observations are indicated as a solid line on the plots, while fits are dashed lines. See text for further explanation.

730 nm in order to conserve the proper intensity ratio based on the branching ratio between emissions originating from the same upper electron state vibrational level. For example, the $N_2(B^3\Pi_g(v'=7)\rightarrow A^3\Sigma_u^+(v''=6))$ to $N_2(B^3\Pi_g(v'=7)\rightarrow A^3\Sigma_u^+(v''=4))$ intensity ratio must be 0.35 based on the branching ratio of the two bands, as discussed in Section 3.2.

Although the solid line is above the dashed line in the upper image of Figure 4.1, apparently indicating that the solid line is at a high altitude, triangulation reveals that the Fogle spectrograph slit (solid line) intersects the sprites at a lower altitude (53 km) than the Deehr spectrograph slit, which intersects the sprites at 57 km. This is because the brightest light entering the Fogle spectrograph slit is from the apparent right edge of the sprite, while the Deehr spectrograph is observing light from apparently more central sprites. The lower altitude observations require N_2^+ (Meinel) ionized emissions for a robust fit to the observed spectrum.

The observations of N_2^+ (Meinel) emissions at lower altitudes runs counter to expectations based on simple quenching considerations. Two effects may explain the low altitude N_2^+ (Meinel) emissions. First, because the thunderstorm is the source of the electric field, the electric field due to the charge rearrangement in the thunderstorm is stronger at lower altitudes. More $N_2^+(A^2\Pi_u)$ molecules would be excited at lower altitudes. Perhaps a sufficiently large number of upper state N_2^+ (Meinel) ($N_2^+(A^2\Pi_u)$) molecules are excited at lower altitudes to overcome quenching effects. The 427.8 nm filtered blue imager observations, which had only $N_2^+(1NG)$ ionized emissions in the bandpass, recorded emissions only from the lower altitudes of sprites, are in agreement with the hypothesis that more energetic processes are occurring at lower altitudes. Blue emissions from $N_2^+(1NG)$ require slightly higher threshold energies than N_2^+ (Meinel) emissions. Second, because collisional effects increase with pressure, any ICT effects increase with decreasing altitude. The $N_2^+(A^2\Pi_u)$ emission duration can be increased via ICT processes with the $N_2^+(X^2\Sigma_g^+)$ state, so an increase in N_2^+ (Meinel) emissions due to ICT would be expected at lower altitudes (*cf.* Section 3.2.3).

Because of the two different types of readout in ISIT and ICCD systems[1] greater than 17 ms resolution is achieved. The July 24, 1996 3:58:24 sprite emissions begin 7 ms after the beginning of the first field of the spectral observations. Therefore, the initial brief, high

[1]Scan vs. dump readout is described in Section B and illustrated in Figure B.3 using observations of this sprite.

energy emissions would have greater temporal weighting against the lower energy emissions of a sprite which was not fortuitously resolved with greater temporal resolution than the 17 ms of video data. Photometric observations indicate that sprite emissions have two components: a brief (0.3-2 ms) emission with significant blue emissions at lower regions followed by a longer (2-10 ms), mainly red, emission (*cf.* Figure 2.14 and Armstrong *et al.* [1998]). An initial higher energy component combined with lower energy emissions is also postulated by runaway breakdown models [Yukhimuk *et al.*, 1998b]).

4.1.2 Theory

All of the theories which predict optical emissions agree that the predominant optical sprite emissions are $N_2(1PG)$. Several models do not even consider N_2^+ (Meinel) emissions [Milikh *et al.*, 1998a; Cho and Rycroft, 1998; Valdivia, 1997]. Taranenko *et al.* [1992] only predict N_2^+ (Meinel) emissions above 80 km. Bell *et al.* [1995] predict weak N_2^+ (Meinel) emissions from 50 km altitude and up (but also predict $O_2^+(1NG)$ emissions that are brighter than the N_2^+ (Meinel) emissions-$O_2^+(1NG)$ emissions have not been observed to date). Pasko [1996] predicts a peak in N_2^+ (Meinel) emissions at ~50 km. Several other proposed models of sprites are concerned with the energization of the middle atmosphere but do not predict optical emissions, and therefore cannot be compared with optical spectral observations of sprites.

As an illustration of the considerations that enter into comparison between observations and modeling, the remainder of this section presents one model for sprite emissions, which provides specific predictions of optical emissions and a method for the determination of the electric field strengths at high altitudes using observed spectra [Milikh *et al.*, 1998a]. This model uses a Fokker-Planck code to include both elastic and inelastic collisions and assumes energization of "ionospheric" electrons by both the electromagnetic and the electrostatic fields due to tropospheric lightning. After deriving electron energetization between altitudes of 60-90 km, this model calculates the steady state electron distribution function after the initial energization process, and then allows the cascading and quenching of the excited molecules to produce optical emissions. The fundamental parameter of the model is the

electron quiver energy,

$$\bar{\epsilon}(E,\upsilon) = \frac{e^2E^2}{m[\Omega_e^2+\upsilon_e^2]}\left\{1+\left(\frac{\Omega_e}{\upsilon_e}\right)\cos^2\theta_0\right\}$$

which parameterizes the excitation rates of N_2 electronic states in terms of E, the electric field strength (V/m); e, the electron charge (C); m_e, the electron mass; Ω_e, the electron gyrofrequency (1/s); and υ_e, the electron-neutral collission frequency. Optical emissions are not predicted for $\bar{\epsilon} < 0.02$ eV, while for $0.02 < \bar{\epsilon} < 0.1$ eV optical emissions and molecular dissociation are predicted, and ionization occurrs with higher quiver energies, $\bar{\epsilon} > 0.1$ eV.

The model is deficient in some respects. First, no consideration of N_2^+ (Meinel) emissions is included (presumably on the basis that the $N_2^+(A^2\Pi_u)$ state is collisionally quenched at sprite altitudes). Additionally, no intersystem collisional transfer (ICT) effects are considered (between the $W^3\Delta_u$, $B^3\Pi_g$, and $B'^3\Sigma_u^-$ states). The low altitude observations of N_2^+ (Meinel) emissions presented in Section 4.1 is evidence that ICT processes are important in ionized molecular nitrogen states. ICT effects are significant in electronically excited neutral molecular nitrogen at sprite altitudes as well, as suggested by auroral observations [Morrill and Benesch, 1996; Hallinan *et al.*, 1998]. The model does include excitation of the $N_2^+(B^2\Sigma_u^+)$ state (leading to N_2^+(1NG) emissions), but does not self-consistently include the effects of ionization of N_2, which produces enhancements of up to five orders of magnitude in the local conductivity [Pasko *et al.*, 1995, Figure 3].

Under the assumption of local thermodynamic equilibrium, Milikh *et al.* [1998a] propose that "...by comparing the two peaks of the N_2(1PG) band, *say 5-2 and 4-2* which undergo different absorption, one can estimate the zenith angle of the observed sprite." The use of emissions from different upper states (5 and 4 in the example) is flawed by any deviation in the vibrational distribution away from local thermodynamic equilibrium. However, the observed variations observed in sprite spectra (discussed in Section 3.4) implies that the excited species are not in local thermodynamic equibilibrium. Emissions due to transitions from a single upper state (*e.g.* the 4-3 and 4-4 transitions) are reasonable candidates for the atmospheric transmission analysis suggested by Milikh *et al.* [1998b].

Milikh *et al.* [1998b] further suggest the vibrational distributions of spectral observations can be used as a direct probe of the electron quiver energy, $\bar{\epsilon}$. They provide analysis of the June 22, 1995 7:04:39.07 event (Figure 4 of Hampton *et al.* [1996]) and obtain

$\bar{\epsilon} = 0.1$eV (which corresponds to electric field strength of 35 V/m at 80 km altitude). According to the model, this is just below the ionization threshold, so no observable ionized emissions (N_2^+ (Meinel), N_2^+(1NG)) are predicted. Because the electron quiver energy can be determined based on observed optical spectral observations and the quiver energy is parameterized by the electric field strength, this model could be used with observed optical spectra to provide a diagnostic for remotely determining high altitude electric fields associated with sprites. However, a preliminary study of the variations of optical spectra briefly discussed in Section 3.4 found no direct correlation between the N_2(1PG)(4-2)/N_2(1PG)(2-0) ratio and the NLDN reported current (a possible proxy for electric field strength at high altitudes). An improved study of spectral variability is required, but the lack of correlation between NLDN current and spectral features indicates the need for either a better proxy for the electric field strength at high altitudes or improved lightning parameters are needed order to test the predictions of the electron quiver energy model.

4.2 Interpretation of near-UV/Blue Observations

Compared to the large number of unfiltered sprite observations, there are only a few observations of sprites made with blue filters. (Ground based broadband observations are primarily red, due to strong Rayleigh scattering of blue light.) Aircraft color camera observations from 1994, discussed in Section 2.2, first measured the existence of blue emissions from sprites. The 1998 EXL98 campaign used a narrowly filtered 427.8 nm imager, a 340.7 nm filtered imager, and an near-UV/blue spectrograph for blue observations of sprites. Three blue images of sprites obtained from ground based cameras (at the Yucca Ridge Field Station) have been published [Suszcynsky *et al.*, 1998][2].

Blue observations are of interest for several reasons. As discussed in Section 3.2.2, the $N_2(C^3\Pi_u)$ state, which is the N_2(2PG) upper state is not affected by cascading or ICT processes to the same degree as the $N_2(B^3\Pi_g)$ state (the N_2(1PG) upper state). In addition to fewer processes leading to the population of the upper state of the blue N_2(2PG) emissions, the relaxation of the excited molecules in the $N_2(C^3\Pi_u)$ state is simpler because quenching is much less critical (the quenching altitude of N_2(2PG) is 30 km). Aside from difficulties

[2]The brightest ground based imagery of a sprite is the July 24, 1996 3:58:24 event, the same event discussed in the previous section with the strongest N_2^+ (Meinel) spectral emissions

due to atmospheric transmission, the blue ionized molecular nitrogen $N_2^+(1NG)$ emissions are much easier to observe and interpret than the red N_2^+ (Meinel) ionized emissions. The quenching altitude of $N_2^+(1NG)$ is 48 km, while N_2^+ (Meinel) is more strongly affected by collisional quenching (and has a quenching altitude of 85-90 km). Also, as with auroral observations, the $N_2^+(1NG)$ brightness is a direct observation of the rate of ionization [Vallance Jones, 1974]. Observations of ionized emissions in sprites are of great interest because of the observations of radar echoes (or lack of radar echoes) from sprites [Roussel-Dupré and Blanc, 1997; Groves *et al.*, 1998] and VLF observations of enhanced electron densities by approximately four orders of magnitude [Rodger, 1999].

Some models based on the original spectral observations of red $N_2(1PG)$ emissions as the predominant emission from sprites also predict blue emissions. Because of the low slant range and long path length through the atmosphere of all observations to date, atmospheric transmission corrections must be applied to the predictions in order to make comparisons of the theory with ground or aircraft based observations. Pasko [1996], using the quasi-electrostatic heating (QEH) model, predicts that at the source the instantaneous blue $N_2^+(1NG)$ band emission is approximately three orders of magnitude below than that of the red $N_2(1PG)$ band, and when temporally integrated to correspond to video field rates, the red $N_2(1PG)$ emission at 60 km are seven orders of magnitude greater than blue $N_2^+(1NG)$ emissions[3], but only about two orders of magnitude greater than blue $N_2(2PG)$ emissions. Bell *et al.* [1995] investigate the runaway electron model and find that the red $N_2(1PG)$ to blue $N_2(2PG)$ ratio is $\sim$2 at all altitudes above 60 km, while the QEH model predicts $N_2(1PG)/N_2(2PG)$ $\sim$10 above 80 km.

A series of recent photometric studies have examined time-resolved blue/near-UV emissions. Armstrong *et al.* [1998] report photometer observations using two filters: one centered at 431.7 nm with a FWHM (full width, half maximum) of 10.6 nm, one at 399.2 nm with a FWHM of 9.6 nm. These filters include both $N_2^+(1NG)$ and $N_2(2PG)$ emissions in their bandpass, making definitive observations regarding ionized emissions from sprites difficult.

Figure 4.4 illustrates the difficulties descriminating between $N_2^+(1NG)$ and $N_2(2PG)$ emissions, particularly for the '427.8' nm filter used on the EXL98 campaign. Figure 4.4 (B)

[3]Atmospheric attenuation effects are not included, and could contribute two more orders of magnitude difference between the red and blue emissions.

is a plot of the responses of the UAF 427.8 nm filter, the blue channel of the UAF/ACTP color camera, the NRL 340.7 nm filter, and the two filters used by Armstrong *et al.* [1998]. Both N_2(2PG) and N_2^+(1NG) emissions are plotted as well, but the relative amplitude of the two groups of emissions is chosen solely for illustrative purposes[4]. The wavelength range in Figure 4.4 (B) is chosen to correspond to the wavelength range of the NRL Blue/near-UV spectrograph used on the EXL98 aircraft. Figure 4.4 (A) shows improved wavelength resolution of the UAF 427.8 nm filter for direct light and for incoming light which is 5°angle of incidence (AOI). Note the difficulty in resolving the 427.8 nm N_2^+(1NG) emissions and 426.8 nm N_2(2PG) emissions. Despite the inability to definitely identify ionized emissions from molecular nitrogen, the ratio of the two filtered photometers is able to discriminate between lightning, sprites, and elves[5]. The 399.2/431.7 intensity ratio for lightning is approximately unity, in agreement with the expected continuum radiation. For sprites, the 399.2/431.7 intensity ratio is ~2, while elves have a measured 399.2/431.7 intesity ratio of ~3.

The temporal evolution of the 399.2/431.7 intensity ratio observed by the two photometers suggests an initial process with an electron temperature equivalent to ~10 eV (for less than 1 ms) followed by a longer lasting ~1 eV process. Suszcynsky *et al.* [1998] used a 20 nm wide filter centered on 425 nm with a photometer to observe the 427.8 nm N_2^+(1NG)(0,1) emission. However, the filter bandpass also included the lower energy N_2(2PG)(1,5) emission at 426.8 nm (as well as several other less intense N_2(2PG) emissions). Both the photometer studies and filtered blue imagery of sprites indicate the presence of N_2^+ emissions during the initial portion of the sprite.

Before the EXL98 aircraft observations, unambiguous observations of ionized molecular nitrogen emissions from sprites had not been obtained. The N_2^+ (Meinel) emissions dtected in some, but not all, sprites are of interest because the Meinel emissions occurred at altitudes significantly below the quenching altitude for that group of emissions. The ground based blue observations of N_2(2PG) and N_2^+(1NG) emissions could not unambiguously resolve the ionized component of the observations. For these reasons, the EXL98 observations included

[4]Observations of sprites indicate that, at television field rates, the N_2(2PG) to N_2^+(1NG) intensity ratio should be much higher. Auroral spectra have a N_2(2PG) to N_2^+(1NG) intensity ratio which is much lower.

[5]Because Armstrong's study was made with filtered photometers and the emissions identified as elves lasted less than 1 ms, the events were most likely elves rather than halos. A study similar to Armstrong's should compare the 399.2/431.7 ratio of elves and halos.

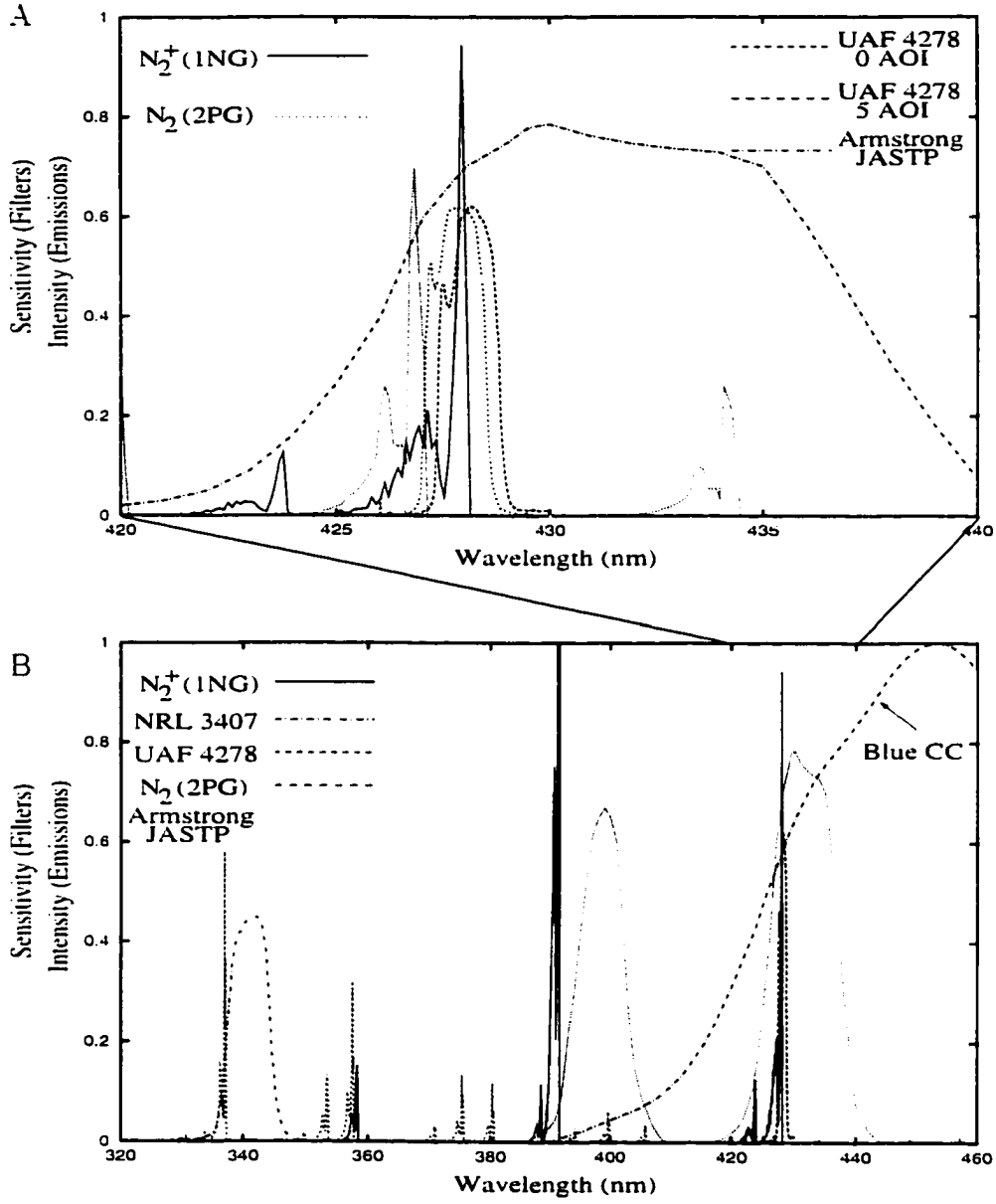

Figure 4.4. Blue Filter Response. The responses of several filters and imagers and the $N_2(2PG)$ and $N_2^+(1NG)$ emissions. The wavelength range of the lower figure is the wavelength range of the near-UV spectrograph. The upper plot illustrates 426.8 nm $N_2(2PG)$ contamination difficulties for 427.8 nm $N_2(1PG)$ emissions observations. The response of the relatively broad '427.8' filter used by Armstrong *et al.* [1998] for infering $N_2^+(1NG)$ emissions is shown. The relative amplitudes of the $N_2(2PG)$ and $N_2^+(1NG)$ bands is arbitrary (see text).

Figure 4.5. Blue Filtered Observations of July 19, 1998 8:59:54. Observations of the July 19, 1998 8:59:54 sprite in three imagers. (A) is from the unfiltered narrow imager, (B) is from the 427.8 nm ($N_2^+(1NG)$) filtered imager, and (C) is from the 340.7 nm ($N_2(2PG)$) filtered imager. The unfiltered and 427.8 nm filtered imagers have the same field of view (FOV), while the 340.7 nm filtered imager has a slightly different FOV. The horizontal white lines are drawn to indicate the approximate same elevations in all three imagers. The ionized (427.8 nm) emissions are observed to be strongest at lower altitudes, while the neutral blue emissions (340.7 nm) emissions are strong throughout the sprite.

a filter selected to observe the $N_2^+(1NG)(0\text{-}1)$ transition with a band head at 427.8 nm. A filtered imager which observed only $N_2(2PG)$ emissions (at 340.7 nm) was used on the same campaign. The two systems were calibrated in order to determine the relative populations of $N_2(C^3\Pi_u)$ and $N_2^+(B^2\Sigma_u^+)$ electronic states. The responses of the two filtered systems are displayed in Figure 4.4.

The quasi-electrostatic heating (QEH) model introduced in Section 2.9 provides predictions of optical output of sprites, which is discussed here for comparison with observations. The predominant emissions predicted is $N_2(1PG)$, in good agreement with the early spectral observations [Hampton *et al.*, 1996; Mende *et al.*, 1995]. Other nitrogen emissions, such as $N_2(2PG)$, N_2^+ (Meinel), and $N_2^+(1NG)$, as well as $O_2^+(1NG)$ emissions, as predicted in Figure 4.4 of Pasko [1996] will be discussed. Pasko *et al.* [1999] notes that because the ionization time scale at 90 km is ~4 ms, only optical emissions having low thresholds ($N_2(1PG)$) will be observed. Additionally, much higher electric fields (about twice E_k, the breakdown threshold field) are required to produce significant ionization [Pasko *et al.*, 1999].

Pasko [1996] (Figure 4.4) predicts that time integrated observations (17 ms) the $N_2^+(1NG)$ (as well as $O_2^+(1NG)$ and N_2^+ (Meinel)) emissions are brightest at lower altitudes (~50 km) with brightness that decreases by three orders of magnitude at ~57 km. [Pasko,

1996, Figure 3.9] presents an instantaneous emission calculation and does not demonstrate the same altitude profile of blue emissions from ionized N_2. The model predicts $N_2^+(1NG)$ emissions brightest above 70 km. The 427.8 nm filtered observations of $N_2^+(1NG)$ emissions do not agree with this model. Simultaneous observations of the July 19, 1998 8:59:54 sprite with the 427.8 nm filtered imager and the 340.7 nm filtered imager are shown in Figure 4.5. Figure 4.5 (A) is the unfiltered imager, while (B) is the 427.8 nm filtered observations (with the same field of view as the unfiltered imager). The 427.8 nm observations have had histogram equalization applied to stretch the contrast of the image. Figure 4.5 (C) is the 340.7 nm filtered observations. The ionized emissions are the strongest at lower altitudes of the sprites, while both the unfiltered observations, primarily red emissions, and the neutral blue observations (340.7 nm) are bright across the entire altitude of the sprite. The horizontal white lines in Figure 4.5 indicate the same elevation in all three images. These observations indicate that atmospheric absorption is not the sole reason that ionized blue emissions are only weakly observed in sprites.

The runaway breakdown theory [Roussel-Dupré *et al.*, 1998; Yukhimuk *et al.*, 1998a] provides altitude dependent optical (400-900 nm) spectral predictions, which are reproduced in Figure 4.6. The emissions are averaged over 17 ms and include atmospheric transmission effects for an observer at 11 km altitude. The atmospheric transmission model is based on observations by Guttman [1968], which is a poor atmospheric transmission model compared to modern models, such as MODTRAN or MOSART (see Section 3.2.5). The spectral predictions from the runaway electron (REL) model of [Yukhimuk *et al.*, 1998a] predict 427.8 nm emission from sprites that do not vary significantly with altitude.

The distance between the sprite and the observer for the predicted emissions presented in Figure 4.6 is not given. The spectral predictions from Yukhimuk *et al.* [1998a] are presented in Figure 4.6 for an aircraft observations of a sprite associated with a 200 C charge neutralization occurring in 7 ms. Figure 3.4, for the 10 km observer, illustrates that difference in the atmospheric transmission between 100 km and 500 km is significant (*e.g.* the ratio of the transmission at 800 nm to transmission at 400 nm is $\sim$4.5 for a distance of 500 km, while it is $\sim$1.7 for a distance of 100 km). The dominant blue emissions are the $N_2^+(1NG)$ 427.8 nm, which does not agree with the reported observations from the EXL98 campaign that the $N_2(2PG)$ emissions are dominant.

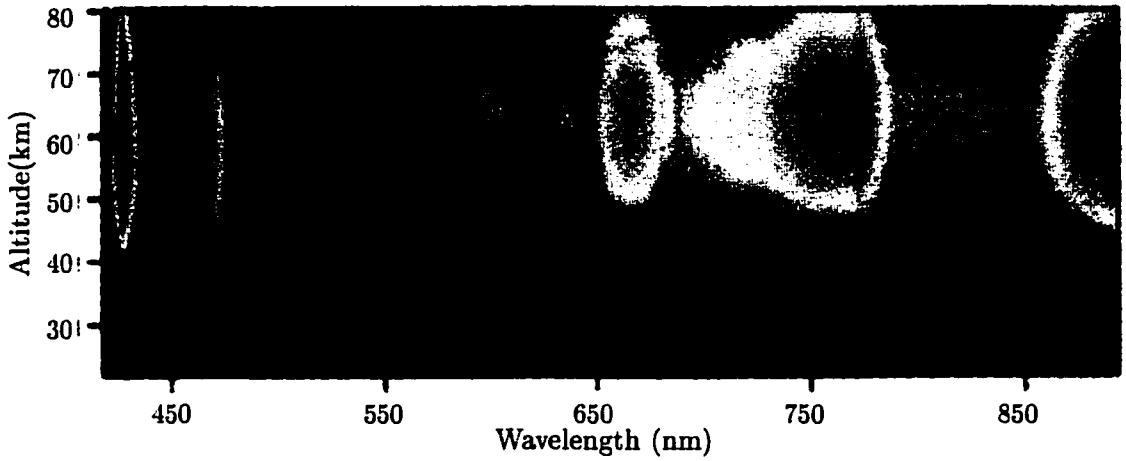

Figure 4.6. Predicted Spectra from Runaway Breakdown. Computed optical emissions for a detector at 11 km altitude for 200 C of charge neutralization by a cloud-to-ground strike in 7 ms at an altitude of 11.5 km. Reproduced from Yukhimuk *et al.* [1998a].

4.3 Spectral Implications for Energetics of Sprites

The dominance of N_2(1PG)emissions indicate that sprites are relatively low energy phenomena, approximately 1 eV [Hampton *et al.*, 1996; Green *et al.*, 1996; Mende *et al.*, 1995]. Electron densities of $\sim 10^3$ cm^{-3}, or four orders of magnitude above ambient at an altitude of 70 km, are predicted by Pasko *et al.* [1995]. Based on VLF scattering observations associated with sprites, electron densities of sprites are estimated to be 2.5×10^3 cm^{-3} [Dowden *et al.*, 2000]. For comparison, the electron density in the first 5 μs of a lightning discharge is 10^{18}cm^{-3} [Uman, 1987].

If the scene viewed by an imager includes several stars, an absolute brightness scale can be established using the published brightness of stars in the image as calibration sources. Using several stars in an image, one obtains a linear relationship between image counts and photons (see Appendix A of Hampton [1996] for more information). Stellar calibrations were used to determine absolute photon flux measurements of sprites in the UAF 1994 measurements, yielding total optical energies of ~50 kJ for the observed sprite. The 1994 observations were based on color camera measurements with response between 395-700 nm. The observed emissions are primarily from the N_2(1PG) group. Based on the vibrational distributions determined by the spectral fitting presented in Section 4.1 and the camera

response convolved with the N_2(1PG) emissions, it is found that only ~5% of the N_2(1PG) emissions are detected by the color camera. Matching the observed photon flux in the image of the sprite to the observed spectrum yields a photon spectrum of the sprite. The color camera photon calibration assumed all emissions were centered at the peak response of the red channel, or 650 nm.

This optical energy flux can be used to estimate the total energy deposited in molecular nitrogen and oxygen as follows. Integrating the apparent brightness of the sprite over its area in the image and folding in the stellar calibrations yields a total flux 1.81×10^{23} photons per sprite. Because only 5% of the photons emitted from radiating $N_2(B^3\Pi_g)$ molecules are in the color camera bandpass, there are 3.62×10^{24} radiating $N_2(B^3\Pi_g)$ molecules. Assuming that half of the $B^3\Pi_g$ state N_2 molecules which are excited via electron impact are quenched, the total $N_2(B^3\Pi_g)$ population is 7.24×10^{24}. For 1 eV excitation energy, the ratio of all N_2 electronically excited states to $B^3\Pi_g$ electronic state excitation is 3.45 [Slinker and Ali, 1982]. This gives 2.5×10^{25} total N_2 electronically excited molecules. Assuming that the upper states all cascade down to the $N_2(A^3\Sigma_u^+)$ state, each molecule has energy ~6.5 eV. Therefore the total energy of electronic excitation is ~26 MJ for this sprite.

Energy is also distributed amongst vibrationally excited states within the electronic states, so we calculate the vibrational energy similarly. From above, there are 3.62×10^{24} radiating $N_2(B^3\Pi_g)$ molecules. The ratio of the total number of vibrationally excited N_2 electronic states to the number of vibrationally excited $N_2(B^3\Pi_g)$ states is 2674 [Slinker and Ali, 1982]. Therefore the total number of vibrationally excited N_2 states is 1.94×10^{28}. Assuming the average vibrational energy is 0.3 eV, there is ~930 MJ of energy in the vibrationally excited N_2 states. Combining the vibrational and electronic energy calculated above, we find ~950 MJ deposited in molecular nitrogen by a sprite whose optical energy is 50 kJ. Assuming similar excitation in O_2 and scaling by the relative densities of N_2 and O_2, we obtain a total energy deposition in the middle- and upper-atmosphere of 1.2 GJ for this sprite.

A second estimate of the total energy can be made by including considerations of ICT (see Section 3.2.1) and cascading. These processes decrease the total N_2 to $B^3\Pi_g$ electronic excitation ratio because the observed emissions from the $B^3\Pi_g$ state include cascade from the $C^3\Pi_u$ state and collisional transfer from the $B'^3\Sigma_u^-$ and $W^3\Delta_u$ states. The ratio between

all N_2 electronically excited states and the observed $B^3\Pi_g$ states must therefore be revised from 3.45 to 1.43, yielding 5.18×10^{24} total N_2 electronically excited states. As calculated above, the total electronic energy is 5.39 MJ. Above, the $N_2(B^3\Pi_g)$ vibrational energy was leveraged to calculate the entire vibrational excitation of N_2. Including the $C^3\Pi_u$ cascading and $B'^3\Sigma_u^-$, $W^3\Delta_u$collisional transfer excitation of $B^3\Pi_g$ state, the ratio of these excitations to the total N_2 vibrational excitation is 769 [Slinker and Ali, 1982]. Therefore, with ICT considerations, a total of 3.98×10^{27} vibrationally excited N_2 molecules is calculated. Assuming an average vibrational energy of 0.3 eV as before, the total vibrational N_2 energy is 191.2 MJ. The total vibrational and electronic energy combined (with strong ICT and cascading effects) is 197 MJ. As above, the density ratio of N_2 and O_2 is used to get a total energy deposition in the middle- and upper-atmosphere of ~250 MJ.

These two estimates for the total energy, 1.2 GJ and 250 MJ, bracket the total energy deposited to the upper atmospheric neutrals, based on the optical spectroscopic observations discussed previously. Thus, the 50 kJ optical energy seen in the images of sprites represents approximately 0.004-0.02% of the total energy associated with these events. Therefore, the largest portion of the energy (more than 99.98%) resides in states that do not lead to optical observations, but which may drive other processes.

Marshall *et al.* [1998] find an upper limit on the order of a megajoule for energy emission in the ELF. However, they are not specific in attributing this energy to the sprite or the causative +CG. They state "...red sprites and elves are generally accompanied by unipolar 'slow tail' wavelets ... *[which]* apparently propagate in the expected TEM mode, and their amplitude is such that, when extrapolated to the source, the total ELF electromagnetic energy approaches a megaJoule." More recent estimates of ELF/VLF energy directly attributable to a sprite are presented by Cummer and Stanley [1999].

The total energy of a negative cloud-to-ground (CG) discharge is approximately 1 GJ [Uman, 1987]. Positive cloud to ground discharges are generally more energetic than negative CGs, by factors of 2-10 [Uman, 1987]. The total energy of 250-1200 MJ calculated is deposited into the upper atmosphere by a typical sprite is therefore of the same order of magnitude as the causative +CG lightning stroke. The energy of sprites is presumably ultimately dissipated by heating of the neutrals within the mesosphere. If we assume a sprite volume of 10^3 km^3 and a mean mesospheric neutral number density of $10^15/cm^3$ and that

the total energy is converted to heat, this would correspond to average heating of neutrals of 0.015-0.075 K within the sprite volume.

4.4 Global Energy Deposition

The previous calculation yields a total energy of a single sprite of 250-1200 MJ. Using an estimated global occurrence rate of one per second (see Section 2.8), the average power is 250-1200 MW. Globally, this corresponds to 2.2-8.4 TJ/day deposited by sprites in the middle atmosphere. The corresponding global average energy flux is 2-10$\mu W/m^2$.

This is only about one hundredth of the mesospheric energy budget [Mlynczak and Solomon, 1993]. However, the local heating associated with a single sprite or several hundred sprites concentrated over a single thunderstorm would produce a substantially enhanced local effect above thunderstorms, or in regions where thunderstorms dominate globally.

For threshold effects in chemistry, the localization of the heating of the middle atmosphere of sprites may be critical. Improved claculations of middle atmospheric effects of sprites is a critical area for future work.

4.5 Chemical Effects

Modeling efforts of the effects of thunderstorms on the middle and upper atmosphere suggest significant electron heating in the lower atmosphere [Pasko *et al.*, 1998]. If the energy from the heated electrons couples into the neutrals on time scales of hours, it would be possible to observe the effects of such heating. The theoretical modeling of such effects is beyond the scope of this thesis, as it requires non-local thermal equilibrium effects to be taken into account (such efforts have yet to be pursued for the lower ionosphere/upper atmosphere). An upper bound estimate by Pasko *et al.* [1998] at 85 km altitude is given as $\sim 10^{\circ}$ K on a time scale of 2-3 h. For comparison, this rate would possibly compete with the integral daily heating produced by solar radiation [Hines, 1965] and is on the order of the energy flux measured in the mesosphere above thunderstorms and interpreted as heating by internal gravity waves generated by the tropospheric convection of thunderstorms [Taylor, 1979] .

The long term heating of neutral N_2 leads to a slightly vibrationally excited ground

state population. This is also known as superelastic vibration collisions, and introduces a new term for the Boltzmann equations solutions. Dissociation of molecular nitrogen is usually considered to be

$$e^- + N_2(X^1\Sigma_g^+)(v = 0) \rightarrow e^- + N(^2D) + N(^2S)$$

but for non-equilibrium nitrogen plasmas the excitation of vibrationally excited. ground state electronic molecular nitrogen should be considered:

$$e^- + N_2(X^1\Sigma_g^+)(v = 0) \rightarrow e^- + N_2^* \rightarrow e^- + N(^2D) + N(^2S)$$

As molecular nitrogen does not have a dipole moment, $N_2'X(v > 0)$ states are metastable. However, collisional transfer of this excitation to infrared active molecules (such as CO_2) has been suggested [Picard *et al.*, 1997]. The frequency of occurrence of sprites and the rate of energy loss from vibrationally excited ground state N_2 needs to be understood to determine if the above dissociation process may be important.

Capitelli and Molinari [1980] consider the processes of molecular dissociation under non-equilibrium plasma conditions. Of critical importance to atmospheric chemistry issues is their finding that "... depending on the system and on the relevant discharge parameters, a variable but generally large fraction of the energy pumped into the type of plasma under consideration is transferred to the vibrotational system of the molecule which can then dissociate via a ladder-climbing mechanism across the vibrotational manifold of the ground electronic state." After a thorough case study of molecular hydrogen the authors discuss molecular nitrogen, but conclude that the total contribution of triplet states to overall dissociation rates of N_2 can not be evaluated with presently available data.

However, if enough of the energy couples into the neutral ground state of nitrogen ($N_2(X^1\Sigma_g^+)$), this would serve to change the vibrational distribution of $N_2(B^3\Pi_g)$ (since, for example $\langle N_2(X^1\Sigma_g^+)(v = 1)| r |N_2(B^3\Pi_g)(v = 0)\rangle \neq \langle N_2(X^1\Sigma_g^+)(v = 0)| r |N_2(B^3\Pi_g)(v = 0)\rangle$, leading to variations in observed ratios of different vibrational upper states in sprite spectra on a time scale of hours.

Brasseur and Solomon [1986] attribute all stratospheric nitrogen atoms to dissociative ionization and dissociation of molecular nitrgen by galactic cosmic rays. However, since sprite emissions are $N_2(1PG)$, there is most likely also some atomic nitrogen formed via

dissociation. Any atomic nitrogen will rapidly react with molecular oxygen to form nitric oxide. Nicolet [1975] indicates cosmic radiation leads to a height integrated NO production of about $5 \pm 1 \times 10^7 cm^{-2}s^{-1}$ in polar regions and $3 \times 10^7 cm^{-2}s^{-1}$ in the tropics. Sprites may constitute an independent source of local NO production in the upper atmosphere.

In addition to interest in excitation and production of NO, a second issue of the production of vibrationally excited CO_2 has been suggested [Milikh *et al.*, 1998b]. Observations of emissions at 4.26μ from the $CO_2(001)$ asymmetric stretch mode were attempted as part of the EXL98 campaign. The observations were inconclusive and did not rule out such emissions.

4.6 Conclusions

Chapter 4 begins with analysis of red spectral observations of a sprite containing a component of ionized molecular nitrogen (N_2^+ (Meinel)) emissions. The neutral $N_2(1PG)$ emissions have an excitation threshold of 7.5 eV. The N_2^+ (Meinel) ionized molecular nitrogen emissions have a threshold energy of 16.5 eV, so observation of emissions from ionized molecular nitrogen is indicative of more energetic excitation processes. Additionally, ionized molecular nitrogen is significant for sprite models of the weakly ionized molecular plasma at middle-atmospheric pressures. The blue spectral observations presented in Chapter 3 are analyzed in the context of other blue filtered observations, and lead to the conclusion that the dominant blue emission is neutral molecular nitrogen emissions ($N_2(2PG)$), with an minor ionized molecular nitrogen ($N_2^+(1NG)$) component observed in only some sprites. Based on the spectral analysis, the total amount of energy deposited in middle atmospheric neutral species is calculated to be between 250 megaJoules and 1 gigaJoule. The optical emissions correspond to only 0.004-0.02% of this energy. After the energy deposition associated with a single sprite is determined, the cummulative effects of sprites is considered.

Chapter 5

Summary and Conclusions

This dissertation describes the optical spectrum of sprites obtained by the University of Alaska Fairbanks during summer campaigns of 1995, 1996, and 1998, and its implication to the understanding of the electrodynamics of the middle atmosphere. The single most signficant result is the determination that a typical sprite deposits up to one gigajoule into the mesosphere. In this chapter, the numerous results presented in the dissertation are summarized. Suggestions are provided for future observations that will improve the characterization of the brief mesospheric optical phenomena associated with thunderstorms, as well as the broader effects of the transfer of energy from the tropospheric thunderstorm to the middle- and upper-atmosphere.

Chapter 2 describes the first decade of scientific study of sprites, blue jets, and elves. Research advances by many research groups are described with an emphasis on results obtained by University of Alaska researchers. Before 1993, observational efforts were directed towards verifying the existence of optical transient events occurring in the middle atmosphere. Several results of the 1994 observations included the identification of blue jets, determination of the accurate dimension of sprites and blue jets, the identification of unique ELF/VLF signature of sprites, and the first observation of palm trees. Significant results from studies of blue jets are the relationship between blue jets and lightning activity, and the accurate triangulation of blue jets to determine the upward propagation speed of 110 km/s. The 1995 observations included red spectroscopic study of sprites, two aircraft campaigns outside of the United States, and the observation of elves/"sprite halos". Exper-

imental work since 1995 includes extending the spectral observations to the blue, filtered blue observations of sprites, improved spatial and temporal resolution of sprites and halos, and observations of sprites in Japan and Australia.

Chapter 3 begins with the identification of N_2(1PG) as the primary source of the red light of sprites. The N_2(1PG) identifications is followed by a discussion of molecular nitrogen optical emissions as a prerequisite for the remainder of the dissertation. A comparison of spectal observations of aurora, sprites, lightning, and St. Elmo's fire illustrates the spectroscopic differences of the emissions and the relationship between the spectral signature and the processes leading to optical emissions, and highlights several signifcant subtle points of the interpretation of the sprite spectrum. Results from a preliminary study of the variability of spectral observations is presented. Chapter 3 concludes with the description of blue spectral observations of sprites and spectral observations of halos.

Chapter 4 begins with analysis of red spectral observations of a sprite containing a component of ionized molecular nitrogen (N_2^+ (Meinel)) emissions. The neutral N_2(1PG) emissions have an excitation threshold of 7.5 eV. The N_2^+ (Meinel) ionized molecular nitrogen emissions have a threshold energy of 16.5 eV, so detection of emissions from ionized molecular nitrogen is indicative of more energetic excitation processes. Additionally, ionized molecular nitrogen is significant for sprite models of the weakly ionized molecular plasma at the low middle-atmospheric pressures. The blue spectral observations presented in Chapter 3 are analyzed in the context of other blue filtered observations, and lead to the conclusion that the dominant blue emission is neutral molecular nitrogen emissions (N_2(2PG)), with a minor ionized molecular nitrogen (N_2^+(1NG)) component. Based on the spectral analysis, the total amount of energy deposited in middle atmospheric neutral species is calculated to be between 250 megaJoules and 1 gigaJoule. The optical emissions correspond to only 0.004-0.02% of this energy. After the energy deposition associated with a single sprite is determined, the cummulative effects of sprites is considered.

Seventeen anectodal reports of optical emissions associated with thunderstorms are reproduced in Appendix A. Appendix B describes the instruments used by the University of Alaska Fairbanks group for sprite observations.

The following bulleted list is the distilled contributions of the author to understanding sprites, blue jets, halos and elves presented in this dissertation:

- Measurement and identification of sprite red spectrum ($N_2(1PG)$)
- Determination and interpretation of sprite ionization observations (N_2^+ (Meinel))
- Measurement and interpretation of sprite blue spectrum ($N_2(2PG)$)
- Observations and analysis of 427.8 nm emissions from $N_2^+(1NG)$ in sprites
- Calculation of total energy transferred to neutrals (N_2, O_2)
- Preliminary estimate of energy deposition rates from sprites
- Identification and interpretation of halos red spectrum ($N_2(1PG)$)
- Prelinary study of variability of sprite spectra
- Identification of "palm tree" events
- Mapping of extensive morphology of sprites
- Triangulation of sprites, blue jets, and halos to determine absolute dimensions
- Determination of blue jet-lightning relationship
- Analysis of sprite distributions over South and Central America
- Collection of additional anecdotal reports

Suggestions for Future Work

In only ten years, the study of optical emissions in the middle atmosphere associated with electrical activity has literally gone from simple anecdotal reports to an established field with several dedicated groups of researchers and significant interest from scientists in other related fields. However, significant research remains to understanding some basic properties of sprites, blue jets, and elves.

One crucial issue which must be resolved is the global distribution and occurrence rate of sprites, blue jets, and elves. Ground based optical observations (with range limited to approximately 1000 km and limited field of view, as well as dependence on relatively clear skies) will most likely be unable to provide the synoptic measurements required to determine global distribution and rates. Reising *et al.* [1999a] propose ground based VLF observations as a possible diagnostic for the determination of global sprite occurrence. However, such work has not been performed to date. Single satellite observations of sprites, as proposed by Chern *et al.* [1998], could provide global maps of sprite occurrence with limited temporal coverage of any specific region of the global.

In addition to the 1000 km range limitation of ground based observations, optical measurements of sprites occurring during the daytime are not yet possible. Daytime observations of aurora are currently being investigated via long time exposure narrow band filtered observations (Mark Conde, personal communications), but because of the brief duration of sprites, this technique is not likely to work for sprite observations. Most thunderstorm activity develops and occurs during the daytime, so some indication of the daytime sprite, blue jet, elves, and halos activity would be valuable to determine the total energy input of sprites, blue jets, elves and halos into the middle atmosphere.

Attempts have been made to observe daytime sprites. One active sprite producing storm studied in 1996 by the University of Alaska persisted until scattered light from the impending sunrise prevented further observations. Sprites were observed almost up to the point of solar illumination at sprite altitude. One observation of the VLF signature of a sprite during a daytime Texas storm has been reported [Stanley *et al.*, 1998]. However, occurrence rates of daytime vs. nighttime sprites remain to be determined. The issue of time-of-day of occurrence is critical for estimating the total energetic input of sprites, blue jets, and elves into the middle atmosphere.

The National Lightning Detection Network data has been an integral part of observational campaigns within the United States, and similar systems have benefitted Australian sprite observations. However, the NLDN data provides minimal parameters of detected lightning discharges (latitude and longitude of ground connection location, millisecond resolution temporal location, peak current, and multiplicity). More recently developed lightning mapping systems provide much greater detail observations of lightning [Rison *et al.*, 1999; Krehbiel *et al.*, 1999]. A much improved understanding of the lightning discharge associated with sprites could be important for understanding the fine scale structure of sprites and jets. An improved characterization of electrical activity in thunderstorms associated with blue jets will also be critical for understanding if the decrease of cloud to ground lightning observed with NLDN data is a true decrease of all electrical activity in the thunderstorm or perhaps a redirection of the activity to higher altitude charge levels. Lightning discharge observations with increased spatial and temporal resolution will improve understanding of the development and morphology of sprites.

Increased temporal resolution of sprites is necessary to understand the development of

the structures observed at video rates. As illustrated in Figure 2.16, imagers with one kiloHertz sampling are not sufficient for fully resolving the development of sprites. Photometer observations with ten kiloHertz sampling do not fully resolve the development of sprites [McHarg *et al.*, 1999]. Observations of the spatio-temporal development of sprites, especially in conjunction with similar high resolution observations of the causative lightning discharges, will improve the understanding of the physics leading to the optical emissions.

Increased temporal resolution in spectral observations of sprites will provide two important improvements. First, the identification of initial high energy processes (>10 eV) followed by a lower energy 'after-glow' (1 eV) [Armstrong *et al.*, 1998] could be verified. Secondly, such a temporal evolution of the characteristic energy of the processes producing optical emissions implies that ionized N_2 is produced only during the intial phase of sprite emissions. Improved time resolution spectral measurements would provide the opportunity for N_2^+ (Meinel) observations and analysis. An imaging spectrograph would provide two-dimenionsal spatially resolved sprite spectra. The limited number of photons from a sprite provides instrumental design challenges for both high time resolution and spatially resolved spectral observations of sprites.

Benesch [1983] discusses the lack of measurements of ICT processes because of the 85 km "turn-on" altitude for ICT between $B^3\Pi_g$ and $W^3\Delta_u$ states, and suggests "... the staging of further high altitude nuclear tests would furnish fine opportunities for the measurement of very bright and stable electron auroras with precisely predictable points of particle injection." Realizing that "... there are, however, several countervailing arguments concerning the merits of such tests ..." the author proceeds to examine data existing at the time. Spectral observations of sprites, especially the vertically resolved spectrum of a single sprite, provides a natural environment for the further study of ICT processes in the excited N_2 manifold. High time resolution spectra that span sprites vertically will provide data that can be used to study processes (such as ICT) in the excitation and relaxation of N_2.

This dissertation presents optical observations of sprites, and several future improvements in optical spectral measurements have been suggested. Improvements in other types of observations of sprites remain to be made in the near future as well. The identification of a unique ELF/VLF signature of sprites [Reising *et al.*, 1999a] provides the possibility for

routine monitoring of sprite activity on a global scale rather than the current campaign-mode observations which occur every summer in the midwestern United States. Radar observations to confirm the spectral measurements of electron densities in sprites should be made (Groves *et al.* [1998] observed no radar echoes from more than 200 sprite events, while Roussel-Dupré and Blanc [1997] reported HF echoes possibly associated with sprites).

The discovery of optical excitation of the middle and upper atmosphere by lightning has opened a new window for observing this traditionally difficult to study region of the terrestrial system. Exploiting the remote sensing possibilities of this discovery will permit systematic investigation of electrically driven linkages between the troposphere and the near space environment of the earth.

Appendix A

Recent Anecdotal Reports of Sprites

As part of the public outreach from the sprites research at the Geophysical Institute of the University of Alaska Fairbanks, a web page (at http://elf.gi.alaska.edu/) describing the observations and ongoing experiments was setup in 1994. An additional web page soliciting reports of similar observations from the public was published to the world wide web (at http://elf.gi.alaska.edu/sprite_pages/form.html). In this appendix is reproduced reports of sprite, jet, and "other" observations obtained through this solicitation. A majority of the reported observations are from observers in the United States. While this correlates geographically with the overwhelming majority of sprite observations of the United States, it also correlates with the distribution of population connected to the internet at the current time. It is encouraging that many pilots have seen scientific reports of sprites and jets and have come forward to report their observations. Also, the ease with which people are able to view sprite and jet activity is encouraging to all amateurs who hope to see sprites.

Richard Grant

"I was amazed to read in New Scientist recently, that lightening coming out of the top of a thunderstorm had only recently been accepted as a real phenomenon!

I saw such an occurrence in the seventies. I was driving with my parents along the road from Umvuma to what is now Masvingo in Zimbabwe. We were on our way to spend the

weekend at Kyle Dam.

Ahead of us, perhaps 20 km away, was a single very tall thunderstorm. The rest of the sky was clear.

The top of the storm was not flattened into an anvil, but looked rounded like the dome of a Van de Graff generator.

From the top of this storm I clearly saw several "bolts of lightning" going upwards. I seem to remember it looked like forked lightening going up from the top of the storm and dissipating in the clear air above the storm.

I remarked to my parents that there was lightning coming out of the top of the thunderstorm ahead of us and I am sure they saw it too.

All in all, I must have seen 5 or 6 occurrences of lightning above that storm before it stopped.

I remember thinking that what I had seen was unusual and I have never seen it since!

I hope you find this account interesting and helpful."

Senior Lecturer, Department of Physics and Electronics
Rhodes University
Grahamstown, South Africa

Mallory

"It was at night, during one of the many thunderstorms we get in Georgia during the summer. I was sitting in my living room watching the lightning when I saw a streak of light shoot straight up from the clouds. It happened so quick I couldn't tell what color it was, but I saw a couple more right after I saw the first one. I had no idea what it was at the time, but I know now."

Joe Warmbrodt

"In 1991, I was with my family at a KOA campground in far northeastern New Mexico. That night, a huge thunderstorm developed in the distance. I was in high school at the time but was interested in meteorology.

The thunderstorm was huge and the lightning was very impressive. Lots of branched fingers of lightning which propagated upwards throughout the mesocyclone, illuminating the

entire storm - it was probably the most beautiful storm I have ever seen. The campground was in a flat area and the storm was sufficiently far away to see it in its entirety.

During the storm, I noticed weird blue flashes above the cloud from time to time. I didn't know what they were. I figured they were some weird optical illusion, or maybe reflections off my glasses or something. Several years later I saw a report on TV and realized that I had seen blue jets. They were definitely blue jets because they "poofed" upwards in an inverted cone shape, almost like a fountain. During the storm I noticed maybe 15 to 20 of these.

Only today, I discovered this website (surfing here indirectly from a CNN report on blue jets) and thought I'd write this note."

Tom Clark

"Frequent entertainment for me on a hot desert night in Phoenix, AZ was to watch the glorious multiple t-storms of the "monsoon season." In the late 1960's and 70's before the valley north of Phoenix filled with houses, I'd look north and enjoy hours of viewing pleasure, including what looked like little "backfires" of colored light above the clouds. As I recall, they were not always reddish color and were not directly connected with a lighting flash, but they were fascinating as I'd never seen them elsewhere.

Thanks for shedding some light (so to speak) on what these things are."

Rob Hudson

"I am a meteorologist at American Airlines. An American Airlines captain reported this event at approximately 0850GMT 06/12/99 while flying near the coast of Costa Rica. He said the anvil of a Thunderstorm (located 40NM WNW of his aircraft) lit up with a very bright glow and then several discharges shot vertically to very high altitude. He indicated the color of the event was white. The location of the aircraft was 0925.4N/08512.0W. He indicated that he had read an article about Sprites and Jets."

Lisa Heining

"This probably won't be of any help, but my sighting happened approx. 10 years ago!! It was just before the ending of a very bad electrical storm we had in Lancaster, NY - a

suburb of Buffalo, NY. It was dark, and I had to go to the store, and as I was walking through the parking lot, I was gazing at the sky (I am a big weather buff) and I noticed both red and blue lights in the sky - they looked like little "bleeps" moving very quickly through the sky. This might not be what you are referring to - Sprites - but I wanted to tell someone who might be interested."

Jason Fields

"Over the course of the past few nights, I have observed four sprites over eastern Arizona and southwestern New Mexico from two different observing locations. I was on Mt. Lemmon (about 9000' elev) in the Catalinas (just north of Tucson) and looking almost due north at a line of storms about 80 to 100 miles away. Lightning activity was moderately active to sometimes very active. The sprites were difficult to see because of an intervening cloud layer and I suspect that there were more than the two I saw that night. I saw two more under more favorable conditions the following night from the Chiricahua Mountains in the southeastern corner of Arizona. From an elevation of 6700' and looking east over New Mexico (flat desert around 4000') was a quieter and smaller line of storms. But I did see two sprites off the top of that. I tune my AM radio to a band with no station (typically 1710 kHz) to 'listen' to the lightning (and sprites?). I initially did this because it was a bit odd to watch lightning and not hear any thunder. My girlfriend and I even thought that there may be a difference in the static sound created by cloud-to-ground and cloud-to-cloud lightning. I should also like to note that distant station reception was enhanced compared with other recent nights when it was clear and I was stargazing (notably a station from Lawrence. Nebraska came in clearly when it usually does not)."

Dallas Klassen

"We were cruising at 45000 en route from California to New York on Oct. 4 1998. There was a line of thunderstorms extending from approximately Omaha. Nebraska southwestward. which we were going around. The tops appeared in excess of 45000 ft. It was nearly dark at altitude. We were approximately 25nm northwest of the towering cumulus when it appeared that lightning shot up from the thunderstorm, approx. 15 deg. from straight up. The color was much like normal lightning flashes. There was no stratus layer and no anvil.

I am a captain on a corporate jet with approx. 11000 hours, and this is the only time I have observed this."

Thomas Miller

"Very dark conditions approx 90 miles from Chicago visibility unlimited could see beacon from downtown Chicago. Located on a lake MI beach shielded from local light sources. Obs. on clear cloudless night billions of stars in view. Flashes of light over large areas of the sky. Light source seemed to flash similar to lighting but very faint. These flashes seemed to come from an easterly direction. These sightings happened a few times during the two summers I work at the camp. It could have just been lighting reflection from storms off to the East. Fov from 30 degrees vertical to straight up to East and unlimited to S to N and W. There were a few flashes with a few minutes between them. Do not remember exact time of dates but am sure of the years.

Not sure if any use to you but your opinion would interest me."

Rosemary Moore

"I live on top of a hill in a two story house in a very remote area with only a few distant lights. The topographical configuration seems to split oncoming thunderstorms in two- with very severe weather to the northwest and southeast. So I have incredible long distant views of thunderstorms and can see the tops. I have seen sprites and jets many times and am glad to know they have names. When I first saw them, I had no idea what they were. I must tell you. though, many of the ones I have seen have had a much longer duration than your statistics. I did not time them, but they lasted long enough to travel almost the length of the thunderhead. These were tornado-bearing storms; very. very intense. I have also seen more than once a phenomenon I've not seen mentioned anywhere yet. I have seen rainbow lightening. I've seen an arc from the top of a lightening strike down to the bottom. sort of connecting the top to the bottom with a rainbow. I've also seen a round rainbow. These have always been of very short duration and occur during very intense storms with a lot of cloud to cloud lightening and concurrent strikes. Backlit by multiple flashes. Please let me know if any else reports this rainbow lightening, I'd be interested in any information."

Hans Jensen

"Many years ago, while a lowly student assistant supporting the National Hail Research Experiment on the Pawnee National Grassland of NE Colorado - A research associate from Texas A&M, John Marrs and I were out late at night watching thunderstorms in the distance 15 to 20 miles, with the purpose of catching rattlesnakes, we both observed a very active storm and on one occasion saw a red spike go out of the top of the storm. We questioned each other and made sure we were not seeing things. we definitely saw a red spike. WOW!! The next day,we told the research scientists from the National Center for Atmospheric Research about the sighting. They laughed it off and joked about us smoking too much dope.

I am sure we saw what is now classified as a red sprite. based on the images I have seen."

Jeffrey Showman

"On April 21. 1999 I was flying from Twin Falls. ID to Cincinnati. OH at FL450. We were overflying a large area of very active thunderstorms. many of which actually had tops well above our altitude. Time and location are approximate. I saw a blue ejection from the top of a storm cloud in the shape of an inverted tear drop (narrow end pointed down). It was only an outline. there seemed to be no coloration within the "teardrop" itself. The jet looked as if it were made of particles (grainy). it was not a solid image as a lightning bolt would appear. It was definitely traveling at a very high rate of speed vertically (away from the top of the storms). and lasted no more than a half second. If I had not been looking at the top of the storm. I would have never seen it."

Luke McConoughey

"Several red flashes on top of a thunderstorm to the southwest. There where trees filtering out a majority of the lower portion of the storm. The red flashes seemed to come from separate parts of the storm cloud. They were considerably brighter in the center of each flash circle.

It was quite exciting!"

Tim Fletton

"Maintaining FL 150. Multiple storm cells for entire flight. One substantial cell over Charters Towers. Estimated tops to FL330. Very active cell with continuous discharges. Magenta conical discharge observed from top of cell into the upper atmosphere. 3 or 4 discharges observed lasting only a few seconds."

Mark E. Evans

"I am a pilot for UPS. This evening enroute from Denver to Louisville in our B767 at FL 370. we paralleled an intense line of thunderstorms running from Arkansas to Indiana. Unbelievably. we witnessed around thirty or so sprites (many other airline crews witnessed them as well) and a few jets. We could not make out any particular color because the lightning activity associated with the line of thunderstorm cells (cold front in area) was extremely active and bright. We were shocked at the number of sprites - they tended to shoot out from the most intense line of cells. about 50-60 miles in depth. The whole line of cells extended several hundred miles. At first. we saw a few jets. then they died off for a while and sprites replaced them. An occasional jet would pop up during the sprite show. FANTASTIC!!"

James Marron

"I am a Corporate pilot. and was flying from Kansas City to New York. and was crossing a rather large line of Level 3 to Level 5 thunderstorms associated with a cold front. the Storms extended from just north of Chicago to southern TN/ northern AL. I was Crossing the line of WX at 41.000 Ft.

There was intense cloud to cloud lighting that seemed to travel the length of the system. On several occasions lighting would seem to start from both the south and the north and propagate through the system and when the lighting met a very visible very distinct sprite would rise out of the storm system. In my 8 years flying corporate jets I have had the opportunity to see many thunderstorms from altitude. yet I can not recall ever seeing lighting travel along a storm system in a given direction. nor have I seen such dramatic sprites."

Steve Schendel

"On Aug 28th I witnessed two sprites above a storm 100-150 miles due south of my location. I live in the edge of Phoenix, so there was a lot of background light.

The first Sprite was a series of vertical red streams from the top of the thunderstorm. It extended a considerable distance above the top of the cloud.

The 2nd Sprite was the mother of all Sprites. It was the largest and widest Sprite I have have ever witnessed. I was in the shape of a funnel with the small end at the top of the cloud. It was also red. It was so bright, my wife even saw it.. and she can't see anything at night."

Appendix B

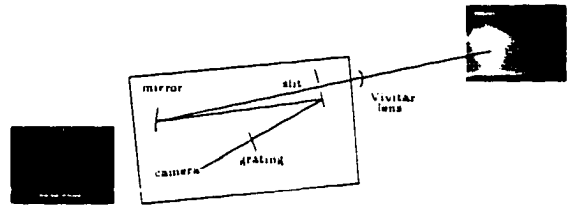

Instrumentation

Interpretation of observations requires understanding of the instruments used to obtain the measurements. The instruments used for the observations in this dissertation are discussed in this appendix.

The most common instrument used for sprite observations to date is the intensified video camera (used on every campaign to date). Following the 1994 aircraft observations, interest in energetics of sprites has driven improved instrumentation in more recent campaigns. The University of Alaska Fairbanks optics group maintains two slit spectrograph systems which have been used for spectral measurements of sprites. During the GASP'95 campaign the Deehr spectrograph [Kimball, 1996] was used to obtain the first spectral observations of sprites. The Sprites'96 ground-based campaign included two spectrographs, allowing observations at two altitudes in a single sprite as well as observations at different wavelength bands (both blue and red) of a sprite. The EXL98 aircraft campaign was specifically designed to answer energetic questions through the use of filtered imagers and a blue spectrograph, provided by the Naval Research Laboratory (NRL). Table B.1 summarizes the campaigns and instruments used for all University of Alaska Fairbanks sprites campaigns.

The Alaska Color Television Project (ACTP) color camera [Osborne *et al.*, 1994] was also used on several campaigns. The color camera consists of three filtered channels and provided the first spectral information about sprites, indicating that they are predominantly red.

Campaign	Dates	Location	Platform	Instruments
Sprites'93	1993/07	South America	NASA DC-8	All Sky Imager
Sprites'94	1994/07	mid-west U.S.	Two Aircraft	ACTP Color Camera
				ELF Search Coil
Peru'95	1995/02	South America	Single Aircraft	ACTP Color Camera
GASP'95	1995/06-07	Evans	Ground	Deehr Spectrograph
Blue Sand '95	1995/08	Central America	Aircraft	ELF Search Coil
Sprites '96	1996/06-07	WIRO & YRFS	Ground	Deehr Spectrograph
				Fogle Spectrograph
EXL '98	1998/07	Central U.S.	Single Aircraft	NUV Spectrograph
				ACTP Color Camera
			WIRO	Photometers
			Evans	Deehr Spectrograph

Table B.1. Campaign Instrumentation Summary. This table presentes a summary of the instruments used on all sprites University of Alaska Fairbanks campaigns, 1993-1998. Intensified black and white cameras were used on all campaigns, so are omitted from the table.

Spectrographs

The optical emissions of sprites are decomposed by wavelength using a dispersion grating. The spectrographs employed for sprite observations have been used for spectroscopic studies of aurora, and the N_2(1PG) emissions observed in sprites are a prominent emission in the aurora. Knowledge of auroral spectroscopy [Vallance Jones, 1974] is therefore a powerful tool for interpretation of spectral sprite observations. Spectrographs are also used to understand lightning [Salanave, 1980; Uman, 1987] and in fact were used even before photography was employed to record lightning discharges. The interpretation of diatomic molecular emissions requires understanding of the underlying quantum mechanical system [Herzberg, 1989]. The instruments used to obtain spectral observations are discussed in detail in the following section. The observations and their interpretations are presented in Chapters 3 and 4.

The Deehr spectrograph, originally built in 1959, has been used extensively for auroral observations [Deehr, 1961; Hallinan *et al.*, 1997, 1998] and coordinated CRRES[1] satellite

[1]Coordinated Radiation Release Experiment Satellite

observations [Delamere, 1998; Stenbaek-Nielsen *et al.*, 1993]. The Deehr spectrograph[2] is a slit spectrograph whose output is recorded using an intensified television camera. The Deehr spectrograph has a spectral range of ~300 nm (slightly dependent on the wavelength of observations, because the dispersion is non-uniform), which can be selected by moving the grating with respect to the light path. The Deehr spectrograph was used on the GASP'95 and Sprites'96 campaigns. For sprite studies, the slit of the spectrograph was horizontally oriented, and indicated in the scene camera image by a dashed horizontal line. The horizontal orientation of the slit was chosen to increase the likelihood of sprite observations. The recorded spectrograph image can be used to determine horizontal structure in the sprite along the slit.

The Fogle spectrograph [Fogle, 1966] is normally instrumented with an IIRelay2 intensifier system, but during the Sprites '96 campaign at the Wyoming Infrared Observatory, a factory-loaned modified Gen II intensifier was used for 'blue' observations, and a modified Gen III intensifier was used for 'red' observations. The Gen III modifications increased the red response from ~900 nm to 1050 nm (at the expense of overall sensitivity decrease of ~30%. The Fogle spectrograph system has angular dimensions of 11° along the slit and 14.67° in the spectral dimension.

The Naval Research Laboratory (NRL) operated a Blue/near-UV instrument on the EXL98 aircraft. In order to address sensitivity concerns, the camera was first used with the 340.7 nm filter as an imager. After this configuration satisfactorily detected emissions from several sprites and starters, the instrument was operated as a spectrograph. The wavelength range of observations with the near-UV spectrograph are shown in Figure B.1.

Filtered Observations

The spectral observations obtained to date provide some of the most important knowledge of sprite energetics, but are lacking in several respects, notably vertical spatial information and high time resolution (<17 ms). Filters have been used in several experiments attempting to address some of these questions, both in front of imagers, to observe spatial structure and variation in both sprites and jets, and in conjunction with high speed pho-

[2]Jen Kimball has written an unpublished report on the performance and tuning of the Deehr spectrograph.

tometers (operating at 20 kHz sampling rates), to obtain high time resolution observations. The ACTP color camera was used as part of the 1994, 1995, and 1998 aircraft flights. Utah State University operated a 665 nm filter (center wavelength, FWHM) with an unintensified CCD in order to observe one specific band of N_2(1PG). As part of the EXL98 campaign, a 427.8 nm filter was used in front of a Dage-MTI imager, alongside an identical (but unfiltered) imager in order to quantify the amount of N_2^+(1NG) emissions observed in sprites. Photometers, with both high temporal resolution and higher sensitivity, provided blue observations of sprites from the ground, using the higher photometer sensitivity to counter the very low atmospheric transmission at the blue wavelengths (see Section 3.2.5). Each system is described in more detail in the following subsections.

The Alaska Color Telelvision Project Color camera is a composite of three separate detectors behind a color dissecting prism block. The responses of each[3] of the three ISIT tubes are adjusted to present the aurora's light on a properly adjusted National Television Standards Committee (NTSC) monitor with the same color balance as the human eye. This adjustment was necessary because typical television scene illumination is from broadband light sources, while auroral emissions are primarily N_2 and O_2 band emissions. The adjustment does not affect the central wavelengths or bandpasses of the three ISIT detectors, only their relative responses. The response of the ACTP camera channels shown in Figure B.1 have all been normalized.

During the Sprites'94 aircraft observations of sprites, a Canon PV10X12B, 12-120 mm, with an auto iris of f/2.0-f/22, zoom lens was used, but operated at all times at 12 mm and f/2.0. This gave a 55° H X 43° V field of view. The same zoom lens was used during the Peru'95 and EXL98 aircraft observations. At all times the camera was operated with external sync so that it was synchronized with all similarly GPS synced camera.

Spectral observations in the range 500-900 nm provided evidence of ionization through the observations of N_2^+ (Meinel) emissions [Morrill *et al.*, 1998; Bucsela *et al.*, 1999]. However, the possible effects of quenching on the N_2^+ (Meinel) emissions (the N_2^+ (Meinel) quenching altitude is 85 km [Vallance Jones, 1974]) and the opportunity to run cameras in an aircraft (above the thickest portion of the atmosphere, so that Rayleigh scattering of

[3]See Wescott *et al.* [1998a] Figure 7 for a plot showing the relative response of each channel of the ACTP camera.

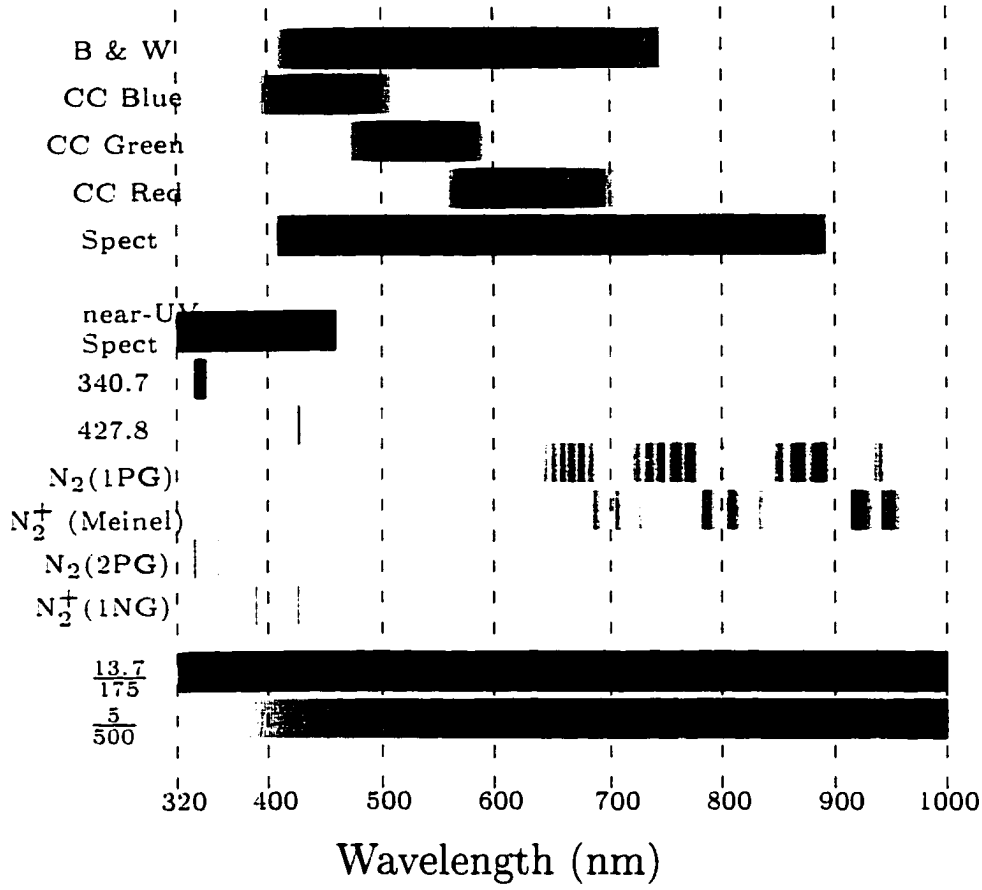

Figure B.1. System Response and Atmospheric Emissions. The normalized logarithmic response of several imaging systems, molecular nitrogen emissions, and two atmospheric transmission plots are shown. The responses plotted include a representative unfiltered imager, the blue, green, and red tubes of the ACTP color camera, the ranges of the Deehr spectrograph and the Fogle spectrograph, the NRL near-UV spectrograph, the 340.7 nm filter, and the 427.8 nm filter. For comparison, the normalized, logarithmic emissions from the N_2(1PG), N_2^+ (Meinel), N_2(2PG), and N_2^+(1NG) groups are shown. The atmospheric transmission as calculated using MOSART (see Section 3.2.5 for more information) is plotted for two different geometries: an aircraft observations (aircraft at an altitude of 13.7 km observing a sprite at 65 km and a distance of 175 km between the plane and sprite), and a mountain top observations (observer at 5 km altitude to a sprite at 65 km altitude and a distance of 500 km between the observer and the sprite. The most striking effect is the loss of blue transmission, largely due to Rayleigh scattering).

blue light is not as bad, see Section 3.2.5) led to the choice of filtered blue imagery. Ground based observations of $N_2^+(1NG)$ (ionized) and $N_2(2PG)$ (neutral) emissions in the blue have been made both with filtered imagers [Suszcynsky *et al.*, 1998] and filtered photometers [Armstrong *et al.*, 1998; Takahashi *et al.*, 1998]. The overlap of the ionized and non-ionized bands, and the relatively broad filters used in those observations made the interpretation of the results difficult.

The EXL98 instrumentation included a narrowly filtered 427.8 nm imager for observations of $N_2^+(1NG)$ emissions, a 340.7 nm imager (from NRL) for $N_2(2PG)$ emissions, and a blue/near-UV spectrograph (also from NRL). The EXL98 campaign used a '427.8 nm' filter, a 1.44 nm FWHM filter actually centered at 428.3 nm, specifically selected slightly red of the $N_2(2PG)$ 426.8 nm emissions which would contaminate the filter if it had been centered on 427.8 nm (see Figure 4.4). Observations of sprites and starters with this filter were conclusive evidence of ionized $N_2^+(1NG)$ emissions [Heavner *et al.*, 1998]. The choice to observe 427.8 nm emissions rather than 391.4 nm emissions was determined by considerations of atmospheric transmission and instrumental response. The 427.8 nm filter was used on a Burle SIT tube in an MTI/DAGE VE-10000 SIT camera which was identical to the narrow field unfiltered camera used on the plane. The filter was the first element in the optical train (rather than placed at a telecentric point), so off-axis incoming light experiences a different filter response, as shown in Figure B.2. At 5° angle of incidence (almost the corner of the image) the peak response has shifted approximately .4 nm, but most significantly the 'skirts' of the filter response have shifted enough to include some response in the $N_2(2PG)$ emissions. Careful analysis must be made to insure that the imaged light is not from the $N_2(2PG)$ band. Analysis of the 427.8 nm filter data in conjunction with data from the blue channel of the ACTP color camera and NRL's 340.7 nm filter allow for such determination.

The EXL98 campaign also used a 340.7 nm filter[4] (~10 nm FWHM) which imaged only $N_2(2PG)$ emissions. The filter was used in front of a Nikor 145 105 mm f/4.5 quartz/fluorite camera. The intensifier is a near-UV/visible ITT Micro Channel Plate, which is imaged using a Pulnix TM6701AN 1/2" CCD array. The 340.7 nm filter was placed in front of the first lens of the camera, so the effects of off-axis light must also be considered, and it is seen that the peak response is shifted by about .4 nm at 10°angle of incidence.

[4]Provided and operated by the Naval Research Laboratory.

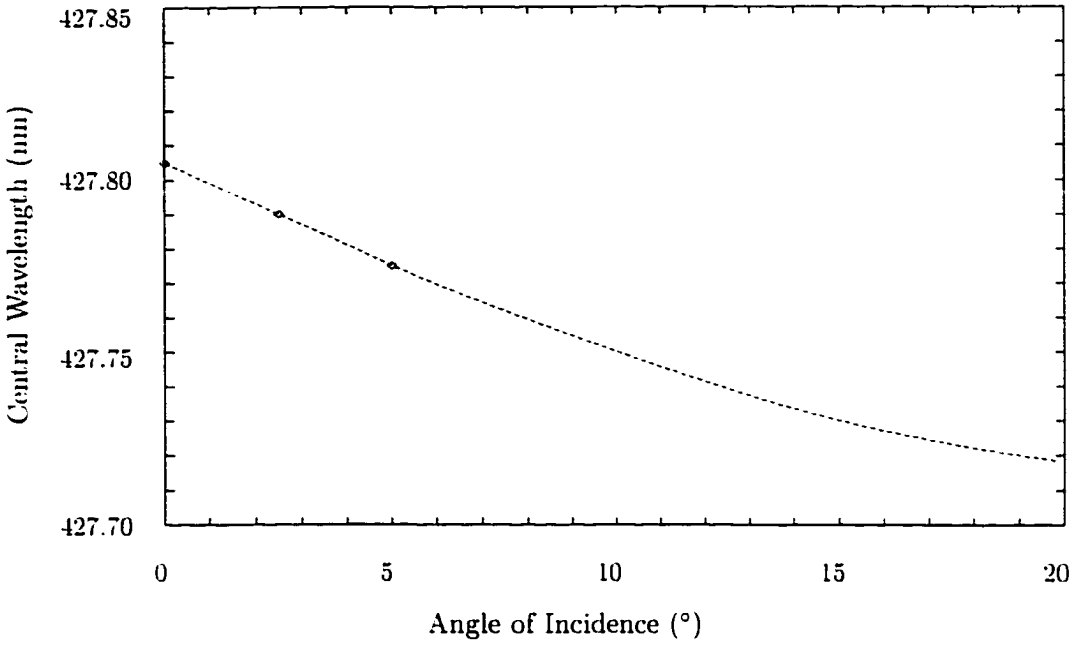

Figure B.2. Angle of Incidence Dependence of 427.8 nm Filter. This plot shows the dependence of the central wavelength of the 427.8 nm filter on the angle of incidence of incoming light. The primary concern is the leakage of 426.8 nm N_2(2PG) light through the filter, and perhaps this would be better illustrated using by showing the full filter response for 3 different wavelengths.

The primary use of intensified television recording systems for the data in this thesis requires that several timing issues be addressed. The television systems used by the Geophysical Institute are drop-frame NTSC systems which run at 29.97 frames per second. The use of the Horita timing system both provides a time stamp (using the SMPTE time code standard) and a common sync pulse to all video cameras. Furthermore, since the Horita system uses GPS for timing, the use of multiple Horita systems allows for spatially separated camera systems (*e.g.* the two aircraft platforms from the summer of 1994, or the simultaneous observations from both Mt. Evans and WIRO) to be sync-locked. The arrival time of the sync pulse to each camera attached to a single Horita synch generator is simultaneous to $<.5\mu$s, and between two spatially separated cameras the synch pulse is

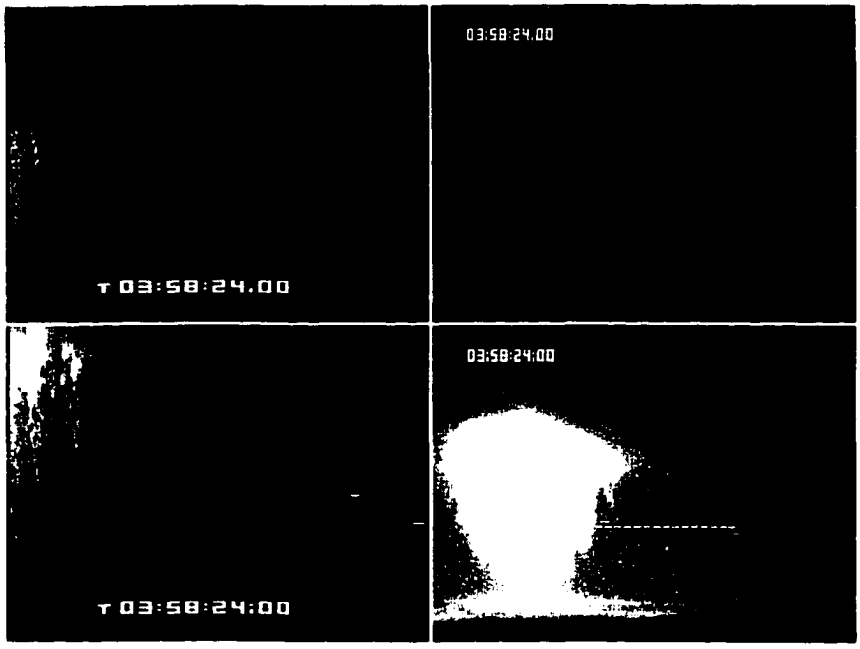

Figure B.3. CCD vs SIT readout, clearly illustrating image dump vs. scan read out.

accurate to $<10\mu s$. The use of several types of cameras (the Dage MTI system, the Pulnix ICCD, and the ISIT) with different types of readout also lead to timing issues.

Camera Readout

The use of multiple synced cameras can provide clear examples of the differences in their respective readout methodology. Figure B.3 illustrates that the CCD integrates the entire image plane for 17 ms and then "dumps" the array when it receives the video sync pulse, whereas the SIT system is a "scan-readout" type devices, meaning that the sync pulse triggers the readout of the top left corner, then the first scan line is readout to the right and the scan lines are readout sequentially. Figure B.3 shows that the sprite observed at July 24, 1996 3:58:24;00 SMPTE, or 3:58:23.970 UTC, actually began on the 177th scan line (out of 243), approximately midway through the first video field. The time code stamp is inserted into the video data stream at the point corresponding to the beginning of the field (the upper left pixel). Because of the scan readout, we can add 12.4 milliseconds to

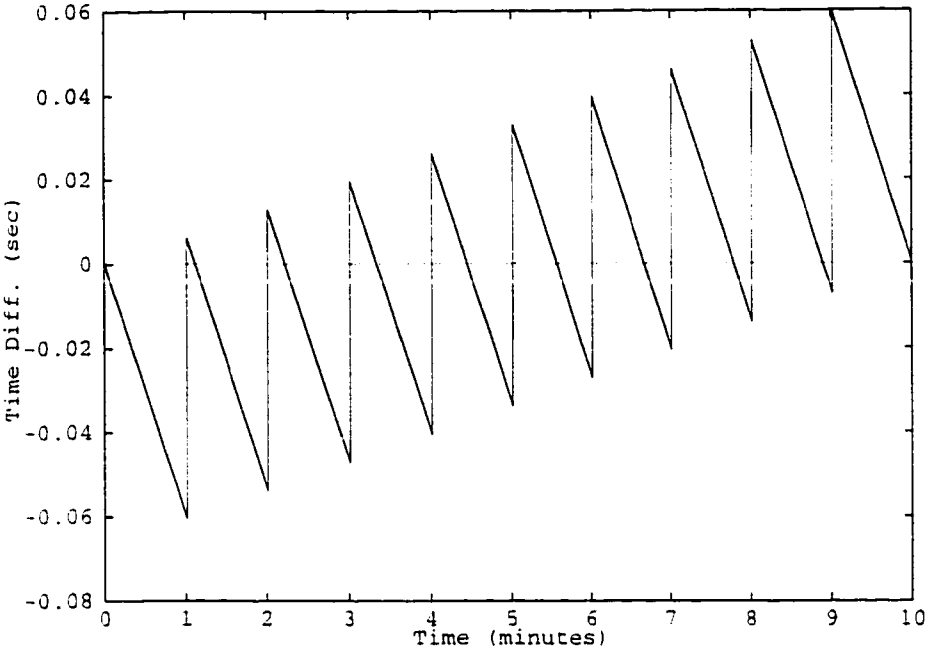

Figure B.4. SMPTE Time Code Showing Effects of drop frames. The plot shows a total of ten minutes worth of frames.

the initiation time of the sprite. so the GPS locked camera first observed light from the sprite at 3:58:23.9824.

SMPTE Time Code

The video observations are time-tagged using the SMPTE time code. a broadcast video time standard that is recorded in the `HH:MM:SS;FF` format where `FF` is a frame number between 00 and 29. This gives the television frame rate of 30 frames/second. Each frame is made of two interlaced fields. so video data resolution of 1/60 of a second is possible with standard VCR equipment (the University of Alaska Group uses 3/4" beta broadcast quality recorders. other groups use SVHS recorders). The interlaced video fields are marked so that when deinterlaced. the first field is tagged such that a comma (,) separates the second and frame numbers. while the second field is tagged so that a semi-colon (:) separates the second and frame numbers. However, SMPTE is actually a drop frame counting method in order

to compensate for the NTSC frame rate of 29.97 frames per second. This means that the 00 and 01 frames are dropped at the start of each minute except minutes which are even multiples of 10. During the drop-frame cycle, error accumulates at .001 sec. per sec. until the minute is reached at which time a .066 second compensation is inserted by dropping 2 frames. Figure B.4 illustrates the saw tooth pattern this creates in time code over a ten minute period.

Bibliography

Armstrong, R. A., J. A. Shorter, M. J. Taylor, D. M. Suszcynsky, W. A. Lyons, and L. S. Jeong, Photometric measurements in the SPRITES '95 & '96 campaigns of nitrogen second positive (399.8 nm) and first negative (427.8 nm) emissions. *J. Atmos. Solar Terr. Physics*, *60*, 787–799, 1998.

Ashmore, S. E., Unusual lightning, *Weather*, *5*, 331, 1950.

Barrington-Leigh, C. P. and U. S. Inan, Elves triggered by positive and negative lightning discharges. *Geophys. Res. Let.*, *26*(6), 683–686, 1999.

Barrington-Leigh, C. P., U. S. Inan, and M. Stanley, Elves: Photometric and video signatures. *EOS Supplement*, *80*(46), F216, 1999a.

Barrington-Leigh, C. P., U. S. Inan, M. Stanley, and S. A. Cummer, Sprites directly triggered by negative lightning discharges. *Geophys. Res. Let.*, *26*(99), 99–99, 1999b.

Bell, T. F., V. P. Pasko, and U. S. Inan, Runaway electrons as a source of red sprites in the mesosphere, *Geophys. Res. Let.*, *22*, 2127–2130, 1995.

Benesch, W., Intersystem collisional transfer of excitation in low altitude aurora, *J. Chem. Phys.*, *78*(6), 2978–2983, 1983.

Berger, K., Blitzstrom-parameter von aufwärtsblitzen, *Bull. Schweiz. Elektrotech. Ver.*, *69*, 353–360, 1978.

Bering, E. A., J. R. Benbrook, J. A. Garrett, A. Paredes, E. M. Wescott, D. D. Sentman, H. C. Stenbaek-Nielsen, and W. A. Lyons, The 1999 sprites balloon campaign, *EOS Supplement*, *80*(46), F216, 1999.

Berk, A., L. S. Bernstein, and D. C. Robertson, MODTRAN: A moderate spectral resolution model for LOWTRAN7, Technical Report GL-TR-89-0122, Phillips Laboratory, 1989.

Boccippio, D. J., E. R. Williams, S. J. Heckman, W. A. Lyons, I. T. Baker, and R. Boldi, Sprites, Extreme-Low-Frequency transients, and positive ground strokes, *Science*, *269*, 1088–1091, 1995.

Boeck, W. L., Lightning activity in typhoon Brenda, *EOS Supplement*, *68*, 1227, 1987.

Boeck, W. L., O. H. Vaughan, Jr., R. Blakeslee, B. Vonnegut, and M. Brook, Lightning induced brightening in the airglow layer, *Geophys. Res. Let.*, *19*, 99–102, 1992.

Boeck, W. L., O. H. Vaughan, Jr., R. Blakeslee, B. Vonnegut, M. Brook, and J. M. McKue, Observations of lightning in the stratosphere, *J. Geophys. Res.*, *100*, 1465–1475, 1995.

Boeck, W. L., O. H. Vaughan, Jr., R. J. Blakeslee, B. Vonnegut, and M. Brook, The role of the space shuttle videotapes in the discovery of sprites, jets and elves, *J. Atmos. Solar Terr. Physics*, *60*, 669–677, 1998.

Borst, W. L. and E. C. Zipf, Cross section for electron-impact excitation of the (0,0) first negative band of N_2^+ from threshold to 3 keV, *Phys. Rev. A*, *1*(3), 834–840, 1970.

Brasseur, G. and S. Solomon, *Aeronomy of the Middle Atmosphere: Chemistry and Physics of the Stratosphere and Mesosphere*, D. Reidel Publishing Company, 2nd edition, 1986, 1995 Reprint.

Brook, M., M. Stanley, P. Krehbiel, W. Rison, C. B. Moore, C. Barrington-Leigh, D. Suszcynsky, T. Nelson, and W. Lyons, Correlated electric field, video, and photometric evidence of charge transfer within sprites, *EOS Supplement*, *78*(46), 1997, Poster.

Bucsela, E., M. J. Heavner, J. S. Morrill, S. Berg, C. Seifring, W. Benesch, E. M. Wescott, D. Sentman, D. L. Hampton, and D. R. Moudry, $N_2(B^3\Pi_g)$ and $N_2^+(A^2\Pi_u)$ vibrational distributions observed in sprites, *Geophys. Res. Let.*, 1999, in prep.

Bucsela, E. J. and W. E. Sharp, NI 8680 and 8629 Å multiplets in the dayglow, *J. Geophys. Res.*, *102*, 2457–2466, 1997.

Capitelli, M. and E. Molinari, *Plasma Chemistry II*, volume 90 of *Topics in Current Chemistry*, chapter Kinetics of Dissociation Processes in Plasmas in the Low and Intermediate Pressure Range, pp. 59–109. Springer-Verlag, New York, 1980.

Chern, J.-L., L.-C. Lee, K.-R. Chen, R.-R. Hsu, H.-T. Su, and C.-C. Tsai, ISUAL project: Observations of red sprites on Taiwan's ROCSAT-2, *EOS Supplement*, *79*(45), F176, 1998.

Cho, M. and M. J. Rycroft, Computer simulation of the electric field structure and optical emission from cloud-top to the ionosphere, *J. Atmos. Solar Terr. Physics*, *60*(7), 871–888, 1998.

Christian, H. J., R. J. Blakeslee, D. J. Boccippio, W. L. Boeck, D. E. Buechler, K. T. Driscoll, S. J. Goodman, J. M. Hall, W. J. Koshak, D. M. Mach, and M. F. Stewart, Global frequency and distribution of lightning as observed by the Optical Transient Detector (OTD), in *11th International Conference on Atmospheric Electricity*, pp. 726–729, 1999.

Corliss, W. R., *Handbook of Unusual Natural Phenomena*, Gramercy Books, 1977.

Cornette, W. M., Atmospheric Propagation and Radiative Transfer (APART) computer code (version 7.00), Technical Report R-062-90, Photon Research Associates, Inc., 1990.

Cornette, W. M., P. K. Acharya, and G. P. Anderson, Using the MOSART code for atmospheric correction, *IEEE Conf. Proc. Int. Geosci. and Rem. Sens. Sympos.*, *1*, 215–219, 1994.

Cummer, S. and M. Stanley, Submillisecond resolution lightning currents and sprite development: Observations and implications, *Geophys. Res. Let.*, *26*(20), 3205–328, 1999.

Cummer, S. A. and U. S. Inan, Measurement of charge transfer in sprite-producing lightning using ELF radio atmospherics, *Geophys. Res. Let.*, *24*(12), 1731–1734, 1997.

Cummer, S. A., U. S. Inan, T. F. Bell, and C. P. Barrington-Leigh, ELF radiation produced by electrical currents in sprites, *Geophys. Res. Let.*, *25*(8), 1281–1284, 1998.

Cummins, K. L., M. J. Murphy, E. A. Bardo, W. L. Hiscox, R. B. Pyle, and A. E. Pifer, A combined TOA/MDF technology upgrade of the U.S. National Lightning Detection Network, *J. Geophys. Res.*, *103*(D8), 9035–9044, 1998.

Deehr, C. S., *A Spectrophotometric Study of the Aurora of 27 November 1959 at College, Alaska*, Master's thesis, University of Alaska Fairbanks, 1961.

Deehr, C. S., E. M. Wescott, D. D. Sentman, H. C. Stenbaek-Nielsen, M. J. Heavner, D. R. Moudry, C. L. Siefring, J. S. Morrill, and E. J. Bucsela, New evidence for ionization of blue starters and blue jets, *EOS Supplement*, *79*(45), F136, 1998.

Delamere, P. A., *Analysis of optical observations and three-dimensional hybrid code simulation of the CRRES G1, G9, and G11A chemical releases*, Ph.D. thesis, University of Alaska Fairbanks, 1998.

Desroschers, J. T., M. J. Heavner, D. L. Hampton, D. D. Sentman, and E. M. Wescott, A preliminary morphology of optical transients above thunderstorms, *EOS Supplement*, *76*(46), F105, 1995.

Dewan, E. M., R. H. Picard, R. R. O'Neil, H. A. Gardiner, J. Gibson, J. D. Mill, E. Richards, M. Kendra, and W. O. Gallery, MSX satellite observations of thunderstorm-generated gravity waves in mid-wave infrared images of the upper stratosphere, *Geophys. Res. Let.*, *25*(7), 939–942, 1998.

Dial, R. and M. Taylor, Investigation of lightning induced elves over the great plains, CEDAR 1999 Workshop.

Dowden, R., C. Rodger, and D. Nunn, Minimum sprite plasma density as determined by VLF scattering, *Geophys. Res. Let.*, 2000, submitted.

Dowden, R. L., J. B. Brundell, and C. J. Rodger, Temporal evolution of very strong Trimpis observed at Darwin, Australia, *Geophys. Res. Let.*, *24*(19), 2419–2422, 1997.

Everett, W. H., Rocket lightning, *Nature*, *68*, 599, 1903.

Fernsler, R. and H. Rowland, Models of lightning-produced sprites and elves, *J. Geophys. Res.*, *101*, 29653, 1996.

Fishman, G. J., P. N. Bhat, R. Malozzi, J. M. Horack, T. Koshut, C. Kouveliotou, G. N. Pendleton, C. A. Meegan, R. B. Wilson, W. S. Paciesas, S. J. Goodman, and H. J. Christian, Discovery of intense gamma-ray flashes of atmospheric origin, *Science*, *264*, 1313, 1994.

Fogle, B. T., *Noctilucent Clouds*, Ph.D. thesis, University of Alaska Fairbanks, 1966.

Franz, R. D., R. J. Nemzek, and J. R. Winckler, Television images of a large upward electrical discharge above a thunderstorm system, *Science*, *249*, 48–51, 1990.

Fritts, D. C. and T. E. vanZandt, Spectral estimates of gravity wave energy and momentum fluxes, I. Energy dissipation, acceleration, and constraints, *J. Atmos. Sci.*, *50*, 3685–3694, 1993.

Fukunishi, H., Y. Takahashi, M. Kubota, and K. Sakanoi, Lower ionosphere flashes induced by lightning discharges, *EOS Supplement*, *76*(46), F114, 1995.

Fukunishi, H., Y. Takahashi, M. Kubota, K. Sakanoi, U. S. Inan, and W. A. Lyons, Elves: Lightning-induced transient luminous events in the lower ionosphere, *Geophys. Res. Let.*, *23*, 2157-2160, 1996.

Fukunishi, H., Y. Takahashi, M. Sato, A. Shono, M. Fujito, and Y. Watanabe, Ground-based observations of ULF transients excited by strong lightning discharges producing elves and sprites, *Geophys. Res. Let.*, *24*(23), 2973–2976, 1997.

Fukunishi, H., Y. Takahashi, A. Uchida, M. Sera, and K. R. Miyasato, Occurrences of sprites and elves above the Sea of Japan near Hokuriku in winter, *EOS Supplement*, *80*(46), F217, 1999.

Füllekrug, M., A. C. Fraser-Smith, and S. C. Reising, Ultra-slow tails of sprite-associated lightning flashes, *Geophys. Res. Let.*, *25*(18), 3497–3500, 1998.

Gales, D., Another account, *Weatherwise*, *35*(82), 72, 1982.

Gerken, E. A., U. S. Inan, C. P. Barrington-Leigh, and M. Stanley, Results from a new telescopic imager: A survey of sprite structures, *EOS Supplement*, *79*(45), F137, 1998.

Gilmore, F. R., R. R. Laher, and P. J. Espy, Franck-condon factors, r-centroids, electronic transition moments, and einstein coefficients for many nitrogen and oxygen band systems, *J. Phys. Chem. Ref. Data*, *21*(5), 1005, 1992.

Gomes, C. and V. Cooray, Long impulse currents associated with positive return strokes, *J. Atmos. Solar Terr. Physics*, *60*, 693–699, 1998.

Green, B. D., M. E. Fraser, W. T. Rawlins, L. Jeong, W. A. Blumberg, S. B. Mende, G. R. Swenson, D. L. Hampton, E. M. Wescott, and D. D. Sentman, Molecular excitation in sprites, *Geophys. Res. Let.*, *23*(23), 2161–2164, 1996.

Groves, K. M., J. M. Quinn, E. R. Shinn, P. Ning, and M. R. Cox, An upper limit on ionization in sprites, *EOS Supplement*, *79*(45), F165, 1998.

Guttman, A., Extinction coefficient measurements on clear atmospheres and thin cirrus clouds, *Applied Optics*, *7*(12), 2377–2381, 1968.

Hallinan, T. J., J. Kimball, H. C. Stenbaek-Nielsen, and C. S. Deehr, Spectroscopic evidence for suprathermal electrons in enhanced auroras, *J. Geophys. Res.*, *102*, 7501–7508, 1997.

Hallinan, T. J., J. Kimball, D. Osborne, and C. S. Deehr, Spectra of type-B red lower borders, *J. Geophys. Res.*, *103*(A6), 11635–11640, 1998.

Hampton, D. L., *Optical Observations of Critical Ionization Velocity Chemical Releases in the Ionosphere: The Role of Collisions*, Ph.D. thesis, University of Alaska Fairbanks, 1996.

Hampton, D. L., M. J. Heavner, E. M. Wescott, and D. D. Sentman, Optical spectral characteristics of sprites, *Geophys. Res. Let.*, *23*(1), 89–92, 1996.

Hardman, S. F., R. L. Dowden, J. B. Brundell, J. L. Bahr, Z. Kawasaki, and C. J. Rodger, Sprites in Australia's Northern Territory, *EOS Supplement*, *79*(45), F135, 1998.

Harris, D. C. and M. D. Bertolucci, *Symmetry and Spectroscopy: An Introduction to Vibrational and Electonic Spectroscopy*, Dover Publications, Inc., 1989.

Heavner, M. and M. Taylor, Transient optical emissions in the upper atmosphere, CEDAR Post, 1999.

Heavner, M. J., D. L. Hampton, D. D. Sentman, and E. M. Wescott, Sprites over Central and South America, *EOS Supplement*, *76*(46), F115, 1995.

Heavner, M. J., D. D. Sentman, D. L. Hampton, and E. M. Wescott, Optical spectra of sprites, in *Proceedings of 10th International Conference on Atmospheric Electricity, June 10-14*, 1996.

Heavner, M. J., D. R. Moudry, D. D. Sentman, E. M. Wescott, J. S. Morrill, C. Siefring, E. J. Bucsela, D. L. Osborne, J. T. Desrochers, H. Stenbaek-Nielsen, J. Winick, J. Kristl, T. Hudson, L. M. Peticolas, and V. Besser, Ionization in sprites, *EOS Supplement*, *79*(45), F165, 1998.

Heavner, M. J., J. S. Morrill, E. J. Bucsela, D. D. Sentman, C. L. Siefring, E. Wescott, and D. R. Moudry, NUV/Blue spectral observations of sprites in the 320-460 nm region: N_2 (2PG) emissions, *Geophys. Res. Let.*, 2000, in prep.

Herzberg, G., *Molecular Spectra and Molecular Structure I. Spectra of Diatomic Molecules*, Krieger Publishing Company, 2 edition, 1989.

Hines, C. O., Dynamical heating of the upper atmosphere, *J. Geophys. Res.*, *70*, 177, 1965.

Hoffman, W. C., The current-jet hypothesis of whistler generation, *J. Geophys. Res.*, *65*(7), 2047-2054, 1960.

Inan, U., C. Barrington-Leigh, S. Hansen, V. S. Glukhov, T. F. Bell, and R. Rairden, Rapid lateral expansion of optical luminosity in lightning-induced ionospheric flashes referred to as 'elves', *Geophys. Res. Let.*, *24*(5), 583–586, 1997.

Inan, U. S., VLF heating of the lower ionosphere, *Geophys. Res. Let.*, *17*, 729-731, 1990.

Inan, U. S., T. F. Bell, and J. V. Rodrigues, Heating and ionization of the lower ionosphere by lightning, *J. Geophys. Res.*, *18*, 705–708, 1991.

Inan, U. S., T. F. Bell, V. P. Pasko, D. D. Sentman, E. M. Wescott, and W. A. Lyons, VLF signatures of ionospheric disturbances associated with sprites, *Geophys. Res. Let.*, *22*, 3461–3464, 1995.

Inan, U. S., C. P. Barrington-Leigh, E. A. Gerken, and T. F. Bell, Telescopic imaging of fine structure in sprites, *EOS Supplement*, *79*(45), F164, 1998.

Kantor, A. J. and A. E. Cole, Zonal and meridional winds to 120 kilometers, *J. Geophys. Res.*, *69*(24), 5131–5140, 1964.

Katayama, D. H., Collision induced electronic energy transfer between the $A^2\Pi_u(v = 4)$ and $X^2\Sigma_g^+(v = 8)$ rotational manifolds of N_2^+, *J. Chem. Phys.*, *81*, 3495–3494, 1984.

Katayama, D. H., T. A. Miller, and V. E. Bondybey, Collisional deactivation of selectively excited N_2^+, *J. Chem. Phys.*, *72*(10), 5469–5475, 1980.

Kimball, J., Calculations for the Deehr TV spectrograph, *Proceedings of UAF*, *1*(1), 1–23, 1996.

Krehbiel, P. R., R. J. Thomas, W. Rison, T. Hamlin, J. Harlin, and M. Davis, Lightning mapping observations in central oklahoma, *EOS*, 1999, in press.

Lehtinen, N. G., M. Walt, U. S. Inan, T. F. Bell, and V. P. Pasko, γ-ray emission produced by a relativistic beam of runaway electrons accelerated by quasi-electrostatic thundercloud fields, *Geophys. Res. Let.*, *23*(19), 2645–2648, 1996.

Li, Y. Q., R. H. Holzworth, H. Hu, M. McCarthy, R. D. Massey, P. M. Kintner, J. V. Rodrigues, U. S. Inan, and W. C. Armstrong, Anomalous optical events detected by rocket-borne sensor in the WIPP campaign, *J. Geophys. Res.*, *96*(A2), 1315–1326, 1991.

Lofthus, A. and P. H. Krupenie, The spectrum of molecular nitrogen, *J. Phys. Chem. Ref. Data*, *6*(1), 113–307, 1977.

Lyons, W. A., A sensor system to monitor cloud-to-stratosphere electrical discharges, *Final Report, NASA contract NAS10-1194*, 1993.

Lyons, W. A., Characteristics of luminous structures in the stratosphere above thunderstorms as imaged by low-light video, *Geophys. Res. Let.*, *21*, 875–878, 1994.

Lyons, W. A. and T. E. Nelson, The Colorado SPRITES '95 campaign: Initial results, *EOS Supplement*, *76*(46), 113, 1995.

Lyons, W. A. and E. R. Williams, Preliminary investigations of the phenomenology of cloud-to-stratosphere lightning discharges, Conf. Atmospheric Electricity, St. Louis, Missouri, AMS, 1993.

Lyons, W. A. and E. R. Williams, Some characteristics of cloud-to-stratosphere 'lightning' and considerations for its detection, Preprint, Fifth Symposium on Global Change Studies, pp. 360–367, Nashville, Tennessee, AMS, 1994.

Lyons, W. A., I. Baker, T. E. Nelson, J. R. Winckler, R. J. Nemzek, P. R. Malcom, E. R. Williams, and D. Boccippio, The 1994 Colorado SPRITE campaign: Initial results, *EOS Supplement*, *75*(44), 108, 1994.

Lyons, W. A., T. E. Nelson, E. R. Williams, J. A. Cramer, and T. R. Turner, Enhanced positive cloud-to-ground lightning in thunderstorms ingesting smoke from fires, *Science*, *282*, 77-80, 1998.

Lyons, W. A., T. E. Nelson, J. L. Eastman, R. A. Armstrong, E. R. Williams, D. S. Suszcynsky, M. A. Taylor, Y. Takahashi, E. A. Bering, and J. R. Benbrook, Sprites'99 campaign highlights and the Yucca Ridge Field Station, *EOS Supplement*, *80*(46), F216, 1999.

MacKenzie, T. and H. Toynbee, Meteorological phenomena, *Nature*, *33*, 26, 1886.

Mackerras, D., M. Darveniza, R. E. Orville, E. R. Williams, and S. J. Goodman, Global lightning: Total, cloud and ground flash estimate, *J. Geophys. Res.*, *103*(D16), 19791–19809, 1998.

Malan, D. J., Sur les descharges orageuses dans la haute atmosphere, *Academie des Sciences*, 1937.

Marshall, L. H., L. C. Hale, C. L. Croskey, and W. A. Lyons, Electromagnetics of sprite- and elve-associated sferics, *J. Atmos. Solar Terr. Physics*, *60*, 771–786, 1998.

McHarg, M., R. Haaland, D. Moudry, and H. Stenbaek-Nielsen, High speed photometric observations of sprites, *EOS Supplement*, *80*(46), F217, 1999.

Mende, S. B., R. L. Rairden, and G. R. Swenson, Sprite spectra: $N_2$1PG band identification, *Geophys. Res. Let.*, *22*, 2633–2636, 1995.

Milikh, G., J. A. Valdivia, and K. Papadopoulos, Spectrum of red sprites, *J. Atmos. Solar Terr. Physics*, *60*(7), 907–915, 1998a.

Milikh, G. M., K. Papadopoulos, and C. L. Chang, On the physics of high altitude lightning, *Geophys. Res. Let.*, *22*, 85–88, 1995.

Milikh, G. M., J. A. Valdivia, and K. Papadopoulos, Model of red sprite optical spectra, *Geophys. Res. Let.*, *24*(8), 833–836, 1997.

Milikh, G. M., D. A. Usikov, and J. A. Valdivia, Model of infrared emission from sprites, *J. Atmos. Solar Terr. Physics*, *60*(7), 895–905, 1998b.

Mishin, E., Ozone layer perturbation by a single blue jet, *Geophys. Res. Let.*, *24*(15), 1919–1922, 1997.

Mlynczak, M. G. and S. Solomon, A detailed evaluation of the heating efficiency in the middle atmosphere, *J. Geophys. Res.*, *98*(D6), 10517–10541, 1993.

Mojzsis, S. J., R. Krishnamurthy, and G. Arrhenius, *Before RNA and After: Geophysical and Geochemical Constraints on Molecular Evolution*, chapter 1, pp. 1–47, number 38 in Cold Spring Harbor Monograph Series, Cold Spring Harbor Laboratory Press, 2 edition, 1999.

Morrill, J. S. and W. M. Benesch, Role of $N_2(A'^5\Sigma_g^+)$ in the enhancement of $N_2B^3\Pi_g(v = 10)$ populations in the afterglow, *J. Chem. Phys.*, *101*(8), 6529 - 6537, 1994.

Morrill, J. S. and W. M. Benesch, Auroral N_2 emissions and the effect of collisional processes on N_2 triplet state vibrational populations, *J. Geophys. Res.*, *101*, 261–274, 1996.

Morrill, J. S., E. J. Bucsela, V. P. Pasko, S. L. Berg, M. J. Heavner, D. R. Moudry, W. M. Benesch, E. M. Wescott, and D. D. Sentman, Time resolved N_2 triplet state vibrational populations and emissions associated with red sprites, *J. Atmos. Solar Terr. Physics*, *60*, 811–829, 1998.

Moudry, D. R., M. J. Heavner, D. D. Sentman, E. M. Wescott, J. S. Morrill, and C. Siefring, Morphology of sprites, *EOS Supplement*, *79*(45), F136, 1998.

Nelson, T., *Spatial Relationships between Radar Reflectivity and Sprite and Elve Producing Cloud-to-Ground Lightning Strokes*, Master's thesis, Mankato State University, 1997.

Nicolet, M., On the production of nitric oxide by cosmic rays in the mesosphere and stratosphere, *Planet. Space Sci.*, *23*, 637, 1975.

Osborne, D. L., D. D. Sentman, E. M. Wescott, D. L. Hampton, and M. J. Heavner, Video imaging systems used in the sprites94 aircraft campaign, *EOS Supplement*, *75*(44), 115, 1994, Poster Presented at Fall AGU Meeting, 1994.

Pasko, V. P., *Dynamic Coupling of Quasi-Electrostatic Thundercloud Fields to the Mesosphere and Lower Ionosphere: Sprites and Jets*, Ph.D., Stanford University, 1996.

Pasko, V. P. and U. S. Inan, Recovery signatures of lightning-associated VLF perturbations as a measure of the lower ionosphere, *J. Geophys. Res.*, *99*(A9), 17523–17537, 1994.

Pasko, V. P., U. S. Inan, Y. N. Taranenko, and T. F. Bell, Heating, ionization and upward discharges in the mesosphere due to intense quasi-electrostatic thundercloud fields, *Geophys. Res. Let.*, *22*, 365–368, 1995.

Pasko, V. P., U. S. Inan, T. F. Bell, and Y. N. Taranenko, Sprites produced by quasi-electrostatic heating and ionization in the lower ionosphere, *J. Geophys. Res.*, *102*(A3), 4529–4561, 1997.

Pasko, V. P., U. S. Inan, and T. F. Bell, Ionospheric effects due to electrostatic thundercloud fields, *J. Atmos. Solar Terr. Physics*, *60*(7), 863–870, 1998.

Pasko, V. P., U. S. Inan, and T. F. Bell, Mesospheric electric field transients due to tropospheric lightning discharges, *Geophys. Res. Let.*, *26*(9), 1247–1250, 1999.

Picard, R. H., U. S. Inan, V. P. Pasko, J. R. Winick, and P. P. Wintersteiner, Infrared glow above thunderstorms?, *Geophys. Res. Let.*, *24*(21), 2635–2638, 1997.

Piper, L. G., State-to-state $N_2(A^3\Sigma_u^+)$ energy pooling reactions. I. The formation and quenching of $N_2(C^3\Pi_u)$ and Herman infrared system, *J. Chem. Phys.*, *88*, 231–239, 1988a.

Piper, L. G., State-to-state $N_2(A^3\Sigma_u^+)$ energy pooling reactions. II. The formation and quenching of $N_2(B^3\Pi_g v = 1 - 12)$, *J. Chem. Phys.*, *88*, 6911–6921, 1988b.

Piper, L. G., B. D. Green, W. A. M. Blumberg, and S. J. Wolnik, N_2^+ Meinel band quenching, *J. Chem. Phys.*, *82*, 3139, 1985.

Piper, L. G., B. D. Green, W. A. M. Blumberg, and S. J. Wolnik, Electron impact excitation of the N_2^+ Meinel band, *J. Phys. B: At. Mol. Phys.* *19*, 3327–3332, 1986.

Rees, M. H., *Physics and chemistry of the upper atmosphere*, Cambridge atmospheric and space science series. Cambridge University Press, 1989.

Reising, S. C., *Remote sensing of the electrodynamic coupling between thunderstorm systems and the Mesosphere/low Ionosphere*, Ph.D. thesis, Stanford University, 1998.

Reising, S. C., U. S. Inan, T. F. Bell, and W. A. Lyons, Evidence for continuing current in sprite-producing cloud-to-ground lightning, *Geophys. Res. Let.*, *23*, 3639–3642, 1996.

Reising, S. C., U. S. Inan, and T. F. Bell, ELF sferic energy as a proxy indicator for sprite occurrence, *Geophys. Res. Let.*, *26*(7), 987–990, 1999a.

Reising, S. C., U. S. Inan, T. F. Bell, Y. Takahashi, and M. Sera, Further evidence of electrical current in sprites using measurements of ELF radio atmospherics and high time-resolution multi-anode array photometer observations, *National Radio Science Meeting*, 1999b.

Rison, W., R. J. Thomas, P. R. Krehbiel, T. Hamlin, and J. Harlin, A GPS-based three-dimensional lightning mapping system: Initial observations in central new mexico, *Geophys. Res. Let.*, *26*(23), 3573–3576, 1999.

Rodger, C. J., *High Altitude Phenomena Associated With Thunderstorms*, Ph.D. thesis, University of Otago, Dunedin New Zealand, 1997.

Rodger, C. J., Red sprites, upward lightning and VLF perturbations, *Reviews of Geophysics*, *37*(3), 317–336, 1999.

Rodger, C. J., J. R. Wait, and R. L. Dowden, Scattering of VLF from an experimentally described sprite, *J. Atmos. Solar Terr. Physics*, *60*, 765–769, 1998.

Roussel-Dupré, R., E. Symbalisty, Y. Taranenko, and V. Yukhimuk, Simulations of high-altitude discharges initiated by runaway breakdown, *J. Atmos. Solar Terr. Physics*, *60*(7), 917-940, 1998.

Roussel-Dupré, R. A. and E. Blanc, HF echoes from ionization potentially produced by high-altitude discharges, *J. Geophys. Res.*, *102*(A3), 4613-4622, 1997.

Rowland, H., R. Fernsler, J. Huba, and P. Bernhardt, Lightning drive EMP in the upper atmosphere, *Geophys. Res. Let.*, *22*, 361-364, 1995.

Rowland, H., R. Fernsler, and P. Bernhardt, Breakdown of the neutral atmosphere in the D-region due to lightning driven electromagnetic pulses, *J. Geophys. Res.*, *101*, 7935-7945, 1996.

Rowland, H. L., Theories and simulations of elves, sprites, and blue jets, *J. Atmos. Solar Terr. Physics*, *60*(7), 831-844, 1998.

Rumi, G. G., VHF radar echoes associated with atmospheric phenomena, *J. Geophys. Res.*, *62*, 547-564, 1957.

Rybicki, G. B. and A. P. Lightman, *Radiative Processes in Astrophysics*, John Wiley & Sons, 1979.

São Sabbas, F. T., *Estudo da relaçõo entre Sprites e os relâmpagos das tempestades associadas (Study of the relationship between Sprites and lightning from the associated storms)*, Master's thesis, Instituto Nacional de Pesquisas Espaciais, São José dos Campos, SP, Brazil, 1995.

Salanave, L. E., *Lightning and Its Spectrum: An atlas of photographs*, The University of Arizona Press, 1980.

Sentman, D., Electrical excitation of the middle and upper atmosphere by lightning: Special issue of the Journal of Atmospheric and Solar-Terrestrial Physics, *J. Atmos. Solar Terr. Physics*, *60*(7-9), 667, 1998.

Sentman, D. and E. Wescott, *From the Sun: Auroras, Magnetic Storms, Solar Flars. Cosmic Rays*. chapter Red Sprites and Blue Jets: Transient Electrical Effects of Thunderstorms on the Middle and Upper Atmospheres, pp. 45–56. American Geophysical Union, 1998.

Sentman, D. D. and B. J. Fraser, Simultaneous observations of schumann resonances in california and australia: Evidence for intensity modulation by the local height of the D region. *J. Geophys. Res.*, *96*(A9), 15973–15984, 1991.

Sentman, D. D. and E. M. Wescott, Video observations of upper atmospheric optical flashes recorded from an aircraft. *Geophys. Res. Let.*, *20*, 2857–2860, 1993.

Sentman, D. D. and E. M. Wescott, Red sprites and blue jets. *Geophysical Institute Video Production, University of Alaska, Fairbanks*, 1994.

Sentman, D. D., E. M. Wescott, J. D. Williams, D. L. Hampton, M. J. Heavner, and D. L. Osborne, ELF/VLF signatures of red sprites and blue jets. *EOS Supplement*, *75*(44), 108, 1994.

Sentman, D. D., E. M. Wescott, D. L. Osborne, M. J. Heavner, and D. L. Hampton, The Peru95 sprites campaign: Overview. *EOS Supplement*, *76*(17), S66, 1995a.

Sentman, D. D., E. M. Wescott, D. L. Osborne, D. L. Hampton, and M. J. Heavner, Preliminary results from the Sprites94 aircraft campaign: 1. Red Sprites. *Geophys. Res. Let.*, *22*, 1205–1208, 1995b.

Sentman, D. D., M. J. Heavner, D. L. Hampton, and E. M. Wescott, Branching structure in sprite tendrils, in *Proceedings of 10th International Conference on Atmospheric Electricity, June 10-14, 1996*, 1996a.

Sentman, D. D., E. M. Wescott, M. J. Heavner, and D. R. Moudry, Observations of sprite beads and balls. *EOS Supplement*, *77*(46), F61, 1996b.

Sentman, D. D., E. M. Wescott, M. J. Heavner, and D. R. Moudry, Horizontal banded structure in sprites. *EOS Supplement*, 1997.

Sentman, D. D., E. M. Wescott, J. R. Winick, C. L. Siefring, L. S. Jeong, R. H. Picard, J. Schummers, P. A. Bernhardt, J. H. Bowles, E. J. Bucsela, and J. S. Morrill. Energetics of upper atmospheric excitation by lightning (EXL), 1998, GI 98-02 NASA proposal.

Sentman, D. D., E. M. Wescott, J. Winick, C. Siefring, J. Morrill, D. Baker, P. Bernhardt, M. Heavner, D. Moudry, D. Osborne, J. Desrochers, L. Peticolas, and V. Besser, The EXL98 sprites campaign, *EOS Supplement*, *79*(45), F164, 1998b.

Shaw, G. E., Above cloud electrical discharges: The effect of aerosol transport. *Geophys. Res. Let.*, *25*(23), 4317–4320, 1998.

Shemansky, D. E., J. M. Ajello, and I. Kanik, Electron excitation functions of the N_2 second positive system, *Astrophysical Journal*, *452*, 472–479, 1995.

Siefring, C. L., J. S. Morrill, E. J. Bucsela, V. P. Pasko, S. L. Berg, W. M. Benesch, E. M. Wescott, and M. J. Heavner, Predicted near-UV spectroscopy of sprites, *EOS Supplement*, *78*(46), 1997, Poster A22C-05 AGU.

Slinker, S. and A. W. Ali, Electron excitation and ionization rate coefficients for N_2, O_2, NO, N, O. Technical report, Naval Research Labs, 1982.

Stanley, M., P. Krehbiel, M. Brook, C. Moore, W. Rison, and B. Abrahams, High speed video of initial sprite development, *Geophys. Res. Let.*, *26*(20), 3201–3204, 1999.

Stanley, M. A., M. Brook, S. A. Cummer, C. P. Barrington-Leigh, and E. A. Gerken, Broadband detection and characterization of day-time sprites and of negative cgs which initiated sprites, *EOS Supplement*, *79*(45), F177, 1998.

Stanton, P. N. and R. M. St. John, Electron excitation of the first positive bands of N_2 and of the first negative and Meinel bands of N_2^+, *J. Optical Soc. Amer.*, *59*(3), 252–260, 1969.

Stenbaek-Nielsen, H., D. R. Moudry, E. M. Wescott, D. D. Sentman, M. J. Heavner, and F. T. São Sabbas, Sprite observations at 1000 frames per second, *EOS Supplement*, *80*(46), F216, 1999.

Stenbaek-Nielsen, H. C., E. Wescott, and T. Hallinan, Observed barium emission rates, *J. Geophys. Res.*, *98*(A10), 17491–17500, 1993.

Sukhorukov, A. I. and P. Stubbe, Problems of blue jet theories, *J. Atmos. Solar Terr. Physics*, *60*, 725–732, 1998.

Suszcynsky, D. M., R. Roussel-Dupré, W. A. Lyons, and R. A. Armstrong, Blue-light imagery and photometry of sprites, *J. Atmos. Solar Terr. Physics*, *60*(7), 801–809, 1998.

Swenson, G. R. and S. B. Mende, OH emission and gravity waves (including a breaking wave) in all-sky imagery from Bear Lake, UT, *Geophys. Res. Let.*, *21*(20), 2239–2242, 1994.

Takahashi, Y., Y. Watanabe, A. Uchida, M. Sera, M. Sato, and H. Fukunishi, Energy distributions of electrons exciting sprites and elves inferred from the fast array photometer observations, *EOS Supplement*, *79*(45), F175, 1998.

Takeuti, T., M. Nakano, M. Brook, D. J. Raymond, and P. Krehbiel, The anomalous winter thunderstorms of the Hokuriku coast, *J. Geophys. Res.*, *83*, 2385–2394, 1978.

Taranenko, Y. N. and R. Roussel-Dupré, High-altitude discharges and gamma-ray flashes: A manifestation of runaway air breakdown, *Geophys. Res. Let.*, *23*(5), 571–574, 1996.

Taranenko, Y. N., U. S. Inan, and T. F. Bell, Optical signatures of lightning-induced heating of the D region, *Geophys. Res. Let.*, *19*(18), 1815–1818, 1992.

Taylor, L. L., Mesospheric heating due to intense tropospheric convection, *NASA Contractor Report 3132*, 1979.

Tsunoda, R. T., R. C. Livingston, J. J. Buonocore, W. A. Lyons, T. E. Nelson, and M. C. Kelley, Evidence of a high-altitude discharge process responsible for radar echoes at 24.4 MHz, *J. Atmos. Solar Terr. Physics*, *60*(7), 957–964, 1998.

Uman, M. A., *The Lightning Discharge*, volume 39 of *International Geophysics Series*, Academic Press, Inc., Orlando, Florida, 1987.

Uman, M. A., *Lightning*, Dover, New York, 1994.

Valdivia, J. A., *The Physics of High Altitude Lightning*, Ph.D. thesis, University of Maryland at College Park, 1997.

Vallance Jones, A., *Aurora*. D. Reidel Publishing Co., 1974.

Van Zyl, B., M. W. Gealy, and H. Neumann, N_2^+ first-negative emission cross section for low-energy H^+ and H impact on N_2, *Phys. Rev. A*, *28*(4), 2141–2150, 1983.

Vaughan, Jr., O. H. and B. Vonnegut, Lightning to the ionosphere?, *Weatherwise*, *35*(82), 70–71, 1982.

Vaughan, Jr., O. H. and B. Vonnegut, Recent observations of lightning discharges from the top of a thundercloud into the clear air above, *J. Geophys. Res.*, *94*, 13179–13182, 1989.

Vaughan, Jr., O. H., R. Blakeslee, W. L. Boeck, B. Vonnegut, M. Brook, and J. McKune, Jr., A cloud-to-space lightning as recorded by the space shuttle payload bay TV camera, *Mon. Weather Rev.*, *120*, 1459, 1992.

Vonnegut, B., Cloud-to-stratosphere lightning, *Weather*, *35*(2), 59–60, 1980.

Vonnegut, B., Vertical lightning "letters", *Weatherwise*, *37*(2), 61, 1984.

Vonnegut, B., O. H. Vaughan, Jr., and M. Brook, Photographs of lightning from the space shuttle, *Bull. Am. Meteor. Soc.* *64*, 150–151, 1983.

Vonnegut, B., O. H. Vaughan, Jr., M. Brook, and P. Krehbiel, Mesoscale observations of lightning from the space shutle, *Bull. Am. Meteor. Soc.*, *66*, 20–29, 1985.

Wescott, E. M., D. D. Sentman, D. L. Osborne, M. J. Heavner, and D. L. Hampton, The Peru95 sprites campaign: Aircraft video observations of equatorial sprites, *EOS Supplement*, *76*(17), S66, 1995a.

Wescott, E. M., D. D. Sentman, D. L. Osborne, D. L. Hampton, and M. J. Heavner, Preliminary results from the Sprites94 aircraft campaign: 2. Blue Jets, *Geophys. Res. Let.*, *22*, 1209–1212, 1995b.

Wescott, E. M., D. D. Sentman, M. J. Heavner, D. L. Hampton, D. L. Osborne, and O. H. Vaughan, Jr., Blue starters: Brief upward discharges from an intense Arkansas thunderstorm, *Geophys. Res. Let.*, *23*(16), 2153–2156, 1996a.

Wescott, E. M., D. D. Sentman, M. J. Heavner, T. J. Hallinan, D. L. Hampton, and D. L. Osborne, The optical spectrum of aircraft St. Elmo's fire, *Geophys. Res. Let.*, *23*(25), 3687–3690, 1996b.

Wescott, E. M., D. D. Sentman, M. J. Heavner, D. L. Hampton, and O. H. Vaughan, Jr., Blue Jets: their relationship to lightning and very large hailfall, and their physical mechanisms for their production, *J. Atmos. Solar Terr. Physics*, *60*, 713–724, 1998a.

Wescott, E. M., D. D. Sentman, M. J. Heavner, D. L. Hampton, W. A. Lyons, and T. Nelson, Observations of 'Columniform' sprites, *J. Atmos. Solar Terr. Physics*, *60*, 733–740, 1998b.

Wescott, L., E. Wescott, H. Stenbaek-Nielsen, D. Sentman, D. Moudry, M. Heavner, and F. S. Sabbas, Triangulation of sprites and elves from the NASA 1999 sprites balloon campaign, *EOS Supplement*, *80*(46), F216, 1999.

Wigner, E. and E. E. Witmer, *Z. Physik*, *51*, 859, 1928.

Williams, E. R., *Atmospheric Electrodynamics*, volume 1, chapter Meteorological Aspects of Thunderstorms, CRC Press, 1995.

Wilson, C. T. R., The electric field of a thunderstorm and some of its effects, *Proc. Roy. Soc. London*, *37*, 32D, 1925.

Wilson, C. T. R., A theory of thundercloud electricity, *Proc. Royal Meteor. Soc. London*, *236*(32D), 297–317, 1956.

Winckler, J. R., Further observations of cloud-ionosphere electrical discharges above thunderstorms, *J. Geophys. Res.*, *100*, 14335, 1995.

Winckler, J. R., Optical and VLF radio observations of sprites over a frontal storm viewed from O'Brien Observatory of the University of Minnesota, *J. Atmos. Solar Terr. Physics*, *60*, 679–688, 1998.

Wood, C. A., Unusual lightning, *Weather*, *6*, 64, 1951.

Yukhimuk, V., R. A. Roussel-Dupré, E. M. D. Symbalisty, and Y. Taranenko, Optical characteristics of blue jets produced by runaway air breakdown, simulation results, *Geophys. Res. Let.*, *25*(17), 3289–3292, 1998a.

Yukhimuk, V. A., R. A. Roussel-Dupré, E. M. D. Symbalisty, and Y. Taranenko, Optical characteristics of red sprites produced by runaway air breakdown, *J. Geophys. Res.*, *103*(D10), 11473–11482, 1998b.

Zuelsdorf, R. S., R. J. Strangeway, C. T. Russel, C. Casler, H. J. Christian, and R. C. Franz, Trans-Ionospheric pulse pairs (TIPPs): Their geographic distributions and seasonal variations, *Geophys. Res. Let.*, *24*(24), 3165–3168, 1997.